Republic of Iraq
Ministry of Higher Education and Scientific Research
University of Misan/Collage of Engineering
Department of Civil Engineering

STRUCTURAL BEHAVIOR OF FERROCEMENT –BRICK COMPOSITE SLAB

By

Ahmed Hatif Obaid

B.Sc. in Civil Engineering, 2016

A Thesis

Submitted in Partial Fulfillment of the

Requirements for the Master of Science

Degree in Civil Engineering

University of Misan

July 2022

Thesis Supervisor: Prof. Dr. Abdulkhaliq A. Jaafer

بِسْمِ اللَّـهِ الرَّحْمَـٰنِ الرَّحِيمِ

(وَقُلْ رَبِّ زِدْنِي عِلْمًا)

صَدَقَ اللهُ العَلِيُّ العَظِيم

سورة طه - الآية 114

ABSTRACT

This study proposes two new techniques for the construction of jack-arch slabs. The first technique is made from two layers. The first layer is a ferrocement precast panel that worked as a formwork, and the second layer is composed of clay brick units (solid and perforated bricks), cellular concrete block prism, and gypsum mortar. The second technique is made from lightweight precast ferrocement elements in the form of sandwich panels. This technique is made up of two layers of ferrocement separated by styropor or cellular concrete block prisms (thermostone). The overall thickness of the sandwich slab is 130 mm (15 mm for each ferrocement layer and 100 mm for the prisms). All the ferrocement layers are consist of different layers of steel wire mesh embedded in a high-flowable cement mortar of 68 MPa. The main parameters included are span length, camber height, volume fraction, and brick types, type of core material (styropor or cellular concrete), span length, and depth of the slab. Twenty- eight samples are manufactured and tested under three-point flexural loads. Five of which are one-way jack arch slabs made from clay bricks and cellular concrete blocks and gypsum mortar to represent control specimens. The remaining twenty-three members are sixteen of which are ferrocement–brick composite slab specimens, five of are precast ferrocement panels to evaluate their capacity to carry construction loads, and seven other specimens are precast ferrocement sandwich slabs. The results regarding ultimate loads and ductility index showed that all-composite ferrocement slabs specimens, have (19.53-264.33%) and (48.78-243.21%) higher ultimate loads and ductility index than the control specimen, respectively. Precast panel specimens are capable of securely bearing construction loads without supports. Ferrocement sandwich slab specimens have a higher ultimate loads and ductility index, ranging from (571.23-1216.89%) and (60.55-205.50%) than the control specimens, respectively. Increasing the depth section of the ferrocement sandwich slab increased the ultimate loads and ductility

index by 77.48 and 14.28%, respectively. When compared to control specimens, the weight of the sandwich slabs is reduced by 19.60 to 43.13 %. According to the encouraging results of the study, the proposed ferrocement sandwich slab and ferrocement composite brick slab specimens can use as an alternative to the traditional brick-work slab.

SUPERVISOR CERTIFCATION

I certify that the preparation of this thesis entitled " **Structural behavior of ferrocement–brick composite slab**" was presented by "**Ahmed Hatif Obaid**", and prepared under my supervision at University of Misan, Department of Civil Engineering, College of Engineering, as a partial fulfillment of the requirements for the degree of Master of Science in Civil Engineering (Structural Engineering).

Signature:
Prof. Dr. Abdulkhaliq A. Jaafer
Date:

In view of the available recommendations, I forward this thesis for discussion by the examining committee.

Signature:
Assist. Prof. Dr. Samir M. Chassib
(Head of Civil Engineering Department)
Date:

EXAMINING COMMITTTEE'S REPORT

We certify that we, the examining committee, have read the thesis titled **(Structural behavior of ferrocement–brick composite slab)** which is being submitted by (**Ahmed Hatif Obaid**), and examined the student in its content and in what is concerned with it, and that in our opinion, it meets the standard of a thesis for the degree of Master of Science in Civil Engineering (Structures).

Signature:
Name: Prof. Dr. Abdulkhaliq A. Jaafer
(Member and Supervisor)
Date: / /2022

Signature:
Name: Prof. Dr. Mohammed A. Mashrei
(Chairman)
Date: / /2022

Signature:
Name: Assist. Prof. Dr. Samir M. Chassib
(Member)
Date: / /2022

Signature:
Name: Assist. Prof. Dr. Hayder A. Radhi
(Member)
Date: / /2022

Approval of the College of Engineering:

Signature:
Name: Prof. Dr. Abbas O. Dawood
Dean, College of Engineering
Date: / /2022

DEDICATION

To my most prized asset, my family, my love my wife, and my precious kid, Ali.

ACKNOWLEDGEMENTS

In the name of Allah, the Most Gracious and the Most Merciful All praise to Allah for His strength and His blessing in completing this thesis.

A special appreciation goes to my supervisor Prof. Dr. Abdulkhaliq A. Jaafer for his supervision and constant support. His invaluable help with constructive comments and suggestions throughout the experimental and thesis work contributed to the success of this research.

I would like to express my appreciation to the Dean of the College of Engineering. Prof. Dr. Abbas O. Dawood and also to the college of engineering council.

I would like to thank the Civil Engineering Department's Head, Assistant Professor Dr. Samir Mohammed Chassib, for his help and support during the study period, as well as Associate Dean for Scientific Affairs and Graduate Studies. Prof. Dr. Sa'ad Fahad Resan and the graduate studies rapporteur, Assistant Professor Dr. Faten I. Mussa.

Thanks to the staff of the College of Engineering for their cooperation, Sincere thanks to all my teachers in the civil engineering department.

My gratitude also extends to all of the technicians and office personnel.

Finally, my deepest gratitude goes to my wife Eng. Lawhedh Forat Naeem.

Also, sincere thanks to my brother's son, Karrar Nibras, for his support during the experimental program.

To those who indirectly contributed to this research, your kindness means a lot to me. Thank you very much.

Ahmed Hatif Obaid

TABLE OF CONTENTS

SUPERVISOR CERTIFCATION vi

EXAMINING COMMITTTEE'S REPORT vii

DEDICATION viii

ACKNOWLEDGEMENTS ix

TABLE OF CONTENTS x

LIST OF TABLES xiii

LIST OF FIGURES xiv

LIST OF SYMBOLES xviii

LIST OF ABBREVIATIONS xix

CHAPTER One: INTRODUCTION 1

1.1 General 1

1.2 Jack Arch Slab 1

1.3 Ferrocement 5

1.4 Ferrocement Composite Slab 6

1.5 Problem Statement 9

1.6 Aim of The Study 9

1.7 The Study Layouts 10

CHAPTER Two: LITERATURES REVIEW 13

2.1 Introduction 13

2.2 Jack Arch Slab 13

2.3 Ferrocement Precast Panels..... 22
2.4 Ferrocement Composite Slab 26
2.5 Concluded Remarks 35
2.6 Research Gap Significant 36
CHAPTER Three: EXPERIMENTAL WORK..... 37
3.1 Introduction 37
3.2 Materials Properties..... 37
3.2.1 Clay bricks 37
3.2.2 Gypsum mortar 38
3.2.3 Cellular concrete blocks..... 39
3.2.4 Flexural bonding strength..... 41
3.2.5 Cement..... 44
3.2.6 Styropor Panel..... 44
3.2.7 Fine aggregate..... 45
3.2.8 Water..... 46
3.2.9 Welded square wire mesh..... 46
3.2.10 Superplasticizer..... 48
3.3 Trail Mixes..... 49
3.4 Manufacturing of Specimens..... 51
3.5 Testing Procedure 60
CHAPTER Four: RESULTS ANALYSIS AND DISCUSSIONS..... 63
4.1 General 63
4.2 Ultimate Load..... 64

4.2.1 Ultimate load for the first group specimens (G_1). 64

4.2.2 Ultimate load for the second group specimens (G_2). 65

4.2.3 Ultimate load for the third group specimens (G_3). 69

4.3 Load – Deflection Curves and ductility index..... 72

4.3.1 Load – Deflection Curves and ductility index for specimens of (G_1) 72

4.3.2 Load – Deflection Curves and ductility index for specimens of (G_2) 76

4.3.3 Load – Deflection Curves and ductility index for specimens of (G_3) 83

4.4 Failure Modes..... 89

CHAPTER Five: CONCLUSIONS AND RECMMONDATIONS..... 118

5.1 Conclusions 118

5.1.1 Conclusions for jack arch slab control specimens 118

5.1.2 Conclusions for ferrocement precast and composite brick specimens 119

5.1.3 Conclusions for ferrocement sandwiched slabs specimens .. 120

5.2 Recommendations for Future Works..... 120

APPENDICIES..... 122

APPENDIX A: PRODUCT DATA SHEET OF SIKA VISCOCRETE 5930L IQ 123

REFERENCES 126

الخلاصة 132

LIST OF TABLES

Table 3-1:Clay bricks properties. 37

Table 3-2: Gypsum mortar properties. 38

Table 3-3: Mechanical and physical properties of cellular concrete blocks. 40

Table 3-4: Results of flexural bonding strength according to Khalaf 43

Table 3-5: Chemical properties of cement. 44

Table 3-6: Physical and mechanical properties for cement material. 44

Table 3-7: Grading test result of fine aggregates. 45

Table 3-8:Welded square steel wire mesh testing results. 48

Table 3-9: Trail mixes proportions with tested results. 49

Table 3-10: Jack arch slab specimens details. 52

Table 3-11: Details of ferrocement brick slab specimens. 56

Table 3-12: Details of ferrocement sandwiched slab specimens. 60

Table 4-1: Ultimate load and weight results of G_1 specimens 64

Table 4-2: Ultimate load and weight results of G_2 specimens 66

Table 4-3: Ultimate Load and weight results of G_3 specimens. 69

Table 4-4: Test results of G_1 specimens. 74

Table 4-5: Test results of G_2 specimens. 80

Table 4-6: Test results of G_3 specimens. 87

LIST OF FIGURES

Figure. 1-1: Jack arch slab after construction. 2

Figure. 1-2: Historical market arching in AL-Amarah city 2

Figure. 1-3: Construction of a jack arch slab. 3

Figure. 1-4: Failure modes of masonry jack arch slabs 4

Figure. 1-5: Some of ferrocement applications. 7

Figure. 1-6: Deck slab-steel beam and composite action. 8

Figure. 2-1: Details of a of the proposed two-way arch slab 13

Figure. 2-2: Failure modes of masonry structures 14

Figure 2-3: Retrofitting jack-arch slab by concrete layer method 15

Figure. 2-4: System of jack arch slab 16

Figure. 2-5: Samples with bracings 17

Figure 2-6: Structural roof in both horizontal and vertical positions 18

Figure. 2-7: Loading the slab with people 18

Figure 2-8: Failure in horizontal position 18

Figure. 2-9: Specimens details 19

Figure. 2-10: Ferrocement effect on strength and mid-span deflection 19

Figure. 2-11: Stress distribution of slabs at failure loads. 20

Figure 2-12: Gravity and lateral loading on the specimens 21

Figure. 2-13: The maximum principal stresses obtained from the static analysis. 22

Figure. 2-14: Setup of the tested folded and flat panels 23

Figure. 2-15: Load - deflection relationship of ferrocement slabs 24

Figure. 2-16: Panels used in the casting process 25

Figure 2-17: Test setups. 25

Figure. 2-18: View of the cross-section of the specimens 26

Figure. 2-19: Composite ferrocement masonry slab layout 27

Figure. 2-20: Slab specimen preparations. 27

Figure. 2-21: Flexural two-line load Test setup of slabs 28

Figure. 2-22: Plan and cross-section details for tested specimens 28

Figure. 2-23: Pure shear loading test for slab specimens 29

Figure 2-24: Ferrocement sandwich and hollow core panels 30

Figure. 2-25: Sandwich panels and location of shear connectors 30

Figure. 2-26: A typical section of the composite slab with a ferrocement panel as a permanent form of the slab..... 32

Figure. 2-27: The equivalent elastic bending stress-deflection for panels by different fiber volume proportions 32

Figure. 2-28: Casting ,and testing steps 34

Figure 2-29: Proposed lightweight multi-ribbed composite slabs. 35

Figure 3-1: Clay bricks test. 38

Figure 3-2: Gypsum mortar tests. 39

Figure 3-3: Cellular concrete blocks tests. 40

Figure. 3-4: Free body diagram of flexural bonding test 42

Figure. 3-5: Flexural bonding strength test. 43

Figure. 3-6: Styropor prism of (200 ×100 ×100)mm..... 45

Figure 3-7: Schematic description of mesh tensile test sample and corresponding stress-strain curve 47

Figure. 3-8: Details for the steel-welded wire mesh coupons test..... 47

Figure. 3-9: Stress-strain curves for tested steel-welded wire mesh. 48

Figure. 3-10: Mix used for casting ferrocement precast panels, ferrocement sandwiched and composite brick slab specimens..... 50

Figure. 3-11: Samples testing of trail mix mortar. 51

Figure. 3-12: Steps for preparing jack arch slab G_1 specimens..... 53

Figure. 3-13: Cross section details for G_2 specimens. 54

Figure. 3-14: Steps for made G_2 specimens. 55

Figure. 3-15: Schematics and location of shear connecters..... 58

Figure. 3-16: Cross section details for ferrocement sandwich G_3 specimens..... 58

Figure. 3-17: Steps for made ferrocement sandwiched slab G_3 specimens. 59

Figure. 3-19: Flexural test set-up..... 61

Figure. 3-20: A plan of flexural test set up..... 62

Figure 4-1: Ultimate loads results for jack arch control specimens G_1. 65

Figure 4-2: Ultimate loads results for ferrocement composite-brick slab specimens G_2..... 67

Figure 4-3: Ultimate strength loads results for ferrocement sandwiched slabs specimens G_3. 70

Figure 4-4: The ductility index calculation approach 72

Figure 4-5: Load-deflection curves of G_1 specimens. 73

Figure 4-6: Ductility index results for jack arch slab specimens G_1. 75

Figure 4-7: Load-deflection curves for all precast ferrocement specimens. 77

Figure 4-8: Load-deflection curves for all ferrocement composite solid clay bricks slab specimens. 78

Figure 4-9: Load-deflection curves for all ferrocement composite perforated clay bricks, cellular concrete blocks slab specimens. 79

Figure 4-10: Ductility index results for ferrocement composite-brick slab specimens G_2. 81

Figure 4-11: Load deflection curves for Sp-4-80-0,SHp-4-80-0, SDp-4-80-0, and SHp-4-100-0. 84

Figure 4-11: Load deflection curves for Sc-4-80-0, SHc-4-80-0, and SHc-4-100-0. 85

Figure 4-13: Ductility index results for ferrocement sandwiched slabs specimens G_3. 88

Figure 4-14: Modes of failure for jack arch slab specimens (G_1). 90

Figure.4-15: Failure modes for all five ferrocement precast panels specimens. 93

Figure. 4-16: Failure modes for all ferrocement composite- brick specimens. 96

Figure 4-17: Failure modes for all ferrocement sandwiched slabs specimens. 103

LIST OF SYMBOLES

$f'c$ Compressive strength of concrete in Mpa.

fcu Compressive strength of cube cement mortar in Mpa.

fr Modulus of rupture of cement mortar in Mpa

f_{fb} Flexural bonding strength in Mpa.

l_b Length of brick unit in mm.

l_{mj} Length of mortar joint in mm.

P Failure load in Newton.

t_{bar} Thickness of steel bar in mm.

W Weight of brick in Newton.

w_b Width of brick unit in mm.

Δy Deflection at yield load in mm.

Δu Deflection at ultimate load in mm.

μ_Δ Ductility index.

LIST OF ABBREVIATIONS

ACI	American Concrete Institute.
ASTM	American Society for Testing and Materials.
CFRP	Carbon Fiber-Reinforced Polymer.
DXS	Double X- Strapping.
HCWA	High Calcium Wood Ash.
IQS	Iraqi Specification.
IRG	Iraqi Reference Guide.
PVA	Polyvinyl Alcohol fiber.
SXS	Single X- Strapping.
UBC	Uniform Building Code.

CHAPTER ONE: INTRODUCTION

1.1 General

Slabs are vital structural elements that are used to construct level and safely surfaces on building floors, roofs, bridges, and other structures. It is a horizontal structural element having parallel or nearly parallel top and bottom surfaces. Slabs are usually supported by beams, columns (concrete or steel or a combination of these), masonry bearing walls, or concrete walls. A slab has a depth that is very small in comparison to its span. Slabs can be distinguished according to their structural behavior as one-way slabs, one-way joist floor system, two-way floor systems and other types of the slab [1]. Slabs are classified into several types based on their materials and construction methods, such as jack-arch slabs, reinforced concrete slabs, ferrocement composite slab, steel plate slabs, timber floors and roofs, folded plates, and ferrocement precast slabs, and …. etc. [2].

1.2 Jack Arch Slab

Jack arch slabs are brick slabs supported by steel I-section beams that rest on load-bearing walls or lintels with centers varying from 700-900 mm [2]. The spans between steel I-section beams is constructed using clay brick units that are bonded together along with gypsum mortar as a binding material due to its rapid setting see Figure. 1-1. The height camber of the arch of this kind of slab varies from 10-30 mm, depending on the distances between the steel beams [3]. The bottom face of the brick may not be plastered with cement mortar for aesthetic reasons see Figure. 1-2. For the first time, Victorian architects in Britain developed the jack arch slab in the late nineteenth century. After that, the jack-arch slab spread to most countries, including North America, East Europe, and India. By the mid-twentieth century, it has become a popular flooring system in several Middle Eastern countries, such as

Iran and Iraq. Arching by bricks is a well-known method and is widely used in most regions of Iraq.

Figure. 1-1: Jack arch slab after construction.

Figure. 1-2: Historical market arching in AL-Amarah city [4].

Despite the widespread use of reinforced concrete in construction slabs, arch brick slabs are still used in many countries, especially in Iraqi regions, due to their speed of construction, low cost, no need for skilled labor, no need for complex engineering calculations, effectiveness for small areas, and not required formwork, reinforcement, casting and curing [3]. It is recently found that ceramic panels and cellular concrete block units are used in their construction due to the cellular concrete block's speed of work, thermal insulation, and lightweight see Figure. 1-3.

In spite of the general advantages of a jack-arch slab, there are some drawbacks. In particular, as a primitive building technique, it sustains limited loads, is sensitive to seismic loadings, and uses gypsum mortar, which has low moisture resistance [5].

(a) Cellular concrete blocks. (b) Ceramic panels.

Figure. 1-3: Construction of a jack arch slab.

Under normal static loading, the jack arch slab system is stable because the brick arches transport gravity loads mainly in compression along the arch towards the beams. The load is then transferred to the walls or beams through parallel steel beams. The jack-arch slab system is often regarded as a one-way slab due to its geometric design [6].

The performance of jack arch slabs in previous earthquakes demonstrates that jack arch slabs do not produce a significant diaphragm effect, which is regarded as one of the primary reasons for failure see Figure. 1-4. Furthermore, masonry bearing wall strength losses and steel beam movement owing to ground subsidence are two of the most common causes of jack arch slab failures. Because of their arch geometries, brick arches exhibit more stiff behavior than steel beams under vertical vibration. As a result, loadings on slab systems focus on rigid arches rather than ductile steel beams [7]. The main functions of the brick arches are to carry the load

Figure. 1-4: Failure modes of masonry jack arch slabs [8].

and transfer it to the steel beams safely. However, because of the high stiffness of brick arches, dynamic interaction between steel and brick members produces collapse. Furthermore, the material characteristics of jack arch slab components play a crucial role in the structural response. Poor mechanical properties of mortar, gypsum, and bricks, such as compressive strength ,and flexural bonding strength in particular, might be another cause of the collapse [6].

1.3 Ferrocement

Ferrocement is a form of thin-walled reinforced concrete that is generally made of hydraulic cement mortar and reinforced with closely spaced layers of continuous and relatively fine wire mesh. The mesh might be composed of metallic or other appropriate materials [9]. It is formed so that it acts differently than ordinary reinforced concrete regarding strength, deformation, and applications. It may be formed into panels or thin sections, which are mostly less than 50 mm thick, with simply a cement mortar the covering reinforced layers. Ferrocement is a member of the thin-laminated cementitious composite family [10].

The origins of ferrocement can be traced back to the work of Jean Louis Lambot, who submitted a patent for a substance he named (fer-ciment) in 1855. Jean Louis created a variety of artifacts, including two boats [10].

Constituent materials use in the construction of ferrocement are sand, water, and reinforcement. Sand is often used after it has been passed through sieve No. 8 (2.36 mm). The most common cementitious material is ordinary Portland cement. The water must be drinkable. In addition to the fundamental components, extra admixtures such as silica fume and high-range water reducer may be employed [9].The main reinforcement is wire mesh. Wire mesh provided in a different texture which are comes in square, woven, welded, expanded, and hexagonal shapes. Skeletal steel bars (6–10)mm in diameter are sometimes used in ferrocement

members to create the desired shape of the structure [10]. In addition to mesh, fibers can be used to decrease the number of mesh layers [9].

Many methods available for making ferrocement that depending on the complexity of the shape, size, and operator skills. The goal of all approaches is to completely encapsulate a layered mesh system with cement mortar. These ways are armature, closed-mold, integral-mold, and open-mold [9]. The construction process is determined by the type of section to be created, which influences the composition of the mixed mortar. Typically, mortar is applied by hand, and plaster is done by pressing it through the mesh. Mortar can be shotte through a spray gun mechanism in some cases (shotcreting) .

There are numerous advantages to using ferrocement over other building materials, such as available raw materials, suitable for a wide range of construction techniques, no need for labor skills, lightweight, may be constructed into any shape, durable, not flammable, easily repaired, cost-effective, environmentally friendly technology, high flexibility and ductility, and it has superior cracking resistance [10].

Ferrocement is utilized in a variety of applications, including new construction and the rehabilitation of existing structures, such as marine applications, housing applications, water supply, and sanitation facilities, agricultural applications, and permanent formwork see Figure. 1-5.

1.4 Ferrocement Composite Slab

Composite structures are structures that consist of two or more components and have positive implications. They are a versatile option for a variety of applications. Each material may be chosen according to its primary function in the construction. A composite system reduces the unnecessary and unwanted material properties, such as weight and cost, without effect on required capacity [11].

(a) Interior beam–column joints rehabilitated by ferrocement jackets [12].

(b) Construction septic tank [13].

Figure. 1-5: Some of ferrocement applications.

The significant advancement of material science and modern buildings have been the major sources of composite materials. Also, there is a high need for materials that are both light and strong. This empowers researchers, experts, and organizations to place emphasis on composite materials in their studies.

In most residential structures, the slab structure represents the largest dead load. The weight of slab in any structure almost account of 50-65% of a building's total dead load. Furthermore, the substantial self-weight percentage of the structure has a significant impact on column, beam, and foundation size, as well as the seismic capacity and reaction of conventional residential structures [11].

As a result, even minor weight reductions or increases in the load-bearing capability of this structural element have an impact on the global structure, from design through construction and durability. Several distinct forms of composite slab construction have been used all around the world. The most typical composite slabs

consist of a profiled steel decking that acts as a permanent formwork on the bottom of the concrete slabs, spanning between support beams [14] see Figure. 1-6.

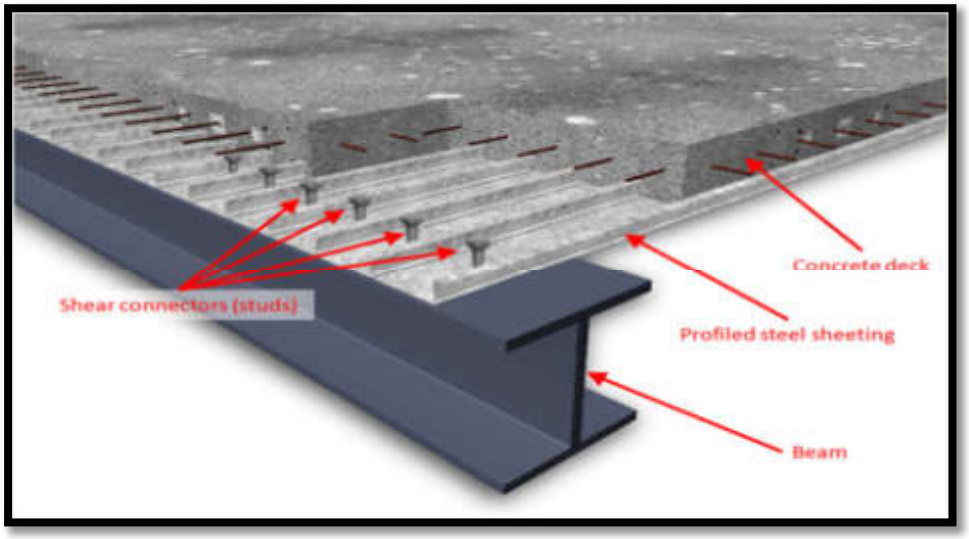

(a) Schematic deck slab-steel beam [15].

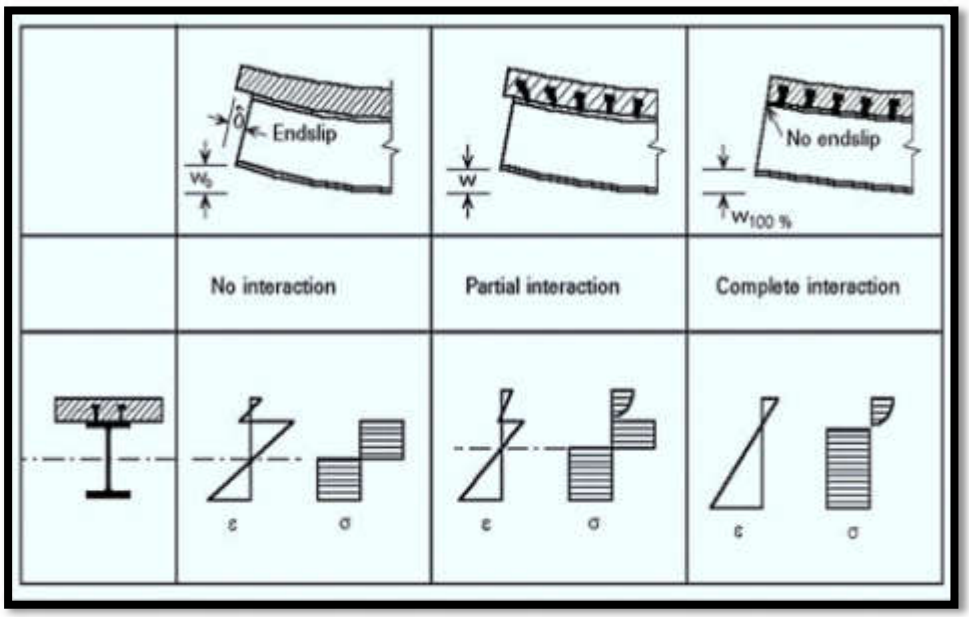

(b) Composite action [15].

Figure. 1-6: Deck slab-steel beam and composite action.

1.5 Problem Statement

The purpose of this study is to develop an alternative method for construction of jack arch slab. A list of the most significant issues and challenges that are taken into consideration when developing roofing for buildings based on the previously stated information are listed below:

1. Many slabs being used in construction are heavy and expensive, hence the development of lightweight, and low-cost slabs depict a solution of such problem.
2. Lower production costs, simplicity of use, and higher material quality are all required by the technical criteria. As a result, modern systems are more important than traditional systems.
3. The jack arch slab can only sustain a limited load and is also prone to earthquakes failure as mentioned early.
4. The majority of traditional roofs need a considerable number of workers.
5. The use of clay bricks in the jack arch slab contributes to pollution because of the local industries distributed throughout Iraq, which rely on primitive production processes.

1.6 Aim of The Study

The main goal of this study is to manufacture an effective jack-arch slab made from ferrocement precast panels and ferrocement sandwich slabs. The reasons for using ferrocement are due to the advantages mentioned in the section 1.3, and because it is an environmentally friendly material due to reduced wastage and reduced energy use for heating and cooling if use in sandwich form. The current study goals include:

1. Manufacturing of precast ferrocement panels and ferrocement sandwiched composite jack-arch slabs with varying depth, core materials, comber height, volume fraction, types of brick, and span length.

2. The structural behavior of jack-arch slabs made of different bricks (solid clay bricks, perforated clay bricks, and cellular concrete blocks (thermostone)) subjected to line load will be investigated.
3. The behavior of ferrocement slab panels, composite ferrocement jack arch slabs, and, ferrocement sandwiched jack arch slabs under a flexural three-point loading (line load) also was examined, and investigated.

1.7 The Study Layouts

The study is divided into **five chapters.** An overview of each chapter's content from the study is listed below.

1. **The first chapter** introduces jack arch slab, ferrocement, ferrocement composite slab, problem description, and the study goals.
2. **The second chapter** presents a literature overview and previous studies of the structural responses of jack-arch slabs, ferrocement precast panels, and composite ferrocement slabs.
3. **The chapter three** is talking about the experimental work, which shows the features and testing of the materials that are used in the study, as well as the descriptions of the jack arch slab, ferrocement panels, ferrocement composite brick slab, and ferrocement sandwiched composite jack arch slab specimens, test equipment, and testing procedure.
4. The results analysis of the structural behavior of studied specimens are shown in **Chapter four**, along with a discussion of these results.
5. **The fifth chapter** presents the research's conclusions and recommendations for further research in future.

CHAPTER TWO: LITERATURES REVIEW

2.1 Introduction

This chapter is divided into five sections, three of which include a review and summary of the most significant studies related to the structural behavior of jack arch slabs, ferrocement precast panels, and ferrocement composite slabs. Concluded remarks on the relevant studies and research gaps are the other two section titles.

2.2 Jack Arch Slab

Maheri and Rahmani in 2003 [5], were proposed a novel two-way jack-arch slab system. In this the proposed technique were used a sequence of transverse steel beams between the main I-beams as shown in Figure. 2-1. This system allows transmission of the vertical load in two directions. It was found that the diaphragm action and resistance to gravity and seismic loads were improved. The proposed flooring system represents an alternative to other flooring types such as reinforced concrete slab due to its low cost and ease of construction.

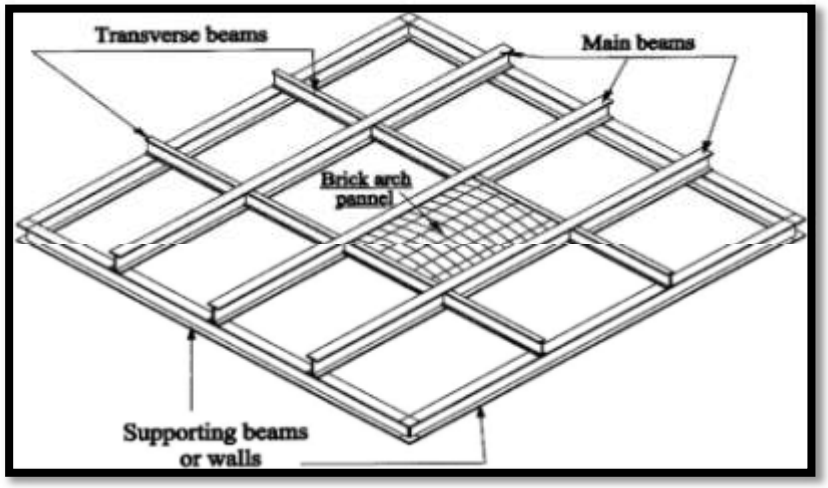

Figure. 2-1: Details of a of the proposed two-way arch slab [5].

Heidarzadeh and Zahrai in 2007 [8], were investigated the performance of existing structures during the 2003 Bam earthquake. The authors of this study concentrated on the most widespread types of structures in the subject zone of the Bam earthquake. The jack arch slab system was the most common in the subject area. The results revealed that the common failure modes of these structures are the shear failure of walls, separation of walls from the slab, and separation of steel I-section beams from each other, as seen in Figure. 2-2.

Figure. 2-2: Failure modes of masonry structures [8].

The effect of using a concrete overlay layer on top of the jack arch slab were experimentally evaluated by **Pourfalah et al. in 2009** [16]. The contact between the concrete and the steel I-section beams would be insufficient. A connecting mechanism comparable to that employed in composite slabs was chosen. Shear keys were used in this approach to enhance the interface between the concrete and the

steel I-section beams see Figure 2-3. The results showed that the strength and ductility increased by 198, and 167%, respectively than tradition jack arch slab. The addition of a layer of concrete increased the weight of the slab by 25%.

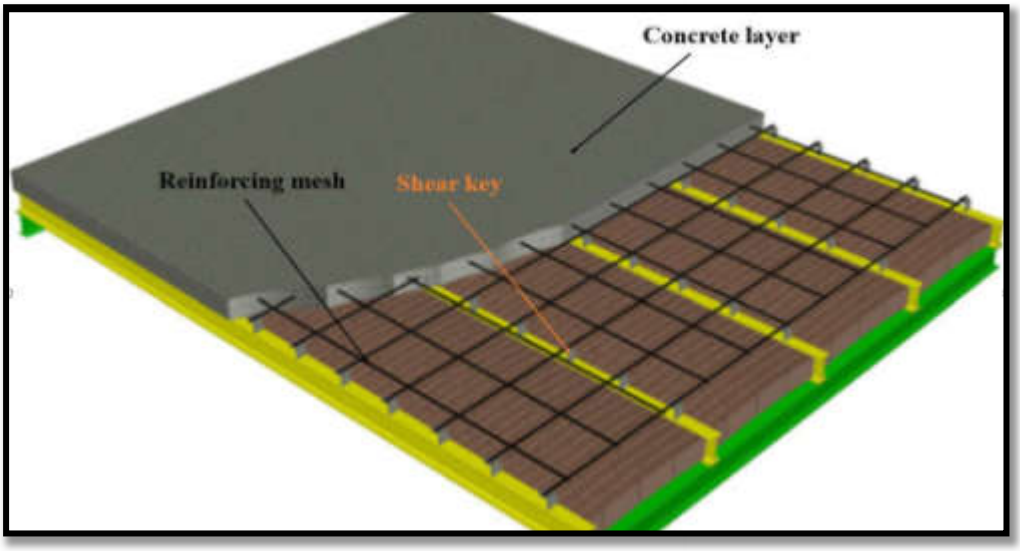

Figure 2-3: Retrofitting jack-arch slab by concrete layer method [16].

Maheri et al. in 2011[6] were performed out-of-plane pushover tests on full-scale retrofitted and ordinary jack-arch slabs as shown in Figure. 2-4. Two strengthening techniques were used in this study. The first one was using a grid of steel beams as shown in Figure. 2-4 (b). Another method was using a concrete layer over the brick jack arch slab shown in Figure. 2-4 (c). The results of the tests are then compared to the slabs' strength capacities and ductility. The results showed that the steel grid, in addition to being simpler, faster, and cheaper, the performance of the system had improved. However, the concrete layer method was effective in increasing strength, but significantly increased the weight of the slab. The concrete layer had higher strength and ductility than the steel grid method by 88.35 and 27.27%, respectively.

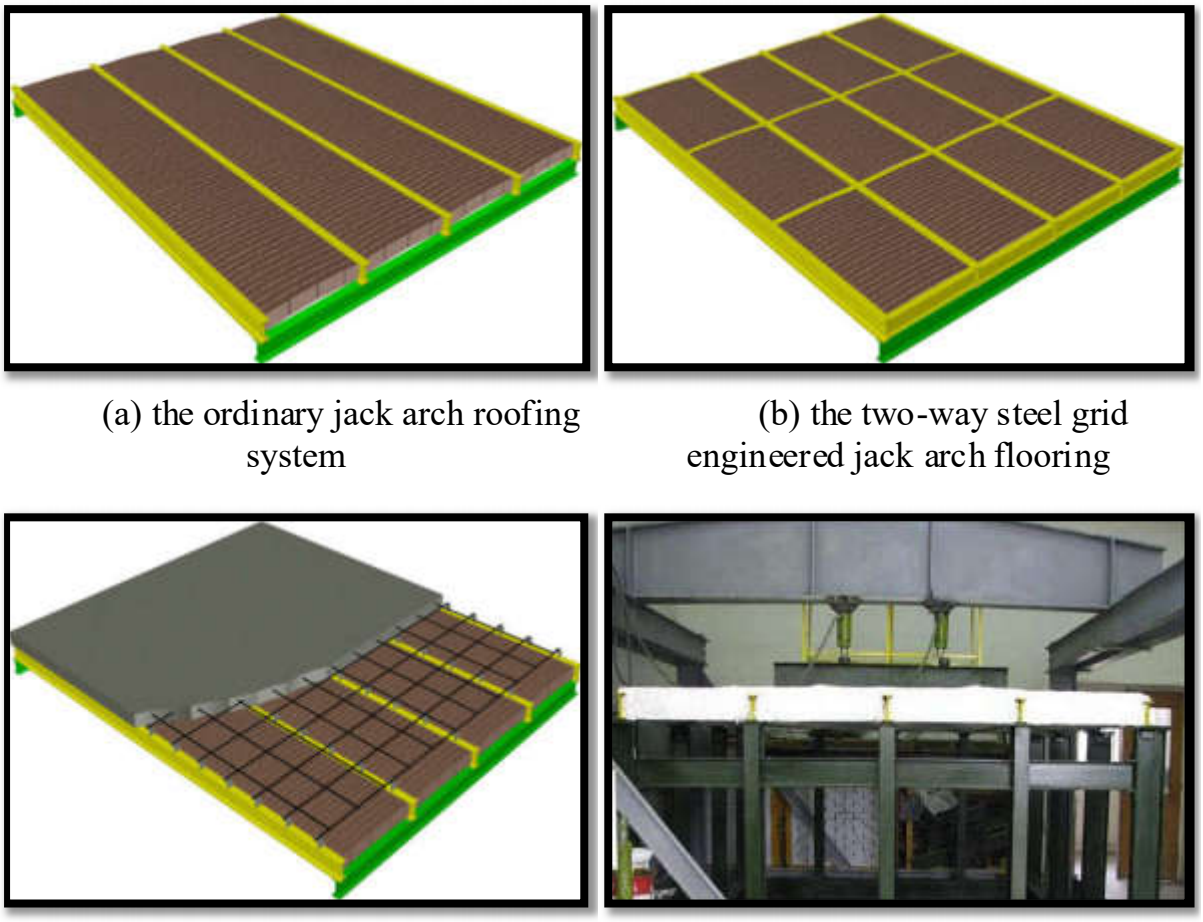

(a) the ordinary jack arch roofing system

(b) the two-way steel grid engineered jack arch flooring

(c) retrofitting of jack arch slab by laying a concrete layer on top

(d) test set-up for out-of-plane pushover loading of the slabs

Figure. 2-4: System of jack arch slab [6].

An experimental study of typical retrofitted jack arch slabs in a single-story 3D steel building was investigated by **Zahrai in 2014** [17]. The proposed retrofitted methods include using single X-strapping (SXS), double X-strapping (DXS) as shown in Figure. 2-5, and a two-way jack arch slab supported by a steel grid. The results revealed that a DXS method can significantly improve diaphragm performance regarding in-plane stiffness, capacity, and even energy dissipation when compared to the other two techniques.

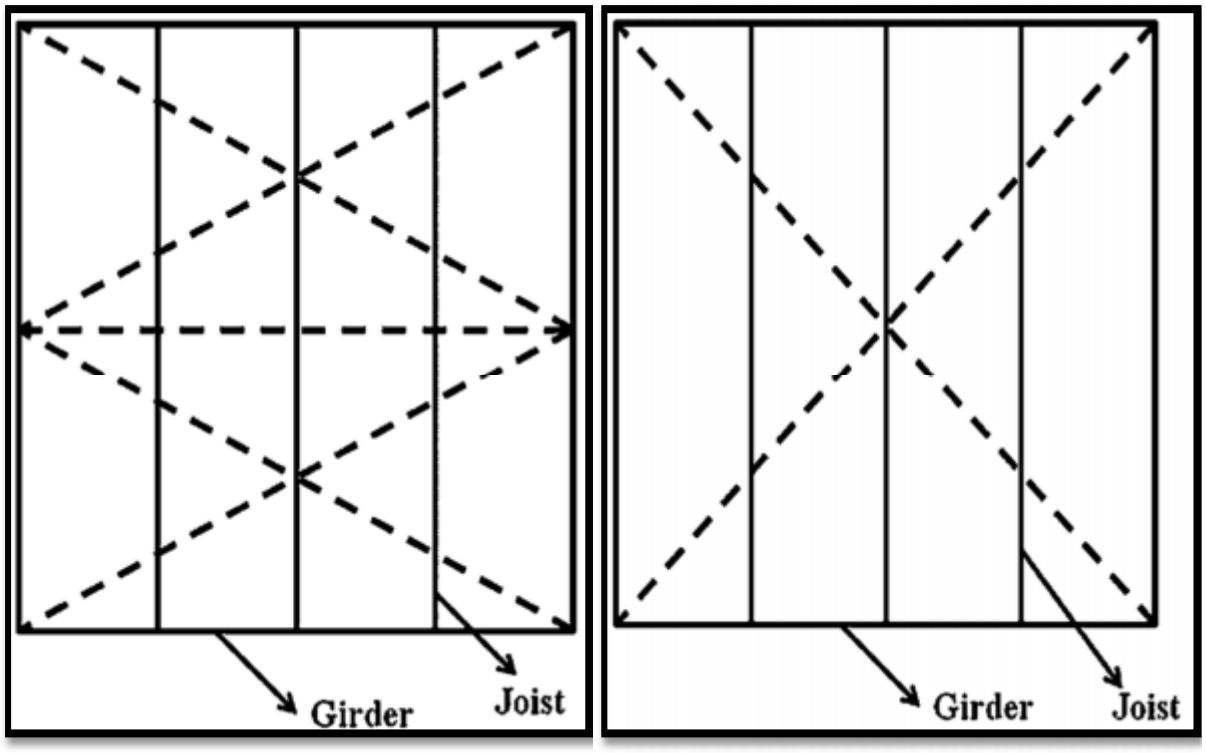

(a) DXS. (b) SXS.

Figure. 2-5: Samples with bracings [17].

The structural behavior of low-cost steel frame and thermo-stone block roof systems was studied by **Alfeehan and Alkerwei in 2014** [18]. The vertical and horizontal modes of thermo-stone blocks were tested. Figure 2-6 depict structural roof in both horizontal and vertical positions and Figure. 2-7 shows loading of slab with people . The results indicated the ultimate vertical loads in the horizontal position are about (18.5) tons/m^2, whereas the ultimate vertical loads in the vertical position are approximately (185) tons/m^2. Flexural failure was the most common failure mode in the cellular concrete block roof structure during the test. The cellular concrete block unit was fractured practically in the mid-span and no crushing of the cellular concrete block see Figure 2-8.

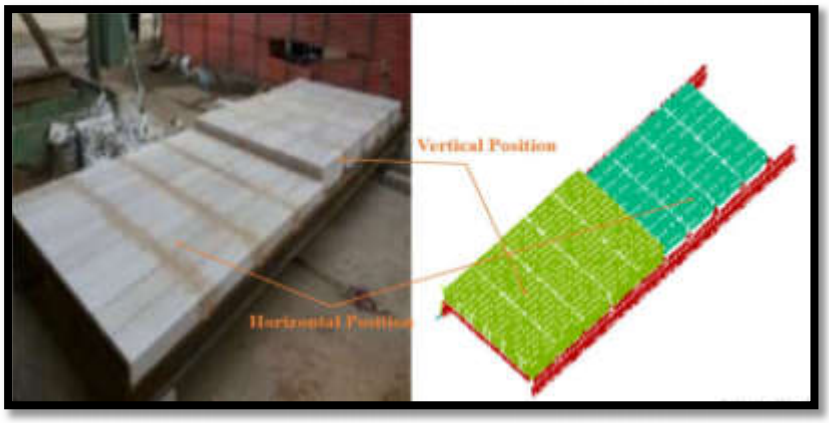

Figure 2-6: Structural roof in both horizontal and vertical positions [18].

(a) Vertical-position loading. (b) Horizontal -position loading.

Figure. 2-7: Loading the slab with people [18].

Figure 2-8: Failure in horizontal position [18].

Resan and Dawood in 2015 [3], were studied the performance of jack-arch slabs strengthened by ferrocement layers as shown in Figure. 2-9. They were used single and double layers of welded steel wire mesh with 12.5 mm square openings and an average wire diameter of 1 mm. The ferrocement layer worked together with the jack-arch slab and provided an improvement in flexural strength, stiffness, and ductility without significantly increasing the slab's weight see Figure. 2-10.

Figure. 2-9: Specimens details [3].

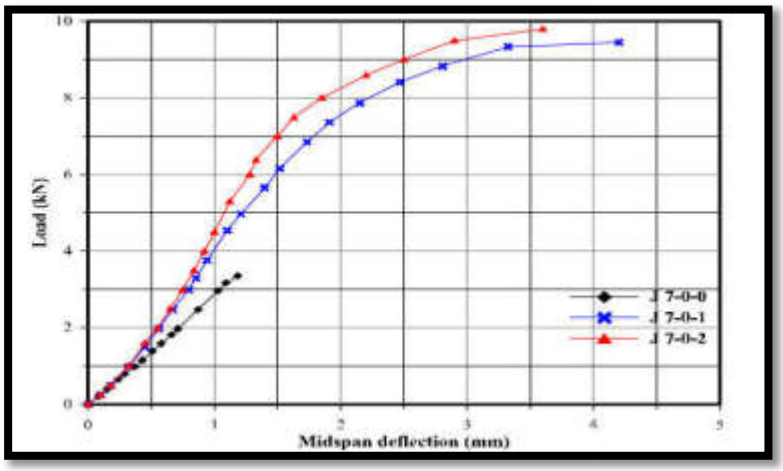

Figure. 2-10: Ferrocement effect on strength and mid-span deflection [3].

The performance of a jack-arch slab in southern Iraq was evaluated using finite element analysis by **Dawood and Resan in 2015** [19]. In this study, the effect of camber height on ultimate load and maximum deflection was investigated for flat and 20 mm camber-height masonry arch specimens. The STAADPRO software was used to perform finite element numerical analyses. As a result, the jack arch slab's tensile strength was crucial, mostly under gravity and seismic stresses. Both camber and flat slabs were governed by flexural stresses. The stress distribution in Figure. 2-11 shows compressive stresses at the top and tensile stresses at the bottom, with values that were maximum at the mid-span. Maximum stresses and deflections of steel I-section beam evaluated using finite element models were 69 MPa and 7.7 mm, respectively. These results were within the acceptable limits of 140 MPa for stresses and 11.11 mm for deflections, respectively.

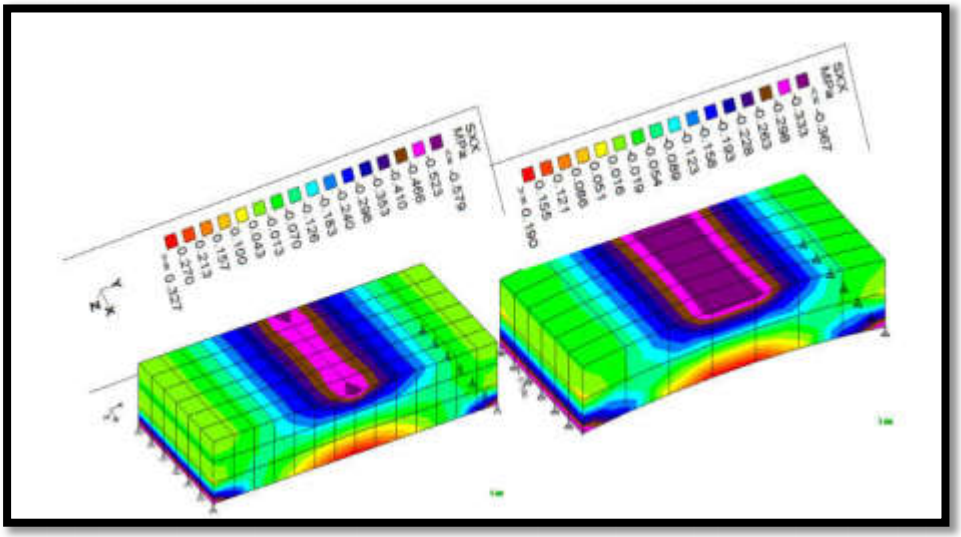

Figure. 2-11: Stress distribution of slabs at failure loads [19].

Experimentally, the in-plane seismic response of typical and retrofitted brick flat arch diaphragms was studied by **Shakib et al. in 2015** [20]. To evaluate the

stiffness and shear capacity of slabs. The influence of tension ties was investigated in diaphragm span tests with and without tension ties. Finally, the retrofitted diaphragms with continuous steel diagonal bracing and steel tension ties in end arch spans were tested under X-and Y-direction loadings. Figure 2-12 shows simultaneous gravity and lateral loading on the study specimens .The results showed that the simultaneous application of diagonal bracing and steel tension ties in end arch spans increased the shear capacity and stiffness by 88 and 108%, respectively. The study recommended using simultaneous diagonal bracing and steel tension ties in end arch spans for retrofitting typical brick flat arch diaphragms.

(a) Gravity loading detail.

(b) Lateral-loading detail.

Figure 2-12: Gravity and lateral loading on the specimens [20].

The structural behavior of masonry jack arch slabs on the old American boarding school for girls in Merzifon, Turkey, was studied by **Ozdemir et al. in 2017** [21]. The school was a one-way masonry jack arch slab. Static analyses were used to evaluate performance. According to the static test results the top of the building, and the connection regions between steel beams, and brick arches experienced the highest compression, and tension stresses see Figure. 2-13 .

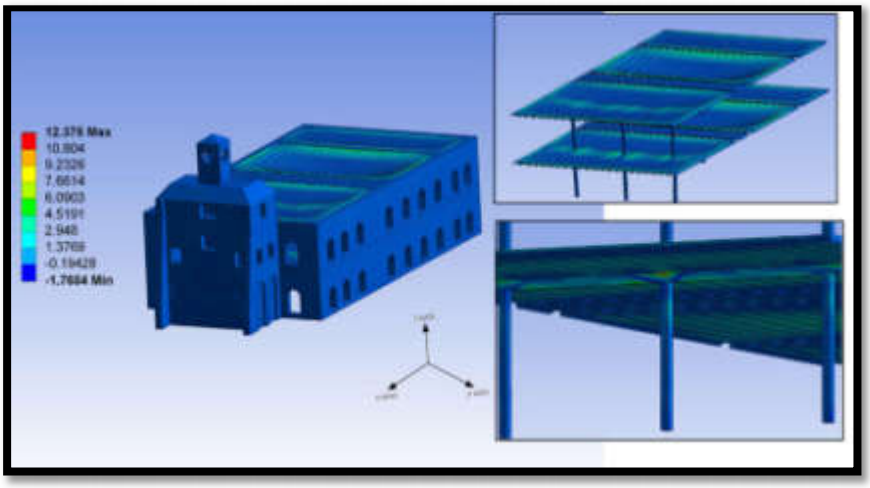

Figure. 2-13: The maximum principal stresses obtained from the static analysis [21].

2.3 Ferrocement Precast Panels

Mahmood and Majeed, in 2009 [22], were tested flat and folded ferrocement panels. The effects of using varying numbers of wire mesh layers on the flexural strength, ultimate strength, and ductility of panels were evaluated and discussed. Seven ferrocement panels were fabricated and tested, each with a horizontal projection of (600×380mm) and a thickness of 20 mm. four flat panels and three folded panels were made. Figure. 2-14 depicts the setup of the tested folded and flat panels. The number of wire mesh layers used was one, two, or three. The

experimental results showed that the ultimate strength of the folded panels with the particular shape used in this study was within the range of 331.81-465.21% of that of the similar flat panels with the same number of wire mesh layers.

Figure. 2-14: Setup of the tested folded and flat panels [22].

The structural behavior of flat ferrocement panels using square welded wire mesh was experimentally investigated by **Gaidhankar et al. in 2017** [23]. The main parameters used were the number of wire mesh layers and the thickness of the panel on flexural strength. Galvanized steel welded square having openings of 20 mm ×20 mm with a wire diameter of 1.6 mm was used in the different 2, 3, and 4 layers for all of the panels. The results revealed that layers of mesh above neutral axis in panels plays role in compressive strength. Their contribution was less in flexural strength as compared to mesh in tension zone. First crack load and ultimate failure load was delay with Increase in the thickness of ferrocement panels.

Eight ferrocement slabs were manufactured and implemented experimentally by **Nawar in 2017** [24]. All of the specimens measured 700 mm long, 300 mm wide, and 50 mm thick. The specimens were divided into two groups according to aggregate size. In the first group standard sand aggregate was used, while in the second group was made from sand that neglected the sand that passed through sieve

No. 8. The results revealed a slight increase in bending strength for the first group of slabs as compared to the second group of slabs see Figure. 2-15.

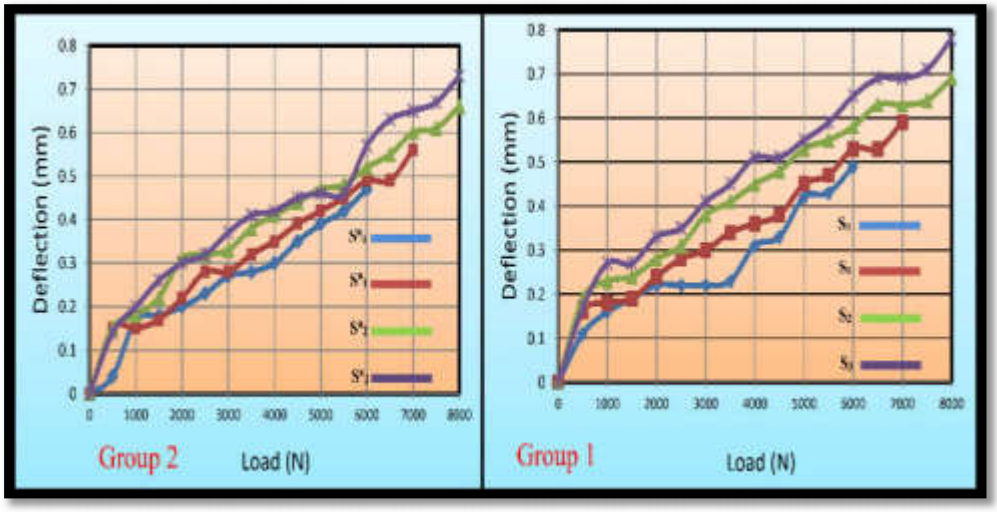

Figure. 2-15: Load - deflection relationship of ferrocement slabs [24].

Mughal et al. in 2019 [25] studied ferrocement panels under flexural and compression loading. Thirty-two specimens are cast and tested. Sixteen of them tested under flexure, while the remaining sixteen specimens are tested under compression load. The panels are reinforced using two different types of materials (galvanized iron mesh and polypropylene mesh) as depicted in Figure. 2-16. Flexure specimens are simply supported on two small edges and tested under four-point load bending. Both ends of the specimens tested in compression are hinged as shown in Figure 2-17. The variables investigated are panel thickness, volume fraction, and mesh material type. The test results regarding flexure and compression strength showed that all the galvanized iron mesh panels higher than the polypropylene mesh panels both in flexure and compression strength. On the other hand, polypropylene mesh panels performed better than galvanized iron mesh panels regarding ductility.

Figure. 2-16: Panels used in the casting process [25].

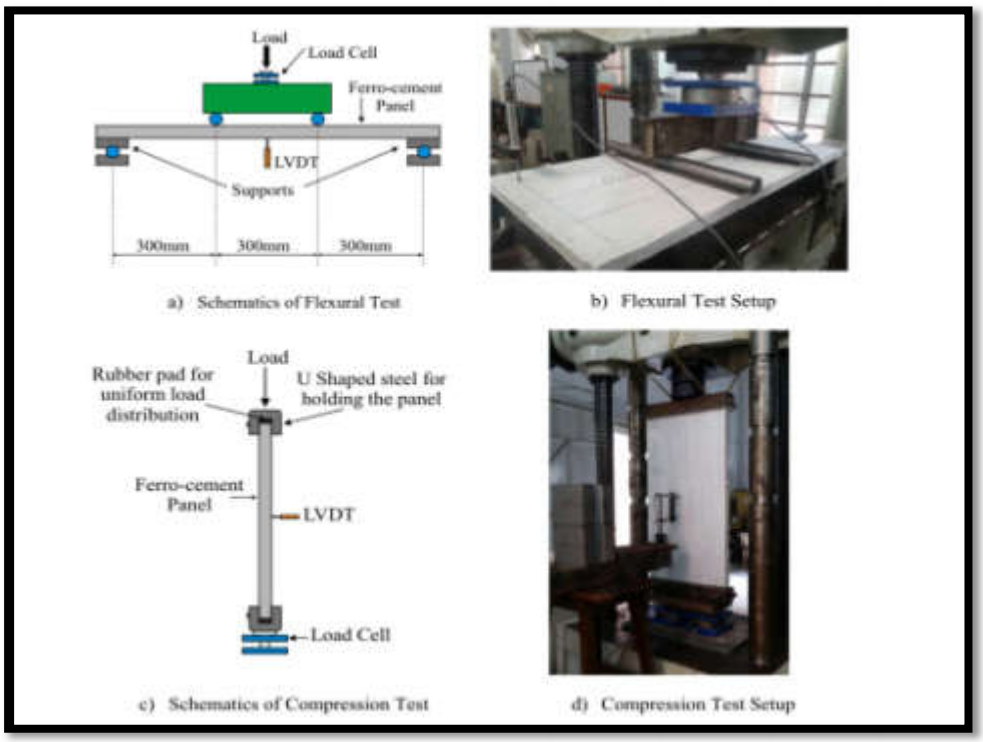

Figure 2-17: Test setups.

2.4 Ferrocement Composite Slab

Memon et al. in (2007) [26] were proposed a new technique for producing lightweight sandwich composite panels. The panels consisted of aerated concrete core confined by a high-performance ferrocement skin layer as shown in Figure. 2-18. The results were compared to a control specimen composed only of aerated concrete. The results showed a significant increase in both compressive and flexural strength of the proposed panels when compared to the control specimens.

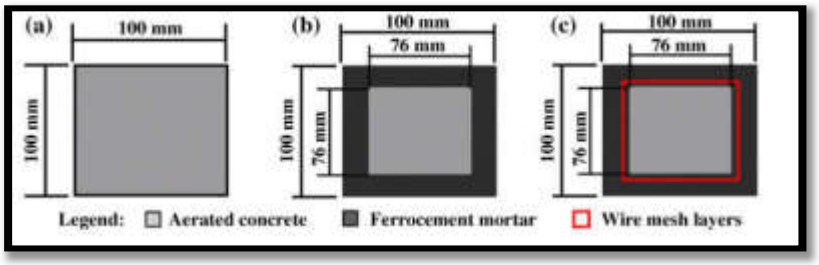

Figure. 2-18: View of the cross-section of the specimens [27].

The flexural performance of a new precast ferrocement thin panel with inverted two-way ribs as permanent formwork was studied by **Yardim et al. in (2008)** [28] see Figure. 2-19. Four panels of one-way ferrocement were made. Two of them were tested as ferrocement precast panels, while the other two were tested as composite slabs. The panels were tested under concentrated two-line loads and uniformly distributed loads. The results of the study showed that, a thin panel with an adequate ribs arrangement sustained the construction loads and can be use as permanent formworks. No separation or horizontal cracks between layers are observed. The panels could resist ordinary construction workers and equipment loads.

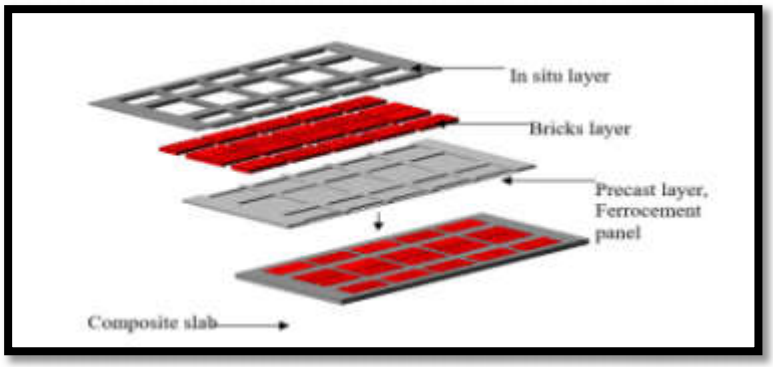

Figure. 2-19: Composite ferrocement masonry slab layout [28].

The structural behavior of a semi-precast model for producing floor slabs was studied by **Thanoon et al. in (2010)** [29]. The slab panel was composed of two layers linked together by a truss shear connection. The first layer was a formwork of precast ferrocement, while the second layer was brick units and mortar see Figure. 2-20. Four full-scale specimens were manufactured and subjected to two-line loads see Figure. 2-21. The investigation focused on the effect of shear connectors and brick units' arrangement on the total structural response of the slab. The findings revealed that the performance of the composite slab's flexural load was acceptable and that it can be employ as a floor slab in construction projects.

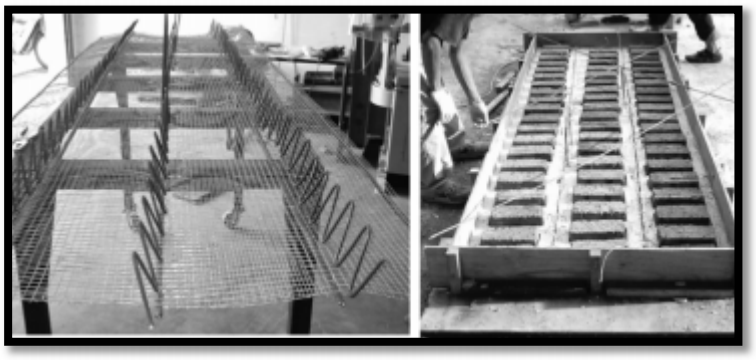

Figure. 2-20: Slab specimen preparations [29].

Figure. 2-21: Flexural two-line load Test setup of slabs [29].

Thanoon et al. in (2011) [30] investigated a semi-precast composite slab system consisted of a precast inverted ribbed ferrocement panel interlocked in situ with a brick–rib layer to create a composite slab, see Figure. 2-22. The efficiency of the composite slab's interlocking mechanism was evaluated under pure shear loading see Figure. 2-23 and flexural loadings. The flexural tests were aimed to obtain the best arrangements and orientations of the bricks. Pure shear loading results indicated that the suggested interlocking technique used was similar in performance to steel truss shear connectors in composite slabs. The observations related to crack patterns, ductility, and failure loads showed that the composite slab has good resistance to flexural loading and can use for structural purposes.

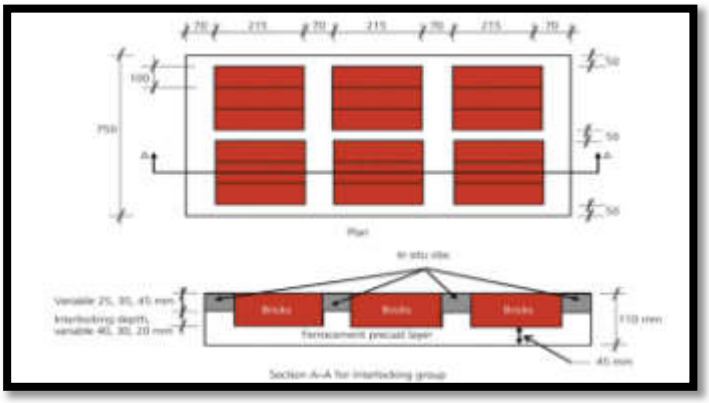

Figure. 2-22: Plan and cross-section details for tested specimens [30].

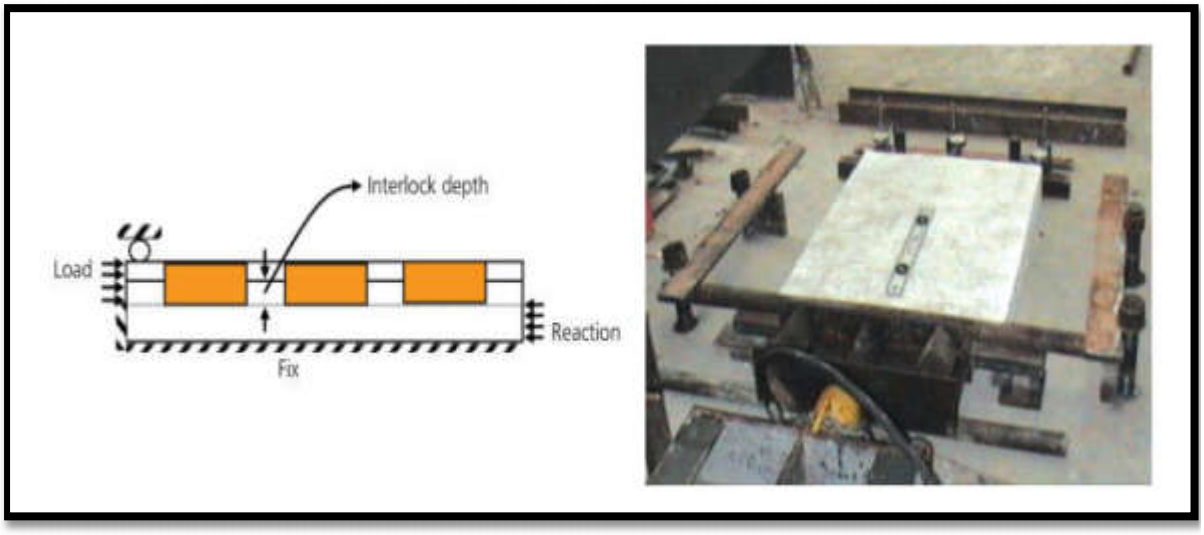

Figure. 2-23: Pure shear loading test for slab specimens [30].

Ezzat et al. in (2012) [31] were present result of a new method to develop ferrocement sandwich and hollow core panels as precast one-way slab components. Sandwich panels were consisted from two ferrocement layers strengthened by steel wire mesh and an autoclaved aerated lightweight concrete brick core. The specimens were divided into two groups based on the core materials used (autoclaved aerated lightweight concrete brick core and hollow core) see Figure 2-24 . Twenty seven specimens were manufactured, fifteen of which are sandwich panels and the remaining twelve are hollow-core panels see Figure. 2-25. The two groups are divided into different groups based on the reinforcement steel provided, the number of steel layers on each face, and the thickness of the two ferrocement layers. The specimens then tested under flexural line loads. The results of the tests demonstrated that the proposed panels could achieve greater ultimate and service loads, fracture resistance, ductility, and energy absorption.

(a) Lightweight brick sandwich panel. (b) Hollow core panel.

Figure 2-24: Ferrocement sandwich and hollow core panels [31].

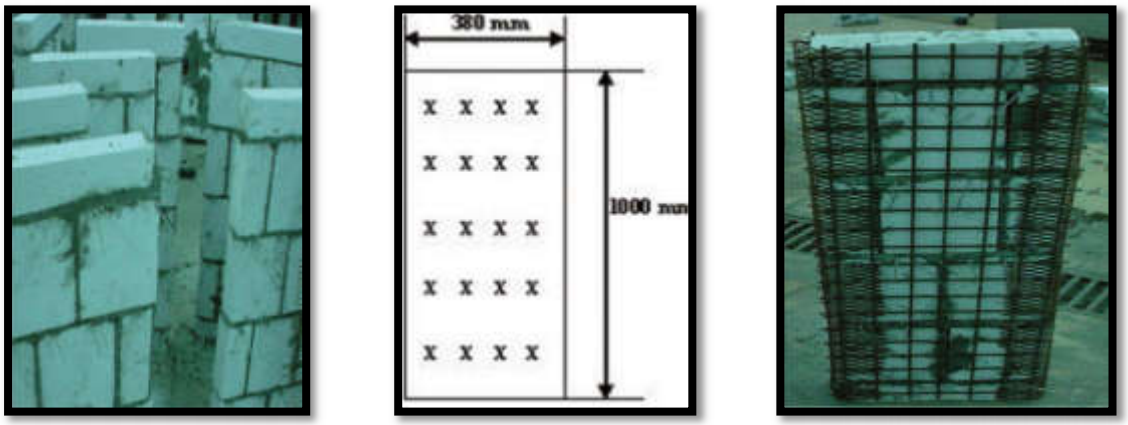

(a) Lightweight brick panel during construction (b) Locations of the shear connectors (c) Steel mesh and side reinforcement before casting the ferrocement layers

Figure. 2-25: Sandwich panels and location of shear connectors [31].

The structural behavior of a ferrocement–reinforced concrete one-way composite slab system with a high calcium wood ash (HCWA) high-strength mortar as the compression zone was investigated by **Chee and Ramli in (2013)** [32]. This system consisted of a typical reinforced concrete slab covered with a layer of high-

strength ferrocement composite containing varying amounts of HCWA by the total weight of the binder. Six one-way composite slab prototypes are manufactured and tested, subjected them to a four-point flexural load test. The investigation's findings showed that using HCWA in the mortar layer as a cement replacement rate of 2% to 8% by binder weight, improves the first crack load and ultimate failure load of the composite slab system significantly

Waryosh et al. in 2013 [33] were studied an experimental program on ten panels of the same length and width (1200×400) mm. All specimens were subjected to flexural two-point flexural loading. Panels were made of a layer of lightweight concrete sandwiched between two outer layers of reinforced concrete joined by truss reinforcement as shear connectors. Three variables were studied these were the thickness of the inner wythe, the strength of the outer wythe, and the type of lightweight aggregate (sawdust, polystyrene, and porecilinite) that was used in the inner wythe. The experimental program's study found that when the thickness of the inner wythe in sandwiched slab panels was increased, their strength improved. Sandwich slab panels with sawdust as aggregate in the inner wythe have a higher strength than sandwich slab panels with a polystyrene inner wythe.

In an experimental series, **Abushawashi and Vimonsatit in 2014** [34] were studied the possible use of ferrocement panels as a permanent type of reinforced concrete slab with lightweight block infill. The specimens in this study are divided into two series. In the first series, all cast panels have dimensions of (620×200×40) mm and were reinforced with distinct wire mesh layers (two, three, four, and six). To investigate the effects of fiber content on strength, three different fiber volume fractions of the hybrid PVA fiber, namely 0.75 percent (FA), 1.00 percent (FB), and 1.50 percent (FC), were applied in three distinct combinations. In the second series, (1220×1000×155) mm, ferrocement panels were manufactured to construct composite slabs with lightweight block infill as shown in Figure. 2-26. The results

indicated that hybrid PVA fiber composites, either as panels or as composite slabs, have higher ultimate strength and yield-strain capacity at the ultimate load than control specimens and may use effectively as permanent forms, see Figure. 2-27.

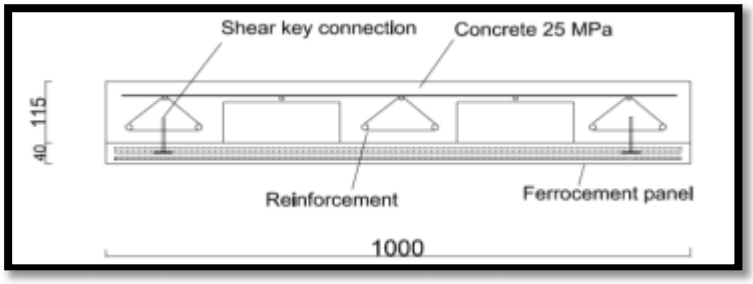

Figure. 2-26: A typical section of the composite slab with a ferrocement panel as a permanent form of the slab [34].

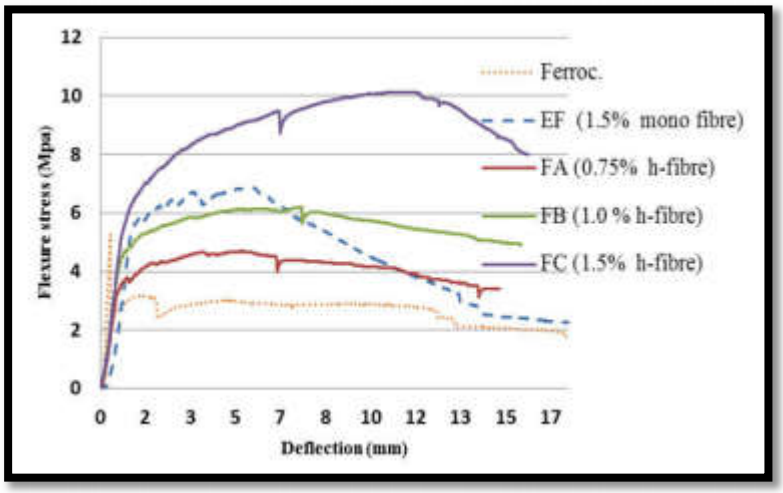

Figure. 2-27: The equivalent elastic bending stress-deflection for panels by different fiber volume proportions [34].

Dharanidharan in 2016 [35] was studied an experimental program to explain the flexural behavior of ferrocement composite reinforced concrete slabs under two-point flexural loading. The purpose of the study was to use the concept of steel-concrete composites to create a similar system in which steel plate was replaced with

ferrocement elements. These elements worked as permanent formwork and also contributed to the slab's structural behavior. Two reinforced concrete slabs and two ferrocement concrete composite slabs were tested in this study. The variables selected were the percentage of reinforcement and the number of mesh layers, while all other factors remained constant. The results indicated that ferrocement as a cover can use successfully for reinforced concrete slabs. The bending strength of the specimens with ferrocement cover was enhanced slightly.

In 2018, Yardim [11] was conducted a comprehensive review of the studies related to the mechanical properties of ferrocement as employed in composite precast and precast slabs. The ferrocement precast slab technology achieved the best composite combination of precast and cast-in-situ systems because ferrocement precast slabs provide a lighter precast layer that enables simpler construction and transportability. By employing ferrocement as a precast layer, the system's initial structural crack load was increased, fracture probabilities during transport and handling were decreased, and the ferrocement thin section decreases the weight of the precast composite and the quantity of in-situ concrete.

Shaheen and Fatema in 2019 [36] were studied the development of a lightweight ferrocement composite plate. Twelve specimens of (500×500×50mm) ferrocement composite plates were prepared and tested. The supports are simply supported along their four sides, and subjected to center flexural loading until failure, see Figure. 2-28. The major goal of this work was to investigate the effect of varying the number of steel wire mesh layers and steel bars on the flexural strength of lightweight ferrocement composite plates. To supply the core material between the two skin ferrocement layers, one type of core material named (Styrofoam) was used, with a density of 32.4 kg/m^3 and a thickness of 20 mm. The results showed that lightweight ferrocement composite plates have superior deformation, ductility, and energy absorption properties. Welded meshes have a higher modulus and hence

stiffness, which results in smaller crack widths in the first region of the load-deformation curve.

(a) Casting of the bottom skin ferrocement layer.

(b) fixing the reinforcement with core material.

(c) Casting of the top skin ferrocement layer.

(d) Flexure test arrangements.

Figure. 2-28: Casting ,and testing steps [36].

Huang et al. in 2019 [37] were proposed new lightweight one-way multi-ribbed composite slab. The slab was divided into two layers, a precast composite layer and a cast-in-situ layer. The precast layer was made from a reinforced concrete base with embedded lightweight blocks (autoclaved aerated concrete blocks) on half of it. The second half of the block was exposed in order to create prominent steel truss shear connectors see Figure 2-29. The cast-in-situ layer was then constructed

by pouring on top of concrete, forming a composite slab. In this study, five specimens are examined, including one normal concrete cast-in-place slab and four composite slabs. The five specimens are (5700×1440×190) mm in size. All one-way slab specimens were tested under two-line flexural loading. The results showed that under fully composite conditions, the measured bearing capacity of the specimens reached more than 70% of the theoretical calculation strength. The overall performance was acceptable. The failure mechanisms of the composite slab specimens were similar to those of a normal concrete slab in terms of crack and deflection propagation. Also, the ductility was fairly good.

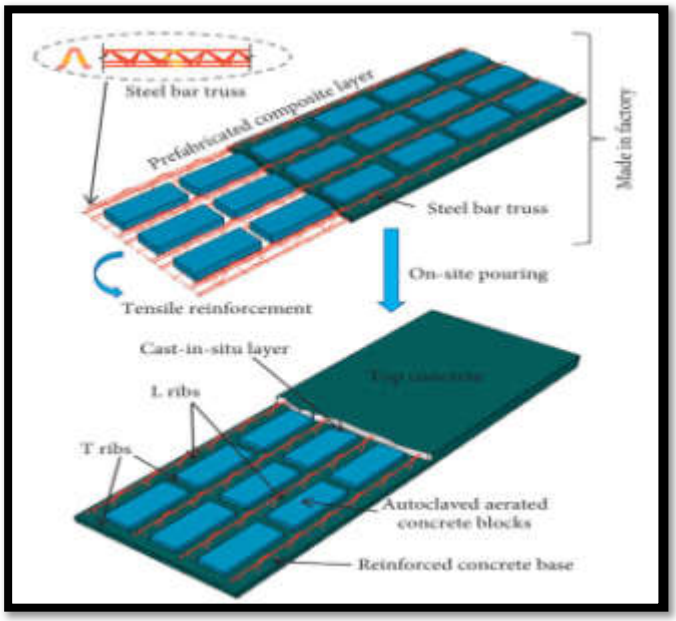

Figure 2-29: Proposed lightweight multi-ribbed composite slabs[37].

2.5 Concluded Remarks

From previous researches, it is possible to conclude that:

1. Applying a concrete layer on top of the jack arch slab is effective in increasing its strength.

2. Provided two-x-bracing welded at the end of the slab corners of the jack arch slab perform well when subjected to lateral loads.
3. The increase in the number of wire mesh layers and panel thickness increased the load-bearing capacity of ferrocement panels.
4. The ferrocement precast panels achieves the best composite combination of precast and cast-in-situ systems.
5. The failure mode of the sandwich components indicated ductile and composite behavior, transforming a brittle failure of material (aerated concrete) into a ductile manner when using the ferrocement encasements.
6. Using steel wire or steel truss as shear connectors in slab enhanced overall performance of slabs.

2.6 Research Gap Significant

Previous research indicated that the topic of investigations into the behavior of ferrocement–brick composite jack-arch slabs under flexural loading has not been adequately covered. The following parameters, for instance, are to be investigate:

1. Behavior of jack-arch slabs construct with different bricks (solid clay bricks and perforated clay bricks), cellular concrete blocks units (thermostone), and gypsum mortar.
2. The structural behavior of a ferrocement–brick composite jack arch slab composes of precast layers of ferrocement composites with solid bricks, perforated bricks, and cellular concrete blocks.
3. The behavior of ferrocement sandwich composite jack arch slabs make of two layers of ferrocement composites with styropor and cellular concrete block units as core material.

CHAPTER THREE: EXPERIMENTAL WORK

3.1 Introduction

This chapter describes objectives of the experimental work, the properties and tested results of all materials used in this study. It also includes the processing of details and manufacturing all specimens, equipment used during experimental work, and testing procedures. The experimental work for the study is conducted in the construction laboratory at University of Misan in Engineering College.

3.2 Materials Properties

3.2.1 Clay bricks

Clay bricks are the most widely employed type of brick in jack arch slab construction. According to Iraqi specifications (IQS 25-1993) [38], its standard dimensions are (240×115×75) mm. The bricks are tested the construction laboratory at University of Misan in college of engineering according to (IQS 24-1989) [39], as shown in the Figure 3-1 and the results of the tests are shown in Table 3-1.

Table 3-1:Clay bricks properties.

Specimen Type		Solid Bricks	Perforated Bricks	Limit of IQS No.25 /1988 [Class C]
Perforated [%]		0	24.44	25% Max
Density [kg/m^3]		1500	1207	-
Dimension Test [mm]		233.00×113.00×72.00	235.20×114.63×73.46	L*, W* =± 3% T*= ± 4 %
Average Water Absorption [%]	10 units	25	22	26
	1 units	25	23	28
Average Compressive Strength [MPa]	10 units	9	7	9
	1 units	8	6	7
Modulus of Rupture [MPa]		2.0	1.2	-
Efflorescence		Light	Light	-

*L= Length, W= Width, T= Thickness

(a) Dimensions test.

(b) Water absorption test.

(c) Efflorescence test.

(d)Compressive strength test.

(e) Modulus of rupture test.

(f) Density test.

Figure 3-1: Clay bricks test.

3.2.2 Gypsum mortar

The gypsum mortar is a mixture of gypsum and water. The gypsum mortar is tested according to Iraqi Reference guide (1042-2011) as shown in Figure 3-2. The results of the tests are shown in Table 3-2.

Table 3-2: Gypsum mortar properties.

Property	Test Result	Limit of IQS No.28/2010 [40]
Fineness [%]	5	8 % Maximum
Setting Time [Minute]	13	[8-25] (for jack arch using 15 max)
Compressive Strength [MPa]	3	3 [MPa] Minimum
Modulus of Rupture [MPa]	0.7	-
Gypsum Water Ratio	0.39	-

(a) Fineness test.

(b) Gypsum water ratio test.

(c) Setting time test.

(d) Compressive strength test.

(e) Modulus of rupture test.

Figure 3-2: Gypsum mortar tests.

3.2.3 Cellular concrete blocks

Cellular concrete blocks (thermostone) are a type of lightweight precast cellular concrete block. It is used in construction due to their ability to provide speed in construction time, thermal insulation, and lightweight. Its mechanical and physical properties are tested according to Iraqi Reference guide (810-2009) [41] as shown in the Figure 3-3. The results of the tests are listed in Table 3-3. The results satisfy Iraqi standards (IQS 1441-2013) [42]. The cellular concrete block units are cut into a prism of (200×100×100) mm to make the necessary measurements for the ferrocement sandwich and ferrocement composite slab.

Table 3-3: Mechanical and physical properties of cellular concrete blocks.

Dimension Test	Standard Dimension [mm]	Test Result [mm]	Limit of IQS 1441/2013	
Length	600	+2	± 3 mm for any dimension	
Height	200	-0.5		
Thickness	100	+ 1		
Specimen [mm]	Average weight for 2 cubes [kg]	Average volume for 2 cubes [m^3]	Density [kg/m^3]	Class according to Limit of IQS 1441/2013
(100×100×100)	0.51	0.00095	536.80	0.50
	Compressive strength [MPa]			Limit of IQS 1441/2013
	One unit	2.16		1.60
	Average for two cubes	2.20		2
600×200×100	Modulus of rupture [MPa] average for two unit			-
	0.8			

(a) Dimensions test.

(f) Density test.

(d) Compressive strength test.

(e) Modulus of rupture test.

Figure 3-3: Cellular concrete blocks tests.

3.2.4 Flexural bonding strength

The flexural bond strength between solid clay brick, perforated clay brick, cellular concrete block units and gypsum mortar is tested and calculated according to Khalaf in 2005 [43]. A new test procedure was proposed to determine the flexural bond strength between masonry units and mortar. In this procedure, bricks are manufactured from two brick units in a Z-shaped arrangement and three-point loading produced a flexural bond failure parallel to the bed joint, as depicted in Figure. 3-4 (a). Two assumptions are made for calculating values of the flexural bond strength (f_{fb}). The first is the distribution of bond stresses at the brick-mortar interface, which is a linear stress distribution, see Figure. 3-4 (b). The second type of stress distribution is the parabolic, see Figure. 3-4 (c). In this study, flexural bond strength values based on linear stress distribution assumption are determined by using equation 3-1, while those for parabolic stress distribution assumption are obtained by using equation 3-2. The results of the tests of flexural bond strength between solid clay brick, perforated clay brick, cellular concrete block units and gypsum mortar are seen in Figure. 3-5 and are listed in Table 3-4.

$$f_{fb} = \frac{(0.5l_b^2 - l_b t_{bar} + 0.5t_{bar}^2)\mathrm{P} + (0.75l_b^2 - 1.25l_b t_{bar} + 0.5t_{bar}^2)W}{(0.333l_{mj}^2 w_b)(1.5l_b - t_{bar})} \quad 3\text{-}1$$

$$f_{fb} = \frac{(0.5l_b^2 - l_b t_{bar} + 0.5t_{bar}^2)\mathrm{P} + (0.75l_b^2 - 1.25l_b t_{bar} + 0.5t_{bar}^2)W}{(0.42l_{mj}^2 w_b)(1.5l_b - t_{bar})} \quad 3\text{-}2$$

Where:

f_{fb} = Flexural bonding strength in Mpa.

l_b =Length of brick unit in mm.

l_{mj}= Length of mortar joint in mm.

P =Failure load in Newton.

t_{bar} =Thickness of steel bar in mm.

W =Weight of brick in Newton.

w_b =Width of brick unit in mm.

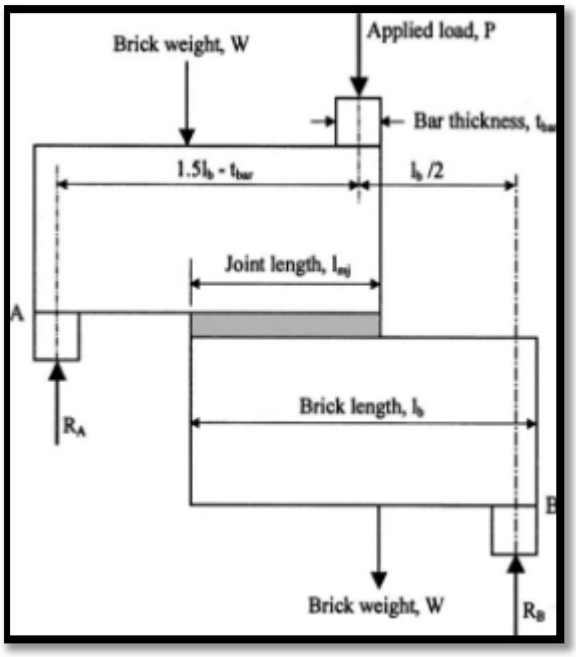

(a) Z-shaped specimen showing applied forces and reactions.

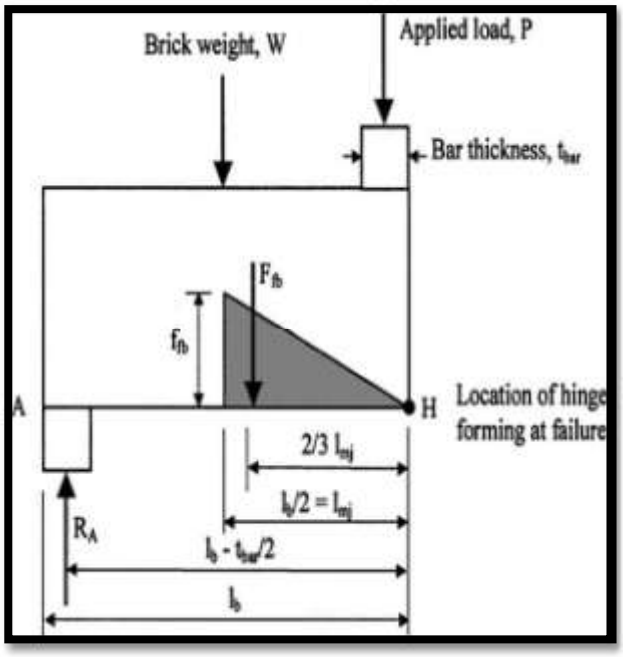

(b) Liner stress distribution.

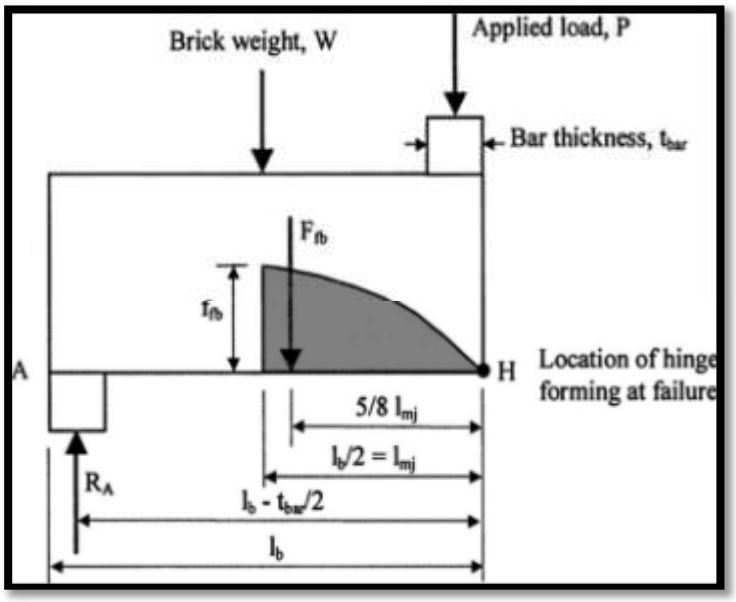

(c) Parabolic stress distribution.

Figure. 3-4: Free body diagram of flexural bonding test [43].

(a) Test set up of solid brick before failure.

(b) Solid bricks after failure.

(c) Perforated clay bricks after failure.

(d) Cellular concrete blocks after failure.

Figure. 3-5: Flexural bonding strength test.

Table 3-4: Results of flexural bonding strength according to Khalaf [43].

Specimen Type	Test Result	
	Average (Two Samples) Flexural Bond Strength by Linear Stress Distribution[MPa]	Average (Two Samples) Flexural Bond Strength by Parabolic Stress Distribution [MPa]
Solid Clay Bricks	0.321	0.253
Perforated Clay Bricks	0.410	0.324
Cellular Concrete Blocks	0.254	0.200

3.2.5 Cement

During the experimental program, all specimens are casted and plastered with ordinary Portland cement type (I). It is saved in a dry place to prevent contact with unfavorable weather conditions. Physical and mechanical properties for cement are tested in the construction laboratory at University of Misan in college of engineering according to Iraqi Reference guide (198-1990) [44], While chemical properties are tested in the construction laboratory at of Amarah technical institute according to Iraqi Reference guide (472-1993) [45]. Table 3-5 and Table 3-6 show the chemical composition and physical characteristics of cement, respectively. They satisfy Iraqi standards (IQS No.5/2019) [46].

Table 3-5: Chemical properties of cement.

Chemical Property	Content [%]	Limit of IQS No.5/2019
MgO	2.73	≤ 5 %
SO_3	2.07	≤ 2.8 %
Loss of Ignition	3.21	≤ 4 %
Insoluble Materials	1.05	≤ 1.5 %
Lime Saturation Factor	0.89	0.66 – 1.02

Table 3-6: Physical and mechanical properties for cement material.

Physical and Mechanical Properties	Test Result	Limit of IQS No.5/2019
Fineness [m^2/kg]	253.60	≥ 250
Setting Time Initial [Hour: Minute] Final [Hour: Minute]	 0 : 55 7 : 17	 ≥ 45 Minutes ≤ 10 Hours
Compressive Strength [MPa] 2- Days 28- Days	 18.0 35.1	 ≥ 10 ≥ 32.5

3.2.6 Styropor Panel

High-density compressed styropor panel (density of styropor 13kg/m^3) are used. The panels are (2000×1000×100) mm in size. The styropor panel are cut into

a prism of (200×100×100) mm to the measurements necessary to make the ferrocement sandwich composite slab see Figure. 3-6.

Figure. 3-6: Styropor prism of (200 ×100 ×100)mm.

3.2.7 Fine aggregate

Locally available natural silica sand is employed in ferrocement and plastering mix as fine aggregate. Its grading is tested according to Iraqi standards (IRG No.30/1984) [47] . The results are satisfy Iraqi standards (IQS No.45/1984) [48] as shown in Table 3-7.

Table 3-7: Grading test result of fine aggregates.

Sieve Size [mm]	Cumulative Retained [%]	Cumulative Passing [%]	Limit of IQS No.45/1984- Zone No.2
10 [mm]	0	100	100
4.75[mm]	0	100	90-100
2.36 [mm]	10	90	75-100
1.18 [mm]	16	84	55-90
600 [Micron]	45	55	35-59
300 [Micron]	72	28	8-30
150 [Micron]	94.5	5.5	0-10
Material Finer Than 75 Micron	1.1		5 % Max
Fineness Modulus	2.375		[2.3-3.1] ASTM C33M/13 [49]

3.2.8 Water

In this experimental study, drinking water is used for mixing all the cement and gypsum mortar, as well as curing specimens and other testing for the materials. It satisfied the Iraqi standard (IQS 1703/2018) [50].

3.2.9 Welded square wire mesh

As reinforcement for ferrocement precast panels, ferrocement composite brick and sandwiched slabs, a locally available welded steel square wire mesh with a 1.0 mm wire diameter and 12.5 mm spacing is used. The mesh is tested according to the report of ACI Committee 549 [51], which represents a design guide for the construction and repair of ferrocement. The test specimens are made by immersing both ends of a rectangular coupons of mesh in mortar for a length at least equal to the sample's width. The mortar-immersed ends work as gripping surfaces. The gripping is reinforced by many layers of square steel mesh larger than number of mesh that represent the free area of the mesh tested. The number of layer was used for samples for the test are five layers. Yield strain of tested mesh reinforcement is taken as the strain at the intersection of the best straight-line fit of the initial portion of the stress-strain curve and the best straight-line fit of the yielded portion of the stress-strain curve, as shown in Figure 3-7. The test sample is represented by the free area of the mesh see Figure. 3-8. The results of test are listed in Table 3-8 and seen in Figure. 3-9. Modulus of elasticity (E_r) is calculated according to equation 3-3) below:

$$E_r = \frac{\sigma_{ry}}{\varepsilon_{ry}} \qquad 3\text{-}3$$

Where:

$E_r = Modulus\ of\ elasticity\ [GPa]$, $\sigma_{ry} =$ Yield stress [MPa], ε_{ry} Yield strain

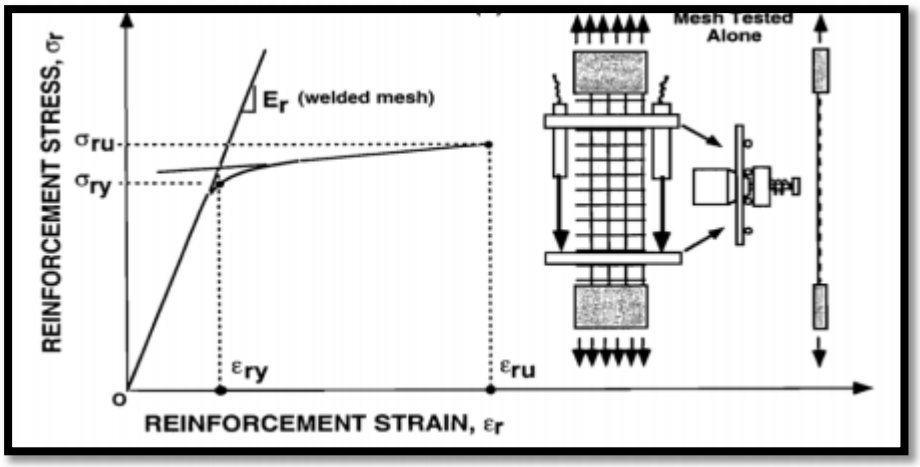

Figure 3-7: Schematic description of mesh tensile test sample and corresponding stress-strain curve [10].

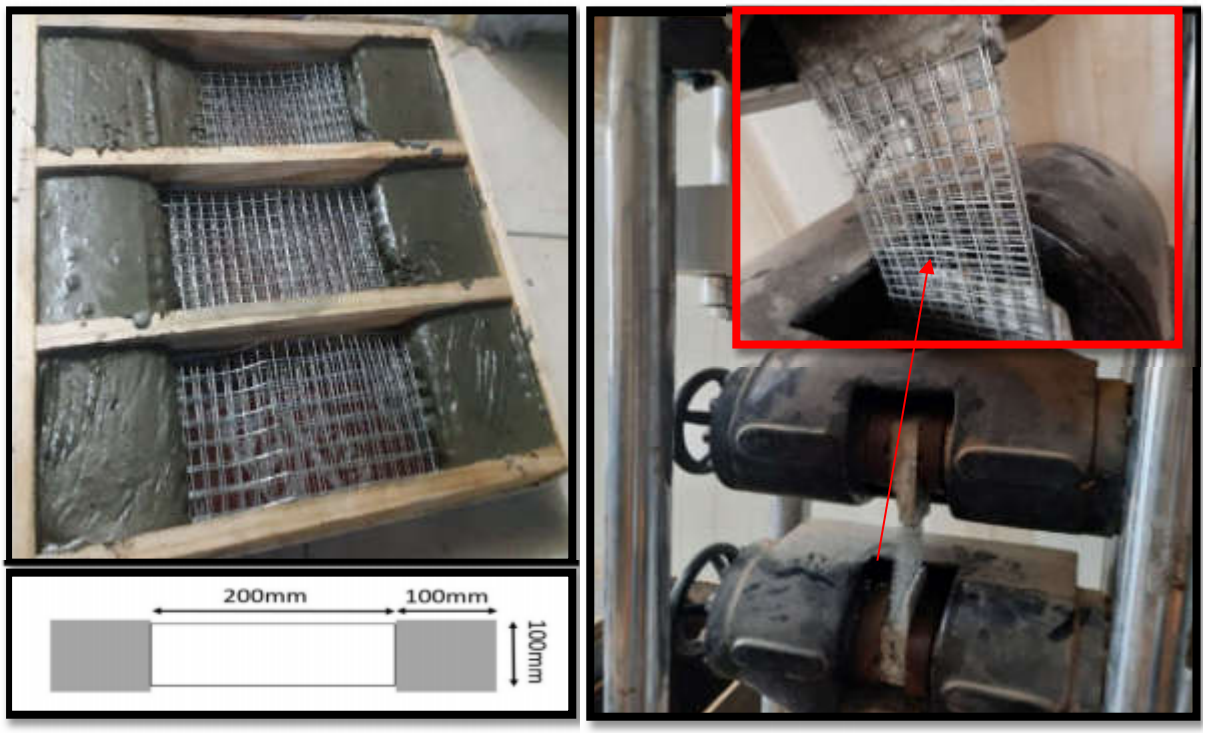

(a) Wire mesh samples with grips.

(b) Test set up and failure of sample.

Figure. 3-8: Details for the steel-welded wire mesh coupons test.

Table 3-8:Welded square steel wire mesh testing results.

Specimens Symbol	Yield Stress [MPa]	Ultimate Stress [MPa]	Modulus of Elasticity [GPa]
W1	470	630	87.037
W2	448	633	89.600
W3	455	610	92.857
Average	457.667	624.333	89.831

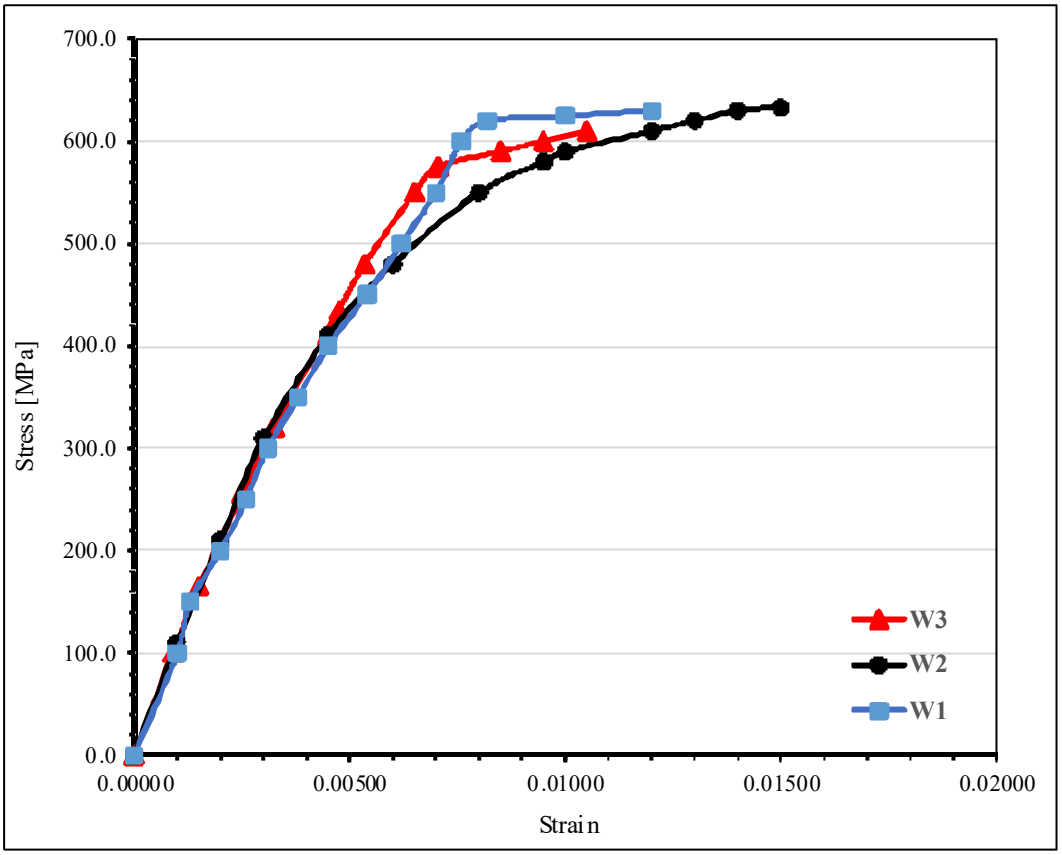

Figure. 3-9: Stress-strain curves for tested steel-welded wire mesh.

3.2.10 Superplasticizer

Sika viscocrete-5930 L is a high-range water-reducing and superplasticizer admixture for concrete and mortar using Sika viscocrete polycarboxylate polymer technology (3rd Generation. It is used in the current study to increase workability by

reducing the water-to-cement ratio and therefore retaining high strength of cement mortar. Product data sheets are attached in appendix A.

3.3 Trail Mixes

Different mixes ratio are cast in this experimental program to produce a flowable, and high-strength cement mortar as listed in Table 3-9 and shown in Figure. 3-10 . The targeted mortar mixes were chosen to get the highest mortar compressive strength. The main parameters were changed W/C, C/S, and superplasticizers. The mortar compressive strength is conducted according to (ASTM C 109-13) [52] on three standard mortar cubes with dimensions of (50× 50× 50) mm for each age of test. The modulus of rupture is conducted for three prisms of (160×40×40) mm according to ASTM C 348-14 [53]. The modulus of rupture are calculated according to equation3-4).

Table 3-9: Trail mixes proportions with tested results.

Trail Mix.	W/C	C:S	S.P/C (%)	f_{cu} (MPa) 7 days	f_{cu} (MPa) 28 days	f_r (MPa) 28 days
T-M-1	0.27	1:1.5	1.66	33.9	46.86	9.84
T-M-2	0.3	1.1.5	1.66	40.6	60.96	10.73
T-M-3	0.3	1:2	1.25	25.55	35.56	9.2
T-M-4	0.28	1:1.5	1.9	36.85	59	10.7
T-M-5	0.34	1:1.5	0.5	36.7	49.9	8.4
T-M-6	0.33	1:1.5	1	31.8	42.5	8.4
T-M-7	0.27	1:1	1	39.64	68	10.76
T-M-8	0.28	1:1	0.7	49.6	60.8	9.6
T-M-9	0.3	1:1.25	1	31.65	57.4	8.26
T-M-10	0.25	1:1.25	1.8	52.8	59.8	11.39
T-M-11	0.29	1:1	0.6	58.3	63	6.9
T-M-12	0.49	1:2	0	26.86	30.2	5.97
T-M-13	0.5	1:2	0	24.85	35.7	7.1
T-M-14	0.29	1:1.5	2	25.9	35.2	9.7
T-M-15	0.28	1:1.25	1	47.9	59	8.4
T-M-16	0.32	1:2.25	1.7	39.88	50	9.9
T-M-17	0.295	1:1.75	1.3	34.4	44.6	8.6

$$f_r = \frac{3PL}{2bd^2} \qquad 3\text{-}4$$

Where:

$f_r = modulus\ of\ ruptuer\ [MPa], P = Failure\ load[N],$

$L = Distance\ between\ supports\ [mm], b = Width\ of\ sampels[mm],$

$d = Depth\ of\ sampels\ [mm].$

Figure. 3-10: Mix used for casting ferrocement precast panels, ferrocement sandwiched and composite brick slab specimens.

For plastering purposes, cement mortar is employed on the bottom face of the jack arch slab. The cement-to-sand ratio was 1:2, with a water-to-cement ratio of 0.5. At age 28 days, the average compressive strength and flexural strength of the cement mortar are 35.7 and 7 MPa, respectively.

For casting ferrocement precast panels, and ferrocement sandwiched and composite brick slab specimens. the water and sand to cement weight ratios are chosen to be 0.27 and 1.0, respectively. Sika viscocrete 5930L IQ is used as a high-range water reducer. The superplasticizer dosage used is 1% of the total cement weight. The average compressive and flexural strengths the cement mortar are 68 MPa and 10.76 MPa, respectively. Figure. 3-11 shows testing of specimens under compression and flexural load.

(a) Tested specimens. (b) Compression test. (c) Flexural test.

Figure. 3-11: Samples testing of trail mix mortar.

3.4 Manufacturing of Specimens

The experimental program focusses on casting and testing one-way ferrocement composite brick and sandwich composite jack arch slab specimens.

twenty-eight samples are made for the current study. The samples are divided into three groups. The first group G_1 consist of five one-way brick jack arch slabs as control specimens. The second group G_2 consist of sixteen specimens, eleven of which are one-way ferrocement–brick composite jack arch slab specimens, while the remaining five specimens are precast panels. The third group G_3 includes seven specimens of ferrocement sandwich composite jack arch slabs.

Five samples of G_1 are fabricated using perforated, solid clay bricks, and cellular concrete blocks with a workable gypsum mixture to bind units together and fill gaps between them. Cement mortar as plastering of 10 mm in thickness is applied on the bottom face of the specimens. Cement mortar as plastering has a compressive strength of (50×50×50) mm cubes and prisms of (160×40×40) mm with a flexural strength of 35.7 MPa and 7 MPa, respectively. After 28 days of plastering five samples with cement mortar, a white painting layers is applied over the plastering layer to prepare the specimens for testing and to obtain a clear view of the cracks during the test. The main variables that are considered for these samples are span length (600-800) mm, camber height (30) mm, and types of brick (solid clay bricks, perforated clay bricks, cellular concrete blocks (thermostone)) use in construction of specimens to show their effects on the structural behavior of the jack arch slab. Table 3-10 summarizes G_1 specimens details. Figure. 3-12 shows the construction process of jack arch G_1 specimens.

Table 3-10: Jack arch slab specimens details.

Group Name.	No.	Specimens Symbol	Span Length [mm]	Width [mm]	Camber Height[mm]	Type of Bricks Used
G_1	1	Js-60-0	600	320	0	Solid brick
	2	Js-80-0	800	320	0	Solid brick
	3	Js-80-3	800	320	30	Solid brick
	4	Jv-60-0	600	320	0	Perforated brick
	5	Jc-60-0	600	320	0	Cellular concrete block

(a) Clean bricks.

(b) Make a mortar.

(c) Construct brick arch.

(d) Apply gypsum mortar on top face.

(e) Apply a plaster layer on bottom face.

(f) All samples after plastering.

(g) Samples after-painting and symbols.

Figure. 3-12: Steps for preparing jack arch slab G_1 specimens.

Sixteen one-way specimens which made ferrocement–brick composite jack arch slab are the second group G_2. The first five samples are made of precast

ferrocement panels with varying span lengths of 600, 800, and 1000 mm, and varying camber heights of (0, and 30) mm, as well as varying numbers of steel wire mesh layers of (2 and 4) layers. The other eleven specimens are precast ferrocement slabs composed of solid bricks, perforated bricks, cellular concrete blocks (200×100×100) mm units, and workable gypsum mortar that binds units together and fills gaps between them. The important variables are the different span lengths of 600, 800, and 1000 mm, the different camber heights of (0, and 30) mm, and the different numbers of steel wire mesh layers of (2, 4, and 6 layers). Figure. 3-13 shows the cross-section of specimens, and Figure. 3-14 depicts the manufacturing process for specimens. The thickness of all precast panels is constant at 15 mm. After 28 days and before the testing day, all specimens are cleaned, and painting by a white layer. Table 3-11 highlights all of the specimens' characteristics and main variables.

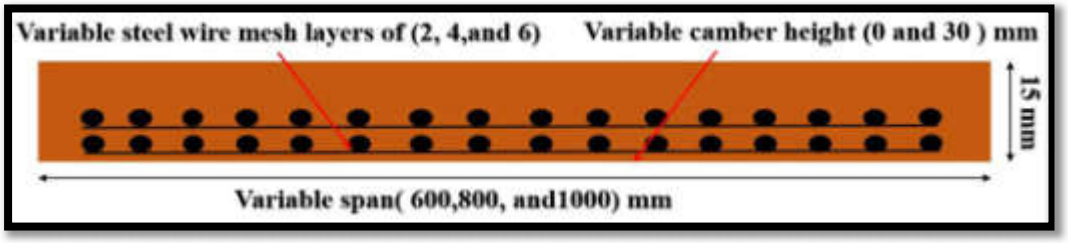

(a) Precast ferrocement layers.

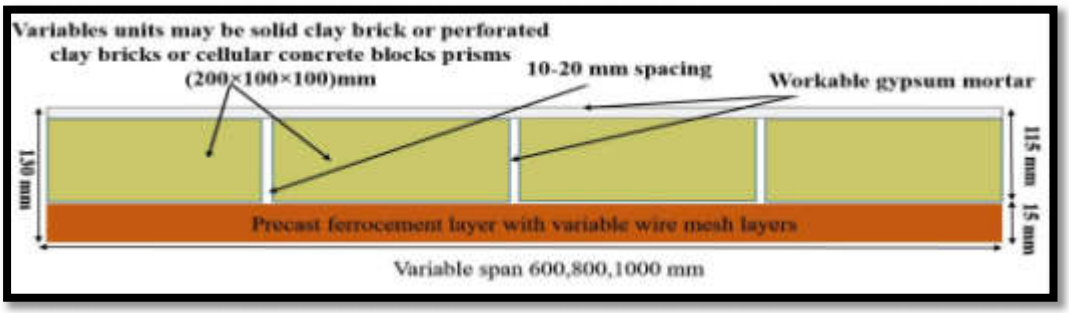

(b) Ferrocement composite brick slab specimens.

Figure. 3-13: Cross section details for G_2 specimens.

(a) Prepare mold .

(b) Apply cement mortar.

(c) Wire mesh layers.

(d) Precast panels.

(e) Layout unit of brick.

(f) Apply mortar.

(g) After painting all specimens and symbols.

Figure. 3-14: Steps for made G_2 specimens.

Table 3-11: Details of ferrocement brick slab specimens.

Group Name	No.	Specimens Symbol	No. of Wire Mesh Layers	Volume Fraction [%]	Span Length [mm]	Width [mm]	Camber Height [mm]	Composite Material Type
G_2	1	P-2-60-0	2	1.67	600	320	0	Precast panel only
	2	P-4-60-0	4	3.35	600	320	0	Precast panel only
	3	P-4-80-0	4	3.35	800	320	0	Precast panel only
	4	P-4-80-3	4	3.35	800	320	30	Precast panel only
	5	P-4-100-0	4	3.35	1000	320	0	Precast panel only
	6	Cs-2-60-0	2	1.67	600	320	0	Precast panel + solid brick
	7	Cs-4-60-0	4	3.35	600	320	0	Precast panel + solid brick
	8	Cs-4-80-0	4	3.35	800	320	0	Precast panel + solid brick
	9	Cs-4-80-3	4	3.35	800	320	30	Precast panel + solid brick
	10	Cs-4-100-0	4	3.35	1000	320	0	Precast panel + solid brick
	11	Cs-6-100-0	6	5.00	1000	320	0	Precast panel + solid brick
	12	Cs-6-100-3	6	5.00	1000	320	30	Precast panel + solid brick
	13	Cv-4-60-0	4	3.35	600	320	0	Precast panel + perforated brick
	14	Cv-4-80-0	4	3.35	800	320	0	Precast panel + perforated brick
	15	Cc-4-60-0	4	3.35	600	320	0	Precast panel + cellular concrete blocks
	16	Cc-4-80-0	4	3.35	800	320	0	Precast panel + cellular concrete blocks

The volume fraction relationship is the ratio of volume of wire mesh (reinforcements) to the volume of composite see equation 3-5 [10]. When the same square or rectangular wire mesh is used the volume fraction can be calculated from equation 3-6) [10].

$$V_r = \frac{V_{\text{reinforcement}}}{V_{\text{composite}}} \qquad 3\text{-}5$$

Where:

V_r = volume fraction.

$V_{reinforcement}$ = volume of wire mesh (reinforcements).

$V_{composite}$= volume of composite (cement mortar).

$$V_r = \frac{N\pi d_w^2}{4h}\left[\frac{1}{D_l} + \frac{1}{D_t}\right] \qquad 3\text{-}6$$

Where:

$N = Number\ of\ mesh\ layers,\ d_w = Daimeter\ of\ mesh\ wire, h = Thickness,$

$D_l = Distance\ center\ to\ center\ between\ longitudinal\ wires,$

$D_t = Distance\ center\ to\ center\ between\ transverse\ wires.$

The remaining seven samples are from the third group G_3 of precast ferrocement sandwich composite jack arch slabs with different span lengths (800, and 1000) mm, depth of section (130, and 160) mm, and core materials (cellular concrete blocks, and styropor) with four layers of wire mesh. The thickness of the ferrocement layers remains constant in the top and bottom layers at 15 mm. A z-shaped steel wire of 3 mm in diameter is used as a shear connector in some specimens to increased interaction between the top and the bottom layers. Figure. 3-15 shows the schematics and the locations of shear connectors . All samples are cast in cement mortar as one unit. Figure. 3-16 shows the cross-section for G_3 specimens, and Figure. 3-17 depicts the manufacturing steps for specimens. After 28 days and before the testing day, all specimens are cleaned, and a white layer is painted over the surface. All of the specimens' characteristics and main variables are highlighted in Table 3-12.

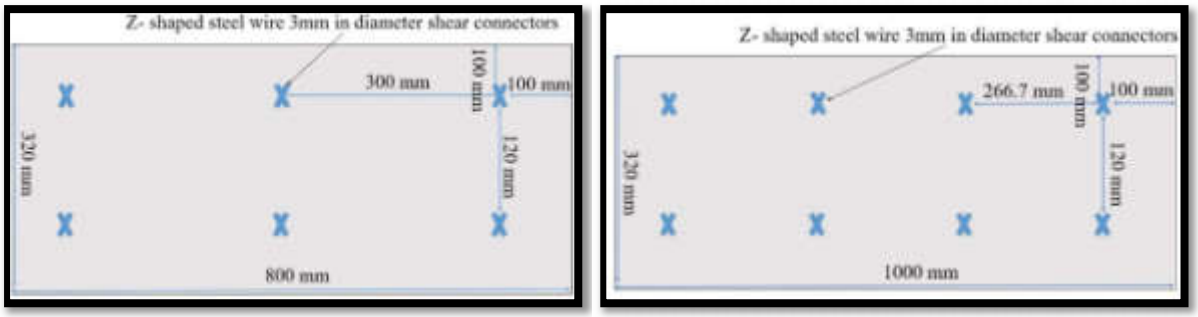

(a) Specimen span (800) mm. (b) Specimen span (1000) mm.

(c) Shear connecters at bottom. (c) Shear connecters at top.

Figure. 3-15: Schematics and location of shear connecters.

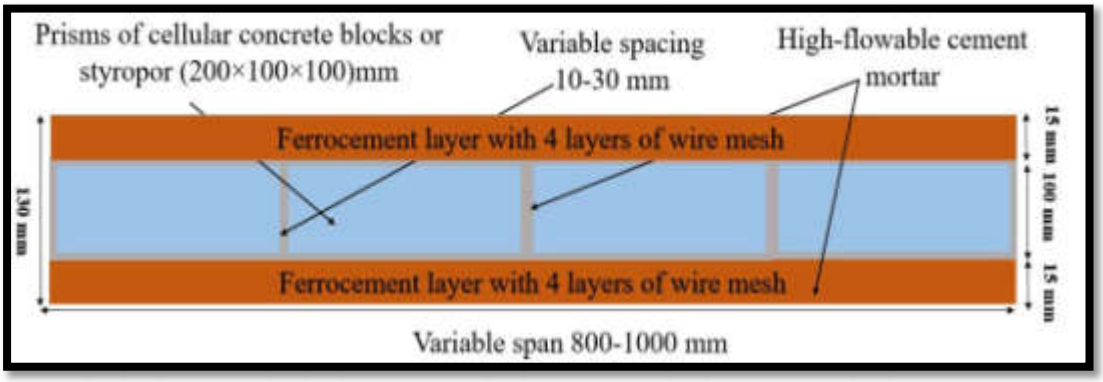

Figure. 3-16: Cross section details for ferrocement sandwich G_3 specimens.

(a) Prepare mold and reinforcement cage for bottom layer.

(b) Layout prisms of styropor or cellular concrete block .

(c) Apply reinforcement cage for top layer.

(d) Apply mortar.

(e) Samples after open molds.

(f) Samples painting and symbols.

Figure. 3-17: Steps for made ferrocement sandwiched slab G_3 specimens.

Table 3-12: Details of ferrocement sandwiched slab specimens.

Group Name	No.	Specimens Symbol	No. of Wire Mesh Layers	Volume Fraction [%]	Span Length [mm]	Width [mm]	Section Depth [mm]	Core Material Type with Notes
G_3	1	Sc-4-80-0	4	3.35	800	320	130	4 layers top and bottom without shear connectors with cellular concrete blocks
	2	SHc-4-80-0	4	3.35	800	320	130	4 layers top and bottom with shear connectors ,and cellular concrete blocks
	3	Sp-4-80-0	4	3.35	800	320	130	4 layers top and bottom without shear connectors with styropor
	4	SHp-4-80-0	4	3.35	800	320	130	4 layers top and bottom with shear connectors ,and styropor
	5	SHc-4-100-0	4	3.35	1000	320	130	4 layers top and bottom with shear connectors, and cellular concrete blocks
	6	SHp-4-100-0	4	3.35	1000	320	130	4 layers top and bottom with shear connectors ,and styropor
	7	SDp-4-80-0	4	3.35	800	320	160	4 layers top and bottom with shear connectors ,and styropor

3.5 Testing Procedure

A three-point bending load (line load) is applied to all thirty-one specimens G_1, G_2, and G_3. A hydraulic jack with a capacity of 10 tons is used for testing slabs. The load is applied monotonically in equal increments and gradually increased at every load step. The slab specimen is supported on both sides by two steel rods. The deflection at mid-span is recorded using a dial gauge with a capacity of 50 mm. The

cracks are observed using a crack microscope. A calibrated load cell is used to measure the applied load at the mid-span of a slab. Figure. 3-18 depicts an image of the test setup, and Figure. 3-19 shows a plan of it.

Figure. 3-18: Flexural test set-up.

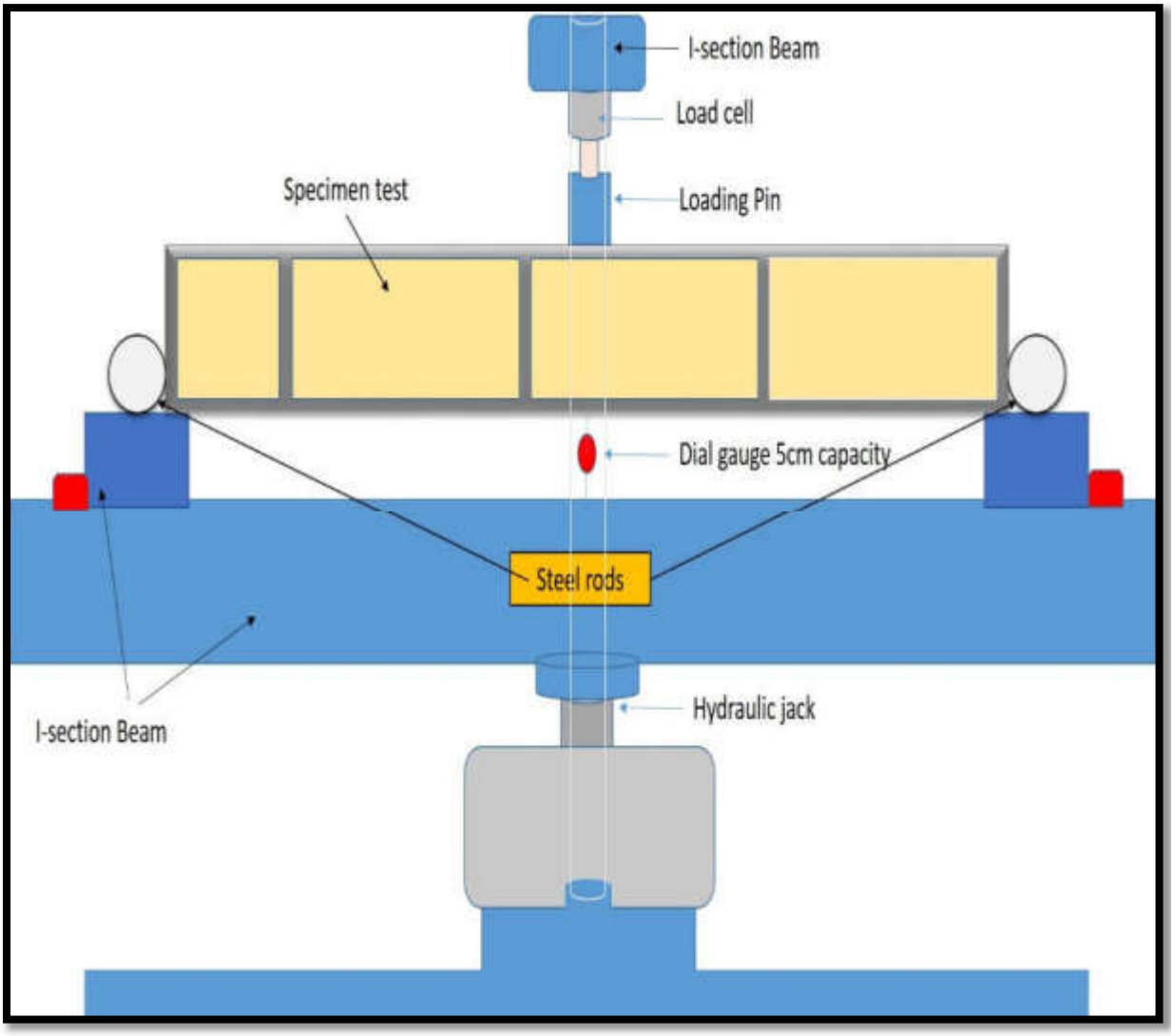

Figure. 3-19: A plan of flexural test set up.

CHAPTER FOUR: RESULTS ANALYSIS AND DISCUSSIONS

4.1 General

The main objectives of this study are to investigate the structural behavior of jack-arch slabs made of various bricks (solid clay bricks, perforated clay bricks, cellular concrete blocks (thermostone)), ferrocement slab panels, composite brick-ferrocement jack-arch slabs, and ferrocement sandwiched jack-arch slabs subjected to flexural three-point loading (line load).

The current study includes three groups of specimens. The first group G_1 consists of jack-arch slab specimens. The second group G_2 consists of the ferrocement panels and ferrocement composite slab specimens. The third group G_3 consists of ferrocement sandwiched slabs. The main variables considered in this study are span length of (600-800) mm, camber height of (0, and 30) mm, and brick types (solid clay bricks, perforated clay bricks, and cellular concrete blocks) used to indicate their effect on the structural behavior of the jack arch slab specimens G_1. As well as varying span lengths of (600, 800, and 1000) mm, varying camber heights of (0, and 30) mm, and varying numbers of steel welded wire mesh layers (2,4, and 6) layers, are used to illustrate their effect on the ferrocement panels and ferrocement brick composite slab specimens G_2. Also, various span lengths of (800 and 1000) mm, depth of sections of (130 and 160) mm, shear connector locations, and core materials (cellular concrete blocks and styropor) are used to demonstrate their influence on the ferrocement sandwich composite jack arch slab specimens G_3. The results of the tests are presented regarding the ultimate load, load-deflection at the slab's mid-span, ductility index, and failure mode.

4.2 Ultimate Load

4.2.1 Ultimate load for the first group specimens (G_1).

Ultimate load results for jack arch slab control specimens G_1 are shown in Table 4-1 and Figure 4-1. The effects of the type of bricks used in the construction of the arch slab on ultimate loads are studied by using three types of bricks. These are solid clay bricks, perforated clay bricks, and cellular concrete blocks for a span length of 600 mm. The results indicate that the specimen with perforation bricks Jv-60-0 has a greater ultimate loads than the specimens with solid clay bricks Js-60-0 and cellular concrete blocks Jc-60-0 by 37.4 and 41.07%, respectively. These results are due to the flexural bonding strengths between brick units and gypsum mortar being higher than those between cellular concrete block units as mentioned in the flexural bonding tests in previous chapter in section 3.2.4 and Table 3-4 . Also, the poor mechanical properties of cellular concrete blocks compared to clay bricks are the expected other reasons. To study the effect of span length on the ultimate loads of jack arch slab is considered for specimens made with solid clay bricks. The selected span is 600 and 800 mm. The results show a clear decrease in the ultimate loads when increasing the span length for solid clay brick specimens. The results show that when the span is increased from 600 to 800 mm for Js-80-0 the ultimate loads decreased by 37.96%. The effect of using camber on the ultimate loads of the jack arch slab is conducted on specimens. For this purpose, one camber of 30 mm is

Table 4-1: Ultimate load and weight results of G_1 specimens.

Group Name	No.	Specimens Symbol	Ultimate Load [kN]	Weight [kg]
G_1	1	Js-60-0	3.53	40
	2	Js-80-0	2.19	51
	3	Js-80-3	3.89	52
	4	Jv-60-0	4.85	33
	5	Jc-60-0	3.44	14

used for specimens made of solid clay bricks. The results show an increase in the ultimate loads for specimens when the camber is increased. Increasing camber from 0 to 30 mm for Js-80-3 improve ultimate loads by 77.62%.

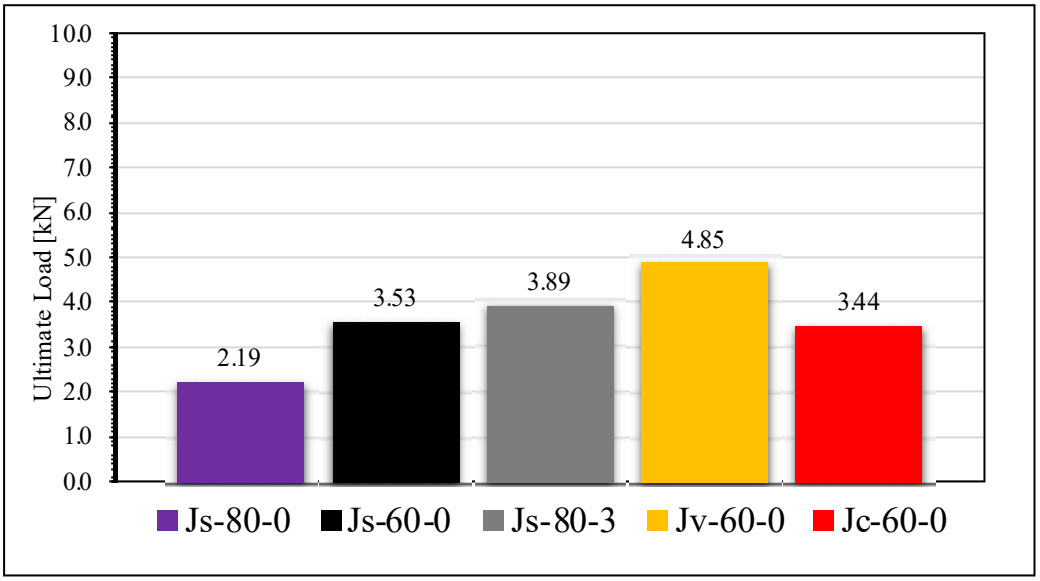

Figure 4-1: Ultimate loads results for jack arch control specimens G_1.

4.2.2 Ultimate load for the second group specimens (G_2).

Ultimate loads results for ferrocement precast and ferrocement composite-brick slab specimens G_2 are listed in Table 4-2 and depict in Figure 4-2 . The effects of the volume fraction on ultimate load strengths of precast ferrocement panels and ferrocement composite-brick slab specimens G_2 are discuss by using 2, 4, and 6 layers of steel wire mesh as mentioned in chapter three section 3.4 and Table 3-11. The results show that increasing the volume fraction by 100% for P-4-60-0 and Cs-4-60-0 increase the ultimate loads by 51.38, and 56.52, respectively. while increasing the volume fraction by 49.3% for Cs-6-100-0 increase the ultimate loads by 8.05%.

Table 4-2: Ultimate load and weight results of G_2 specimens.

Group Name	No.	Specimens Symbol	Ultimate Load [kN]	Weight [kg]
G_2	1	P-2-60-0	1.95	5.0
	2	P-4-60-0	2.95	5.2
	3	P-4-80-0	2.19	7.0
	4	P-4-80-3	2.43	7.8
	5	P-4-100-0	1.80	9.0
	6	Cs-2-60-0	4.86	48.0
	7	Cs-4-60-0	7.60	49.0
	8	Cs-4-80-0	6.27	57.0
	9	Cs-4-80-3	13.22	58.0
	10	Cs-4-100-0	5.46	68.0
	11	Cs-6-100-0	5.90	69.0
	12	Cs-6-100-3	9.36	71.0
	13	Cv-4-60-0	17.67	40.0
	14	Cv-4-80-0	16.87	51.0
	15	Cc-4-60-0	7.40	25.0
	16	Cc-4-80-0	4.65	33.0

The effects of the type of bricks used in the construction on the ultimate loads of ferrocement composite-brick slab specimens are studied by using three different types of bricks (solid clay bricks, perforated clay bricks, and cellular concrete blocks (thermostone)) for a span length of 600 and 800 mm. The results indicate that specimens made with clay bricks have higher ultimate loads than those made with cellular concrete blocks. Also, specimens made with perforated clay bricks have greater ultimate loads than specimens made with solid clay bricks. It can be seen that Cs-4-60-0 and Cv-4-60-0 have higher ultimate loads than Cc-4-60-0 by 2.7 and 138%, respectively. The specimens Cs-4-80-0 and Cv-4-80-0 have higher ultimate loads than Cc-4-80-0 by 34.84 and 262.80%, respectively. The specimens Cv-4-60-0 and Cv-4-80-0 have greater ultimate loads than Cs-4-60-0 and Cs-4-80-0 by 132.5 and 169.05%, respectively. These results are due to the cellular concrete block units have low mechanical properties and flexural bonding strength with gypsum mortar when compared to clay brick units, while perforated brick units and gypsum mortar having higher flexural bonding strengths. The presence of holes in perforated clay

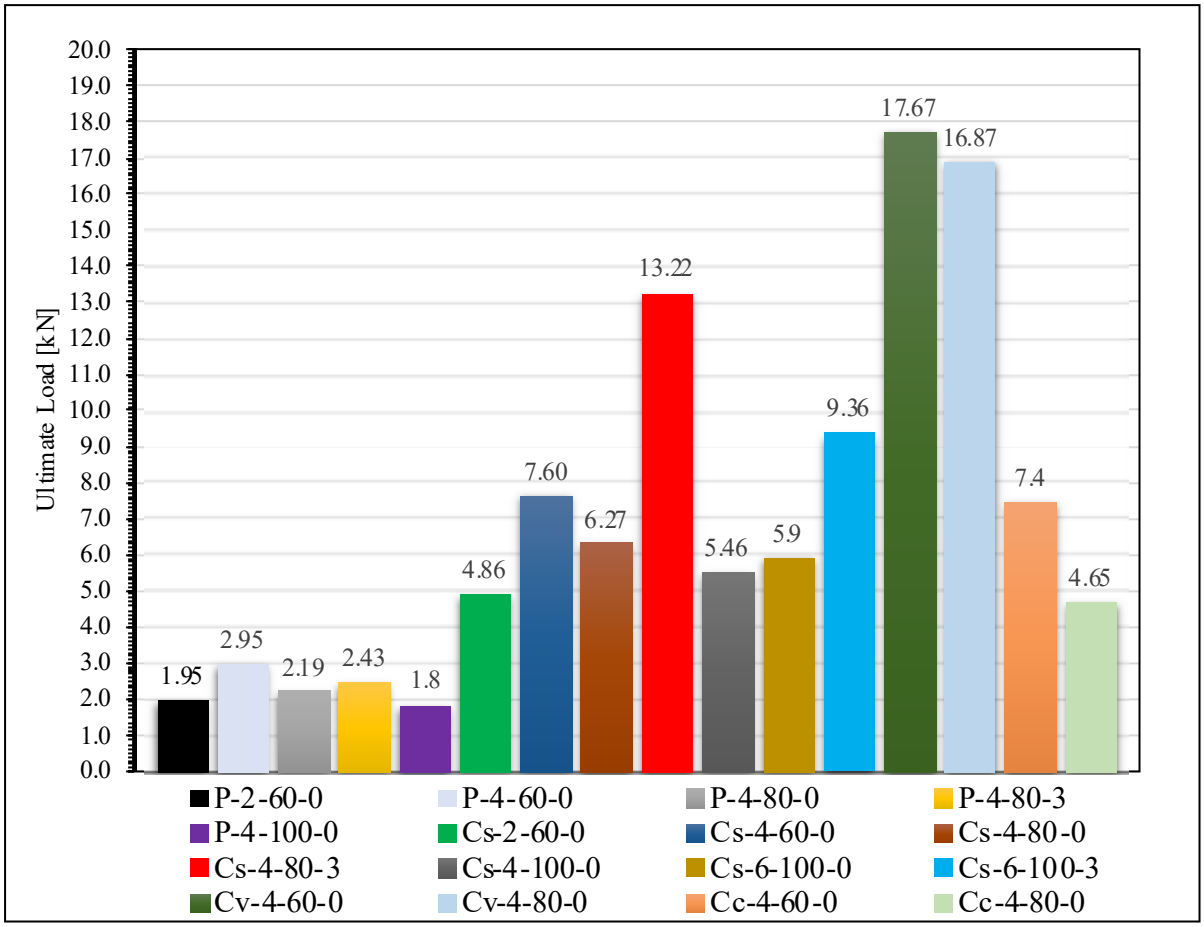

Figure 4-2: Ultimate loads results for ferrocement composite-brick slab specimens G_2.

bricks help to increase the connection between bricks and mortar. This leading improvement of bonding strength, hence max flexural strength can obtain compared with other types of bricks. The effect of span length of this group are considering using three different lengths 600, 800, and 1000 mm, to show their effect on the ultimate loads of ferrocement precast and ferrocement composite-brick slab specimens. The results show a decrease in the ultimate loads when increasing the span length for both precast and ferrocement composite-brick slab specimens. When the span is increased from 600 mm to 800 mm for P-4-80-0, Cc-4-80-0, Cv-4-80-0,

and Cs-4-80-0, the ultimate loads decrease by 25.76, 37.16, 4.52 and 17.50%, respectively. When the span of P-4-100-0 and Cs-4-100-0 is increased from 800 mm to 1000 mm, the ultimate loads decrease by 17.8 and 12.92%, respectively. The effect of increasing camber height on the ultimate strength load of ferrocement precast and ferrocement composite-brick slab specimens is investigated. For this purpose, one camber of 30 mm is used for specimens made of span lengths of 800 mm ferrocement panel, 800 and 1000 mm ferrocement composite-solid brick slab specimens, as mentioned in the Table 3-11. The results show an increase in the ultimate loads for both types of specimens when the camber is increased. The results show that the increasing camber height by 30 mm at mid span for P-4-80-3, Cs-4-80-3, and Cs-6-100-3, lead to improve the ultimate loads by 10.95, 110.84, and 58.64%, respectively. In the comparison between the precast ferrocement panels and ferrocement composite brick slab specimens G_2 and the control jack arch specimens G_1, results show that Cs-2-60-0 and Cs-4-60-0 have higher ultimate loads than Js-60-0 by 37.68 and 115.30%, respectively. The specimen Cs-4-80-0 and Cs-4-80-3 have higher ultimate loads than the specimens Js-80-0 and Js-80-3 by 186.30 and 239.85%, respectively. Although the specimen Cs-4-100-0 and Cs-6-100-0 have a span greater than control specimen Js-80-0, they have higher ultimate loads than Js-80-0 by 149.31 and 169.40%, respectively. As well, although the specimen Cs-6-100-3 has a span greater than control specimen Js-80-3, it has higher ultimate load than Js-80-3 by 140.61%. The specimen Cv-4-60-0 has a higher ultimate load than the specimen Jv-60-0 by 264.33%. The specimen Cc-4-60-0 has a higher ultimate load than Jc-60-0 by 115.24%. Although the specimen Cc-4-80-0 has a span length greater than control specimen Jc-60-0, it has a higher ultimate load than Jc-60-0 by 35.25%. According to experimental test results, all-composite ferrocement slabs with solid and perforated clay bricks, as well as cellular concrete block specimens, have a higher ultimate loads than the control jack-arch slab specimens. This is due

to the precast ferrocement panel, which improve the slab's flexural strength. All precast panels have lower strength when compared to all other specimens because the depth section of them is very low at 15 mm, whereas the other specimens' depth was 130 mm. This cause a reduced lever arm, which cause a reduced flexural strength of the section.

4.2.3 Ultimate load for the third group specimens (G_3).

Ultimate loads results for ferrocement sandwiched slabs specimens G_3 are listed in Table 4-3 and shown in Figure 4-3. The effects of the type of core material used on the ultimate strength loads of ferrocement sandwiched slab specimens are studied by using two types of core materials, styropor and cellular concrete blocks sandwiched between two layers of ferrocement at spans of 800 and 1000 mm with and without shear connectors as mentioned in Chapter Three Section 3.4 and Table 3-12. The results indicated that specimens made with cellular concrete

Table 4-3: Ultimate Load and weight results of G_3 specimens.

Group Name	No.	Specimens Symbol	Ultimate Load [kN]	Weight [kg]
G_3	1	Sc-4-80-0	22.25	40
	2	SHc-4-80-0	28.84	41
	3	Sp-4-80-0	14.70	29
	4	SHp-4-80-0	21.09	30
	5	SHc-4-100-0	22.12	50
	6	SHp-4-100-0	20.84	35
	7	SDp-4-80-0	26.09	38

blocks have higher ultimate loads than those made with styropor. The results reveal that the specimens Sc-4-80-0, SHc-4-80-0, and SHc-4-100-0 have higher ultimate loads than the specimens Sp-4-80-0, SHp-4-80-0, and SHp-4-100-0 by 51.32, 36.75, and 6.14%, respectively. These results because cellular concrete block units have higher mechanical properties when compared to styropor. The effect of increasing span length is studied, and specimens with different span lengths are made, which

are (800 and 1000) mm, to show their effect on the ultimate loads of ferrocement sandwiched slab specimens made with styropor and cellular concrete blocks as core materials. The results show a decrease in the ultimate strength load when increasing the span length for both ferrocement sandwiched slab specimens made with styropor and cellular concrete blocks. The results show that when the span is increased from 800 to 1000 mm for SHc-4-100-0 and SHp-4-100-0, the ultimate strength load decrease by 23.3 and 1.19%, respectively. To study the effect of increasing section depth, specimens with different section depths are made, which are 130 and 160 mm,

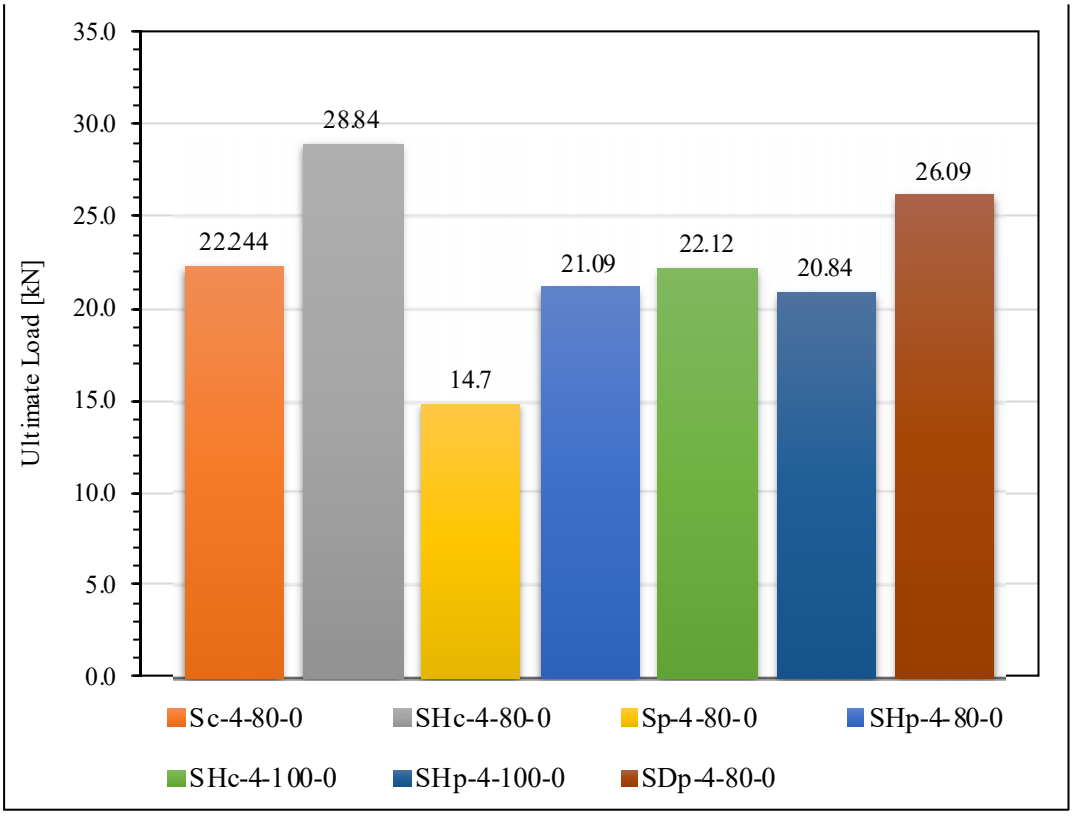

Figure 4-3: Ultimate strength loads results for ferrocement sandwiched slabs specimens G_3.

to show their effect on the ultimate loads of ferrocement sandwiched slab specimens made with styropor as the core material, as mentioned in Chapter Three Section 3.4 and Table 3-12. The results showed an increase in the ultimate loads when increase section depth of specimens. When the section depth of SDp-4-80-0 is increase from 130 to 160 mm, the ultimate load increased by 17.3%. Also, the effect of using a shear connector on the ultimate strength load of ferrocement sandwiched slab specimens made with styropor and cellular concrete as the core material is investigated. The results show that using shear connectors for SHc-4-80-0 and SHp-4-80-0 improve ultimate loads higher than Sc-4-80-0 and Sp-4-80-0 by 29.65 and 43.47%, respectively. This improvement because shear connectors improve interaction between the top and bottom ferrocement layers of specimens. In comparing the ferrocement sandwich slab specimens (G_3) with the control jack arch specimens (G_1), results show that the all specimens of (G_3) of span 800 mm have higher ultimate loads than the specimens Js-80-0 by ranges (571.23-1216.89 %). Although the specimens SHc-4-100-0 and SHp-4-100-0 have a span length 1000 greater than control specimen Js-80-0 800 mm, have ultimate loads higher than Js-80-0 by 863.01 and 851.56%, respectively. When compare between the ferrocement sandwich slab specimens (G_3) and ferrocement composite-brick slab specimens (G_2), the results show that the specimens Sc-4-80-0 and SHc-4-80-0 have higher ultimate loads than Cc-4-80-0 by 378.36 and 520.21%, respectively. According to the test results, all-ferrocement sandwich composite jack arch slab specimens have a higher ultimate strength than the control jack arch slab specimens. These results are due to ferrocement layers, which enhance the slab's flexural strength. Also, all-ferrocement sandwich composite jack arch slab specimens have a higher ultimate loads than ferrocement composite-brick slab specimens except Sp-4-80-0.

4.3 Load – Deflection Curves and ductility index

The ability of a material to resist plastic deformation under load is called ductility. The ratio of total displacement (Δu) to elastic limit displacement (Δy) is defined as the ductility index (μΔ) [54], [55]. The elastic limit deflection is the point at which strength behavior is assumed to change from elastic to plastic. The approach for calculating the ductility indices for each tested specimen in the current experimental study is based on Figure 4-4 [54], [55].

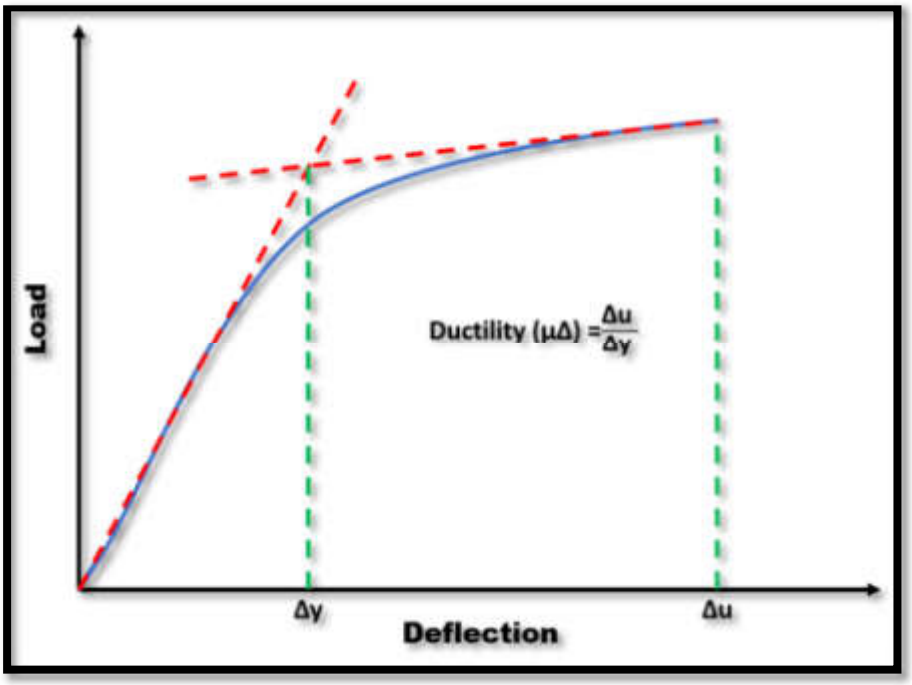

Figure 4-4: The ductility index calculation approach [54], [55].

4.3.1 Load – Deflection Curves and ductility index for specimens of (G_1)

The load deflection curves for the first group G_1 of jack arch slab specimens are shown in Figure 4-5. Figure 4-5 depicts the load-deflection curves of all five ja-

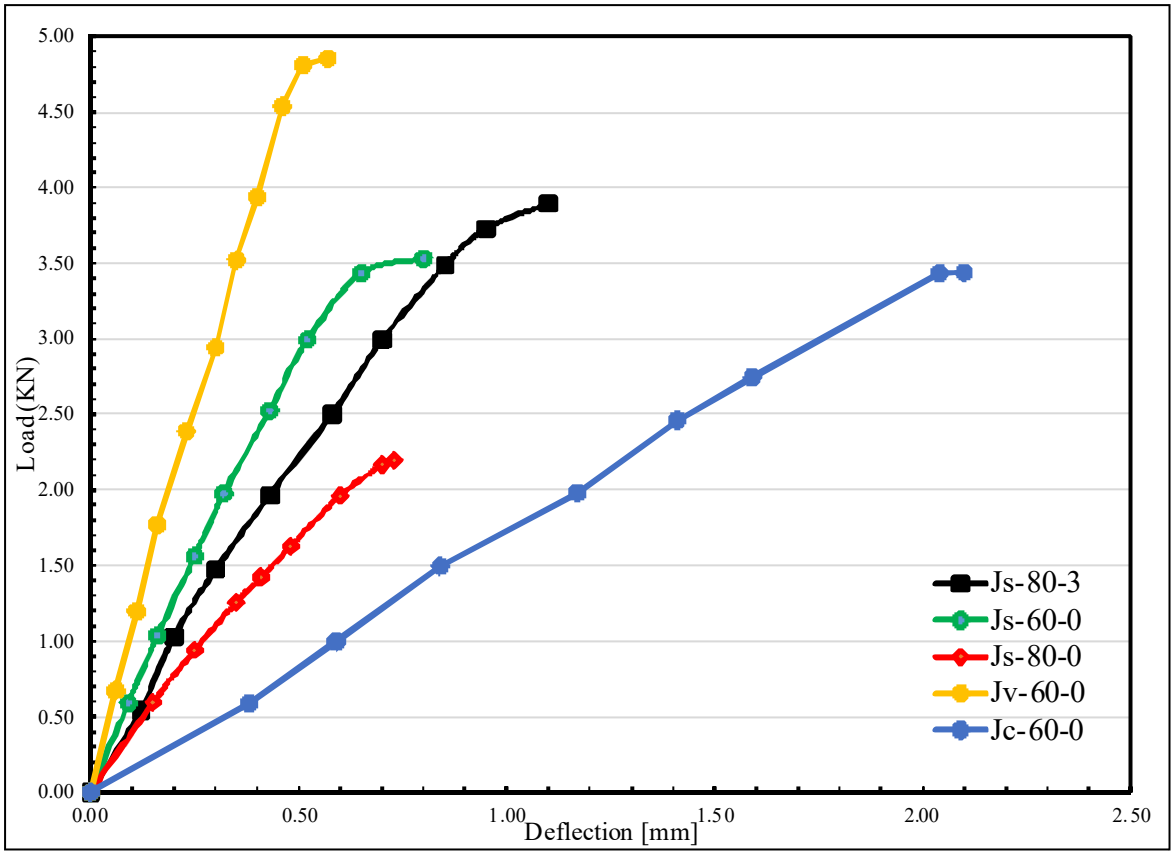

Figure 4-5: Load-deflection curves of G_1 specimens.

-ck arch slab specimens, Js-60-0, Js-80-0, and Js-80-3, Jv-60-0, and Jc-60-0. It can clearly show that the specimens made from perforated and solid clay brick behave approximately linearly until they reach their ultimate load. A sudden failure occurs after reaching ultimate loads. The load-deflection curve for the specimen Jc-60-0, which represents a specimen made with a cellular concrete block (thermostone block) and gypsum mortar that is widely used in recent years in the construction of jack arch slabs. From this figure, it can clearly show that the specimens behave approximately similar to the behavior of jack arch specimens made with solid and perforated clay bricks, where the behavior is linear until reaching their ultimate load. A sudden failure occurs after reaching the ultimate load. This linear behavior of jack-

arch slab specimens made with solid clay bricks, perforated clay bricks, and cellular concrete blocks bonded together using gypsum mortar is due to the fact that they are brittle materials and do not exhibit the ductility of ductile materials. From previous load-deflection curves, the specimen Jv-60-0 has a higher stiffness than the specimens Js-60-0, and Jc-60-0. The specimen Js-80-3 has a higher stiffness than Js-80-0.

Ductility index results for jack arch slab control specimens G_1 are shown in Table 4-4 and Figure 4-6 . The effects of the type of bricks used in the construction of the jack arch slab on the ductility index are studied by using three types of bricks, solid clay bricks, perforated clay bricks, and cellular concrete blocks (thermostone) for a span length of 600 mm. The results show that the specimen with solid bricks, Js-60-0 has a greater ductility index than the specimens with perforation clay bricks Jv-60-0 and cellular concrete blocks Jc-60-0 by 4.46 and 13.59%, respectively. To study the effect of span length on the ductility index of jack arch slab is also considered for specimens made with solid clay bricks. The selected span is 600 and 800 mm. The results show that when the span is increased from 600 to 800 mm for Js-80-0 the ductility index decrease by 6.83. Also, the effect of increasing camber height on the ductility index of the jack arch slab is investigated. For this purpose, one camber of 30 mm is used for specimens made of solid clay bricks The results

Table 4-4: Test results of G_1 specimens.

Group Name	No.	Specimens Symbol	Ultimate Load [kN]	Ultimate Deflection [mm]	Yield Load [kN]	Yield Deflection [mm]	Ductility [Δu/Δy]	Weight [kg]
G_1	1	Js-60-0	3.53	0.80	3.50	0.68	1.17	40
	2	Js-80-0	2.19	0.73	2.16	0.67	1.09	51
	3	Js-80-3	3.89	1.10	3.73	0.95	1.15	52
	4	Jv-60-0	4.85	0.57	4.80	0.50	1.12	33
	5	Jc-60-0	3.44	2.10	3.43	2.03	1.03	14

show an increase in the ductility index for the specimens when the camber is increased. The results showed increase camber by 30 mm for the specimens Js-80-3 improve ductility index by 5.50. From the above results of ductility index, all-control jack arch slab specimens G_1 have a very poor ductility index because their main consistent materials, gypsum mortar, clay bricks, and cement mortar (plastering), are brittle and do not have ductility properties. Also, cellular concrete blocks do not have ductile properties.

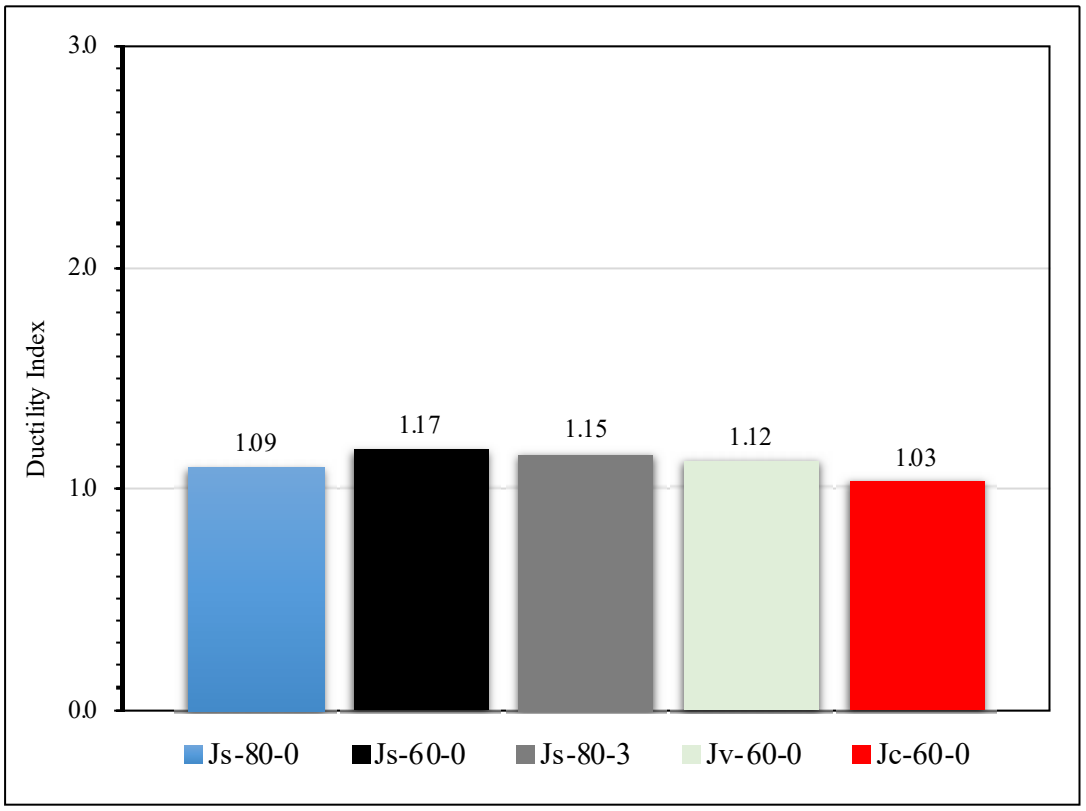

Figure 4-6: Ductility index results for jack arch slab specimens G_1.

4.3.2 Load – Deflection Curves and ductility index for specimens of (G_2)

Load-deflection curves for the second group G_2 that made of ferrocement panels and ferrocement composite-brick slab specimens are discussed here. Figure 4-7 depicts load-deflection curves for all five precast ferrocement panel specimens. These specimens are P-2-60-0, P-4-60-0, P-4-80-0, P-4-80-3, and P-4-100-0, are precast panels made with high-flowable cement mortar reinforced by different layers of steel wire mesh. From this figure, a two-stage load-deflection curve is seen for those specimens. The first zone shows the linear region for the load-deflection relationship at uncracked stage. In this region, both the cement mortar and the wire mesh reinforcement responded elastically. In this stage the cement mortar carrying most of the load. All five ferrocement precast panel specimens exhibit ductile behavior, and the number of cracks increases with increasing the applied load, resulting in considerable deformation. The second zone is indicated by the widening of present cracks with the increase in the applied load. Here the load is carried mainly by reinforcement. When reaching ultimate loads, panels failed in flexural mode by fracturing into two pieces at or near the mid-span of the panels. The ductile and nonlinear behavior of precast ferrocement panels is due to presence of steel wire mesh that has ductile properties. From this figure above, the specimen P-4-60-0 has a higher stiffness than the specimen P-2-60-0. The specimen P-4-80-3 has a higher stiffness than P-4-80-0. Figure 4-8 depicts the load-deflection curves of ferrocement composite solid brick specimens, Cs-2-60-0, Cs-4-60-0, Cs-4-80-0, Cs-4-80-3, Cs-4-100-0, Cs-6-100-0, and Cs-6-100-3. The load-deflection curves for these specimens are linear elastic until the yield load, at which point the curve switches to a nonlinear zone. Throughout the test, failure occurs in the layers of bricks and gypsum mortar. At this stage, no considerable cracks are observed on the bottom face of precast panels of ferrocement composite slab specimens until reaching to the ultimate load, except for the specimens Cs-4-80-3 and Cs-6-100-3, where the first

crack appeared in the bottom face of precast ferrocement panels at loads of 11 and 6.9 kN, respectively. After that, the applied load remained constant while displacement significantly increased, and the cracks developed at the bottom face of the precast panels of ferrocement composite solid clay brick slab. The number of cracks also increase as the displacement increases. The widening of one existing cracks, resulting of excessive displacement of the precast ferrocement panel leading to entire specimen collapse. From Figure 4-8, the specimen Cs-4-60-0 has a higher stiffness than Cs-2-60-0. The specimen Cs-4-80-3 has a higher stiffness than the

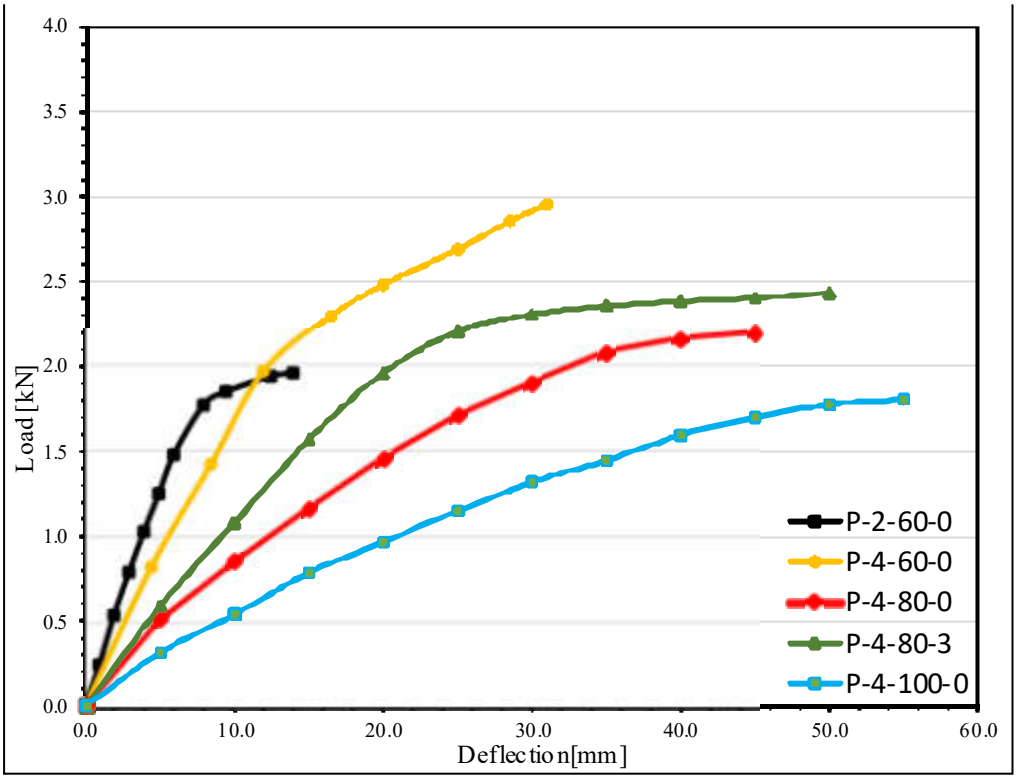

Figure 4-7: Load-deflection curves for all precast ferrocement specimens.

specimen Cs-4-80-0. The specimen Cs-6-100-3 has a higher stiffness than the s specimens Cs-6-100-0, Cs-4-100-0. The load-deflection curves of the ferrocement

composite, perforated clay bricks, and cellular concrete block prism specimens, Cv-4-60-0, Cv-4-80-0, Cc-60-0, and Cc-80-0, are shown in Figure 4-9. Throughout the test, the load-deflection curves for these specimens behave approximately in similar to those of ferrocement composite solid clay brick specimens, which are linear elastic until the yield load at which point the curve switches to a nonlinear zone. The

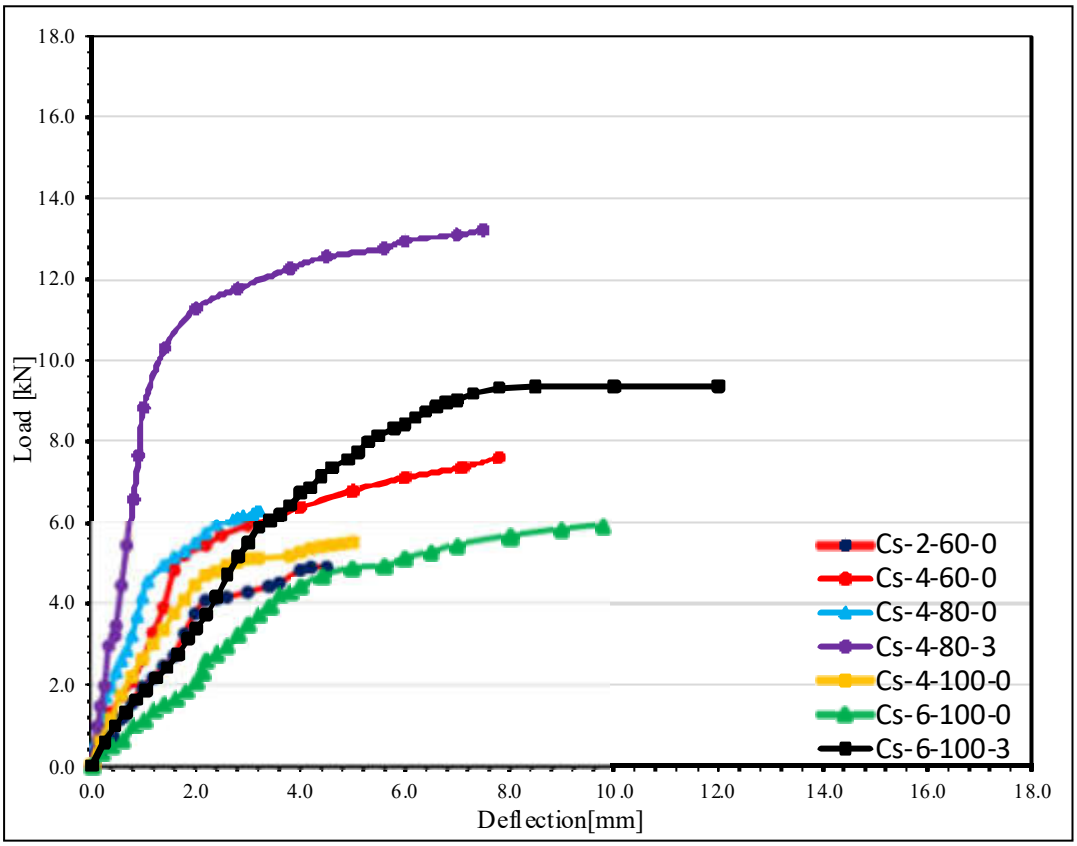

Figure 4-8: Load-deflection curves for all ferrocement composite solid clay bricks slab specimens.

The failure occurs in layers of perforated clay bricks, cellular concrete block prisms, and gypsum mortar. Until the ultimate load is reached, no considerable cracks are observed on the bottom face of the precast panel of ferrocement composite,

perforated clay bricks, cellular concrete block (thermostone) prism, and gypsum mortar. After reaching the ultimate load, the applied load stays constant while the displacement of specimens increase. The cracks are developed in the bottom face of ferrocement precast panels. The number of cracks increased and the widening of existing cracks continued, leading to the severe displacement of the ferrocement composite until collapse. From above, in comparing the load-deflection curves of the second group G_2 with the load- deflection curves of the first group G_1. The results show that the load-deflection curves for the second group G_2 are different from the load-deflection curves for control jack arch specimens G_1 by ductile behavior. From the previous figures, the specimen Cv-4-60-0 has a higher stiffness than the specimens, Cs-4-60-0, and Cc-4-60-0. Also, the specimen Cv-4-80-0 has a higher stiffness than Cs-4-80-0, and Cc-4-80-0.

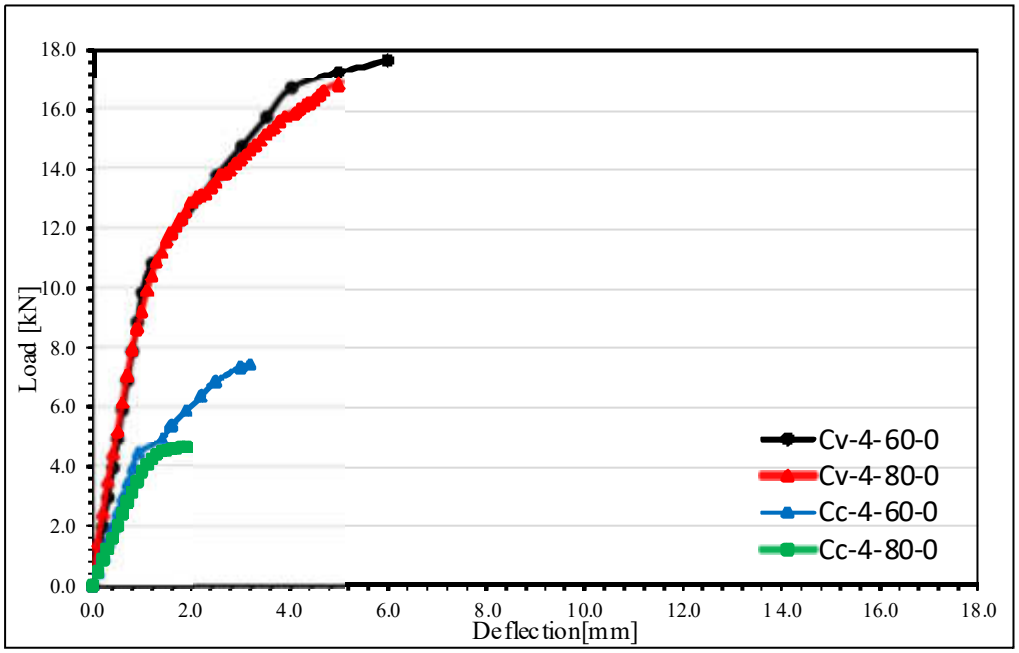

Figure 4-9: Load-deflection curves for all ferrocement composite perforated clay bricks, cellular concrete blocks slab specimens.

Ductility index results for ferrocement precast and ferrocement composite-brick slab specimens G_2 are listed in Table 4-5 and depicted in Figure 4-10. The effects of the volume fraction on the ductility index of ferrocement precast and ferrocement composite-brick slab specimens G_2 are discussed by using 2, 4, and 6 layers of steel wire mesh. The results show that increasing the volume fraction by 100% for the specimens P-4-60-0 and Cs-4-60-0 and by 49.3% for Cs-6-100-0 increase the ductility index by 19.12, 65.38, and 2.39%, respectively. The effects of the type of bricks used in the construction on the ductility index of ferrocement composite-brick slab specimens are investigated by using three types of bricks, solid

Table 4-5: Test results of G_2 specimens.

Group Name	No.	Specimens Symbol	Ultimate Load [kN]	Ultimate Deflection [mm]	Yield Load [kN]	Yield Deflection [mm]	Ductility [Δu/Δy]	Weight [kg]
G_2	1	P-2-60-0	1.95	14.0	1.75	7.8	1.794	5.0
	2	P-4-60-0	2.95	31.0	2.20	14.5	2.137	5.2
	3	P-4-80-0	2.19	45.0	1.70	25.8	1.744	7.0
	4	P-4-80-3	2.43	50.0	2.05	21.0	2.380	7.8
	5	P-4-100-0	1.80	55.0	1.48	38.5	1.420	9.0
	6	Cs-2-60-0	4.86	4.5	4.18	2.5	1.814	48.0
	7	Cs-4-60-0	7.60	7.8	5.80	2.6	3.000	49.0
	8	Cs-4-80-0	6.27	3.2	4.80	1.3	2.461	57.0
	9	Cs-4-80-3	13.22	7.5	11.10	1.9	3.947	58.0
	10	Cs-4-100-0	5.46	5.0	4.50	2.1	2.380	68.0
	11	Cs-6-100-0	5.90	9.8	4.60	4.0	2.437	69.0
	12	Cs-6-100-3	9.36	12.0	7.30	4.7	2.553	71.0
	13	Cv-4-60-0	17.67	6.0	11.40	1.6	3.750	40.0
	14	Cv-4-80-0	16.87	5.0	11.50	1.7	2.941	51.0
	15	Cc-4-60-0	7.40	3.2	4.80	1.4	2.285	25.0
	16	Cc-4-80-0	4.65	1.9	4.10	1.1	1.711	33.0

clay bricks, perforated clay bricks, and cellular concrete blocks (thermostone) for a span length of 600 and 800 mm. The results show that specimens made with both types of clay bricks have a higher ductility index than those made with cellular concrete blocks. Also, specimens made with perforated clay bricks have a greater ductility index than specimens made with solid clay bricks. The results show that the

specimens Cs-4-60-0 and Cv-4-60-0 have a higher ductility index than the specimen Cc-4-60-0 by 31.29 and 64.11%, respectively. The specimens Cs-4-80-0 and Cv-4-80-0 have a ductility index greater than specimen Cc-4-80-0 by 43.83 and 71.88%, respectively. The specimens Cv-4-60-0 and Cv-4-80-0 have a greater ductility index than the specimens Cs-4-60-0 and Cs-4-80-0 by 25 and 19.50%, respectively. This results are because cellular concrete block units have low ductility properties and flexural bonding strength with gypsum mortar when compared to clay brick units and perforated clay brick units and gypsum mortar having higher flexural bonding strengths than solid clay brick units, where the perforations in them enhance the bond

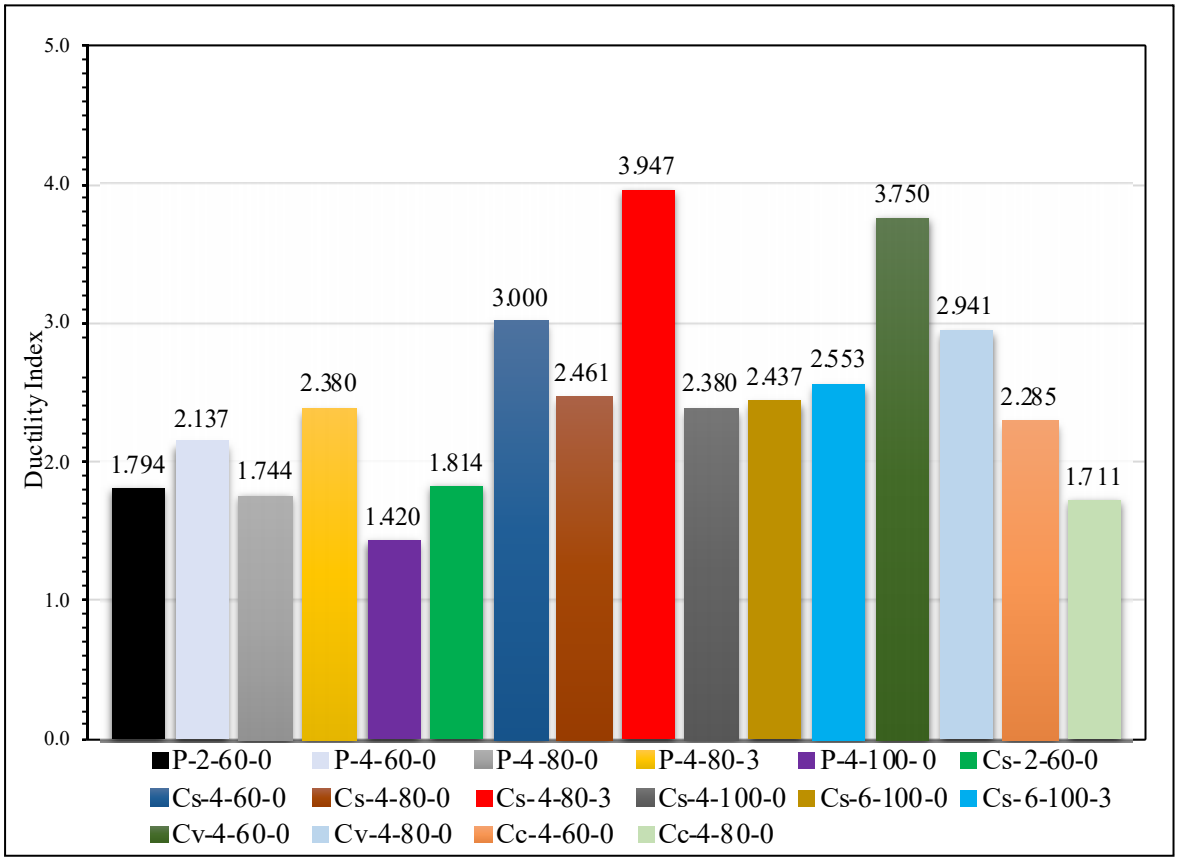

Figure 4-10: Ductility index results for ferrocement composite-brick slab specimens G_2.

-ing strength between units. This is lead to an increase in the interaction action between layers that cause them to resist large deformations. To study the effect of increasing span length, specimens with different span lengths are made, which are of 600, 800, and 1000 mm, to show their effect on the ductility index of ferrocement precast and ferrocement composite-brick slab specimens. The results show a decrease in the ductility index when increasing the span length for both precast and ferrocement composite-brick slab specimens. When the span is increased from 600 mm to 800 mm for P-4-80-0, Cc-4-80-0, Cv-4-80-0, and Cs-4-80-0, the ductility index decrease by 18.39, 25.12, 21.57, and 17.96%, respectively. When the span of P-4-100-0 and Cs-4-100-0 is increase from 800 mm to 1000 mm, the ductility index decrease by 18.57 and 3.29%, respectively. The effect of increasing camber height on the ductility index of ferrocement precast and ferrocement composite-brick slab specimens is investigated. For this purpose, one camber of 30 mm is used for specimens made of span lengths of 800 mm ferrocement panel and 800 and 1000 mm ferrocement composite-solid brick slab specimens. The results show an increase in the ductility index for both types of specimens when the camber is increased. For the specimens P-4-80-3, Cs-4-80-3, and Cs-6-100-3, increasing camber height by 30 mm, improve ductility index by 36.46, 60.38, and 4.76%, respectively. In the comparison between the precast ferrocement panels and ferrocement composite brick slab specimens G_2 and the control jack arch specimens G_1, the results show that the specimens Cs-2-60-0 and Cs-4-60-0 have a higher ductility index than specimen Js-60-0 by 55.04 and 156.41%, respectively. The specimens Cs-4-80-0 and Cs-4-80-3 have a ductility index greater than Js-80-0 and Js-80-3 by 125.78 and 243.21%, respectively. Although the fact that the specimens Cs-4-100-0 and Cs-6-100-0 have a span greater than control specimen Js-80-0, they have a higher ductility index than Js-80-0 by 118.34 and 123.57%, respectively. As well, although the specimen Cs-6-100-3 had a span greater than control specimen Js-80-3, it has a

higher ductility index than specimen Js-80-3 by 122%. The specimen Cv-4-60-0 has a higher ductility index than Jv-60-0 by 234.82%. The specimen Cc-4-60-0 has a higher ductility index than the specimen Jc-60-0 by 121.84%. Although the specimen Cc-4-80-0 has a span length greater than control specimen Jc-60-0, it has a higher ductility index than the specimen Jc-60-0 by 66.11%. From the above results, all-composite ferrocement slabs with solid and perforated clay bricks, as well as cellular concrete block and precast ferrocement panel specimens G_2, have a higher ductility index than the control jack-arch slab specimens G_1. These results are due to the precast ferrocement panel, which improve the slab's flexural strength and ductility by using layers of steel-welded wire mesh that has ductile properties.

4.3.3 Load – Deflection Curves and ductility index for specimens of (G_3)

Load-deflection curves for ferrocement sandwiched slab specimens of group G_3 are discussed in this section. Figure 4-11 shows the load-deflection curves for the specimens Sp-4-80-0, SHp-4-80-0, SDp-4-80-0, and SHp-4-100-0, which represent ferrocement sandwiched slabs formed from two layers of ferrocement with the same core material styropor prism unit between the layers with varying spans 800, and1000 mm and depth sections 130, and 160 mm. The ferrocement layers are reinforced by four layers of steel wire mesh placed at the top and bottom of specimens. These layers are linked together with or without shear connectors. For those specimens, two-stage load-deflection curves are seen, which are different from the load-deflection curves for control jack arch specimens G_1. The first zone shows the linear load-deflection relationship for the uncracked stage. At this stage, both the cement mortar and the reinforcement with styropor response elastically along this zone. The load-deflection curve is approximately linear until the first crack load. The second zone starts after the first crack occurs. With increasing applied load, the numb

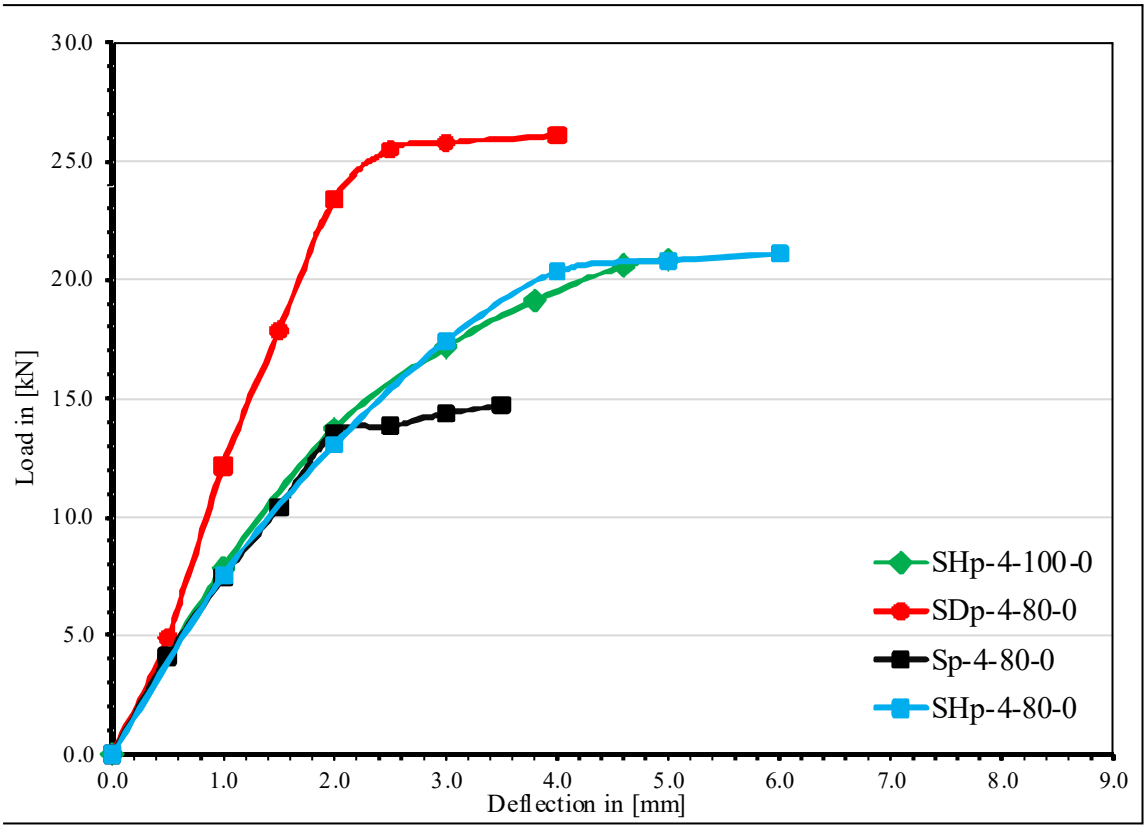

Figure 4-11: Load deflection curves for Sp-4-80-0,SHp-4-80-0, SDp-4-80-0, and SHp-4-100-0.

-er of cracks increases resulting in considerable deformation, and all specimens exhibit ductile behavior. Then the widening of present cracks with the increase in applied load. Here the load is carried mainly by reinforcement. When reaching ultimate loads, specimens failed in flexural mode by fracturing the bottom layer into two pieces. From the previous figure, the specimen SDp-4-80-0 has a higher stiffness than the specimens Sp-4-80-0, and SHp-4-80-0, respectively. Figure 4-12 depicts load-deflection curves for the specimens Sc-4-80-0, SHc-4-80-0, and SHc-4-100-0, which represent ferrocement sandwich slabs formed from two layers of ferrocement with the same core material cellular concrete block prism (thermostone) with varying spans 800, and 1000 mm. The ferrocement layers are reinforced by four

layers of steel wire mesh. Also, for those specimens, two-stage load-deflection curves are seen that are different from the load-deflection curves for the control jack arch specimens. The specimens are approximately similar in behavior to specimens Sp-4-80-0, SHp-4-80-0, SHp-4-100-0, and SDp-4-80-0, in which the first zone shows the linear load-deflection relationship for the uncracked stage. The load-deflection curve is nearly linear until the first crack load. The second zone starts after the first crack occurs. All specimens exhibit ductile behavior, and the number of

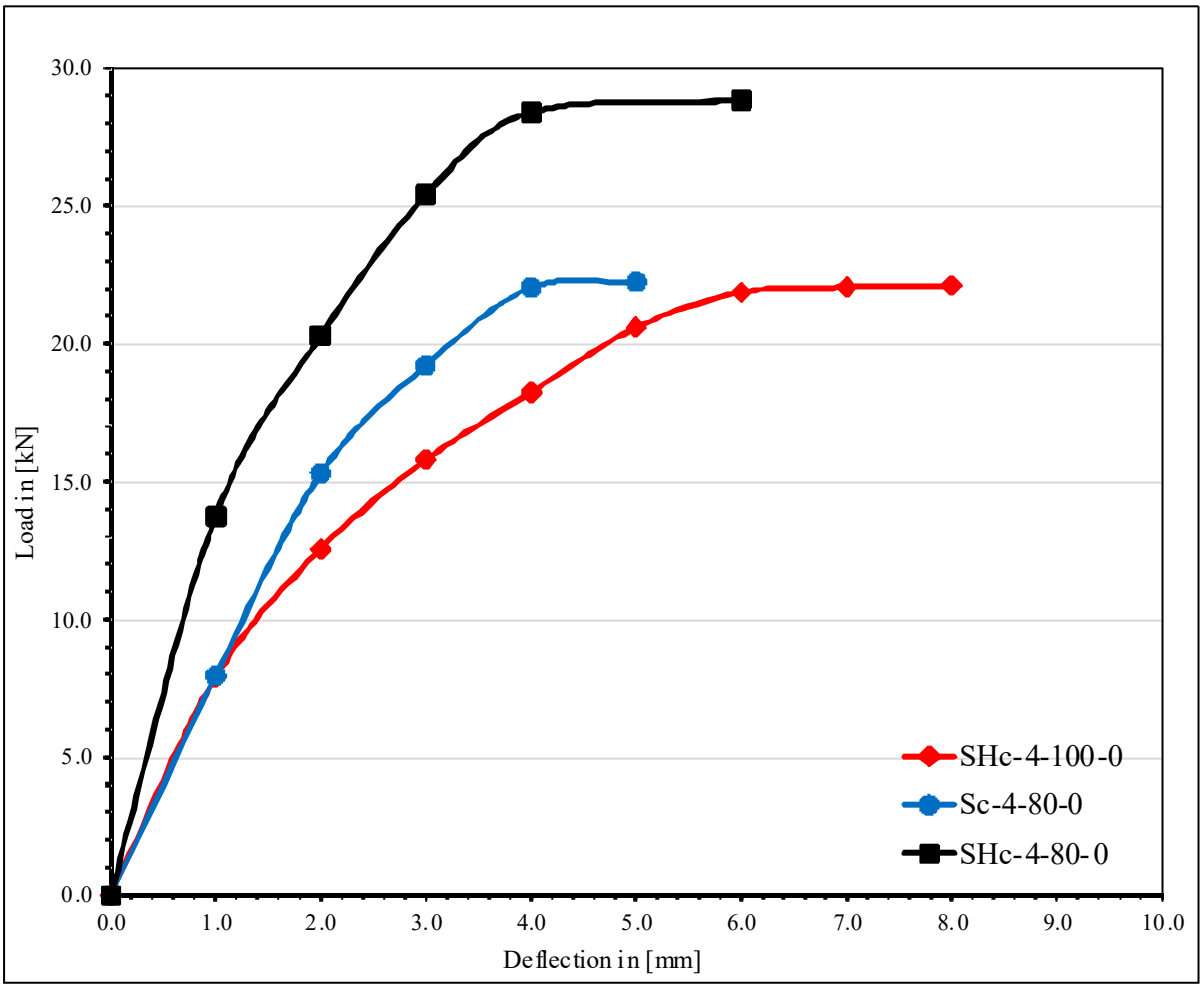

Figure 4-12: Load deflection curves for Sc-4-80-0, SHc-4-80-0, and SHc-4-100-0.

cracks increases with increasing load, resulting in significant deformation. Then the widening of present cracks with the increase in load. When achieving ultimate loads, specimens fail in flexural mode by fracturing the bottom layer into two. The ductile and nonlinear behavior of the all-ferrocement sandwich composite slab specimens G_3 is due to steel wire mesh that has ductile properties higher than cement mortar and core materials (styropor and cellular concrete blocks), which are brittle materials. From the previous figures of load-deflections curves, the specimen SHc-4-80-0 has a higher stiffness than the specimens Sp-4-80-0, and SHp-4-80-0. The specimen SHc-4-100-0 has a higher stiffness than SHp-4-100-0.

Ductility index results for ferrocement sandwiched slab specimens G_3 are listed in Table 4-6 and shown in Figure 4-13. The effects of the type of core material used on the ductility index of ferrocement sandwiched slab specimens G_3 are studied by using two types of core materials, styropor and cellular concrete blocks sandwiched between two layers of ferrocement at spans of 800 and 1000 mm with and without shear connectors. The results indicate that specimens made with cellular concrete blocks have a higher ductility index than those made with styropor. The results reveal that the specimens Sc-4-80-0, SHc-4-80-0, and SHc-4-100-0 have a higher ductility index than the specimens Sp-4-80-0, SHp-4-80-0, and SHp-4-100-0 by 9.71, 55.60, and 53%, respectively. This improvement in ductility index is because cellular concrete block units have higher ductile properties than styropor. The effect of increasing span length is studied, and specimens with different span lengths are made, which are (800 and 1000) mm, to show their effect on the ductility index of ferrocement sandwiched slab specimens G_3 made with styropor and cellular concrete blocks as core materials. The results show that when the span is increased from 800 to 1000 mm for the specimens SHc-4-100-0 and SHp-4-100-0, the ductility index decrease by 8.1 and 6.54%, respectively. To study the effect of increasing

Table 4-6: Test results of G_3 specimens.

G.	No.	Specimens Symbol	Ultimate Load [kN]	Ultimate Deflection [mm]	Yield Load [kN]	Yield Deflection [mm]	Ductility [Δu/Δy]	Weight [kg]
G_3	1	Sc-4-80-0	22.25	5.0	19.00	2.6	1.92	40
	2	SHc-4-80-0	28.84	6.0	20.10	1.8	3.33	41
	3	Sp-4-80-0	14.70	3.5	14.00	2.0	1.75	29
	4	SHp-4-80-0	21.09	6.0	16.20	2.8	2.14	30
	5	SHc-4-100-0	22.12	8.0	14.80	2.6	3.06	50
	6	SHp-4-100-0	20.84	5.0	15.50	2.5	2.00	35
	7	SDp-4-80-0	26.09	4.0	24.50	2.0	2.00	38

section depth, specimens with different section depths are made, which are 130 and 160 mm, to show their effect on the ductility index of ferrocement sandwiched slab specimens made with styropor as the core material. The results show that when the section depth of SDp-4-80-0 is increase from 130 to 160 mm, the ductility index increase by 14.28%. Also, the effect of using a shear connector on the ductility index of ferrocement sandwiched slab specimens made with styropor and cellular concrete as the core material is investigated. For this purpose, steel wire 3 mm in diameter is used as shear connectors for four specimens each having a span length of 800 mm. The results show that using shear connectors for the specimens SHc-4-80-0 and SHp-4-80-0 improve the ductility index by 73.43 and 22.28%, respectively. These improvements in ductility index results are because shear connectors improve interaction between the top and bottom ferrocement layers of specimens, which increase their ability to resist large deformations. In comparing the ferrocement sandwich slab specimens G_3 with the control jack arch specimens G_1, the results show that the specimens Sc-4-80-0, SHc-4-80-0, Sp-4-80-0, SHp-4-80-0, and SDp-4-80-0 have a higher ductility index than the control jack arch specimen Js-80-0 by 76.14, 205.50, 60.55, 96.33, and 83.48%, respectively. Although the specimens SHc-4-100-0 and SHp-4-100-0 have a span length greater than control specimen Js-80-0, they have a ductility index higher than the specimen Js-80-0 by 180.73 and 83.48%, respectively. When compare between the ferrocement sandwich slab

specimens G_3 and the ferrocement composite-brick slab specimens G_2, the results show that Sc-4-80-0 and SHc-4-80-0 have a higher ductility index than Cc-4-80-0 by 12.21 and 94.62%, respectively. These results are due to ferrocement layers, which enhance the slab's flexural strength and its ability to resist large deformations after the yield stage. According to the test results mentioned above, all-ferrocement sandwich composite jack arch slab specimens G_3 have a higher ductility index than control jack arch slab specimens G_1. This is due to the composite behavior of the ferrocement sandwich, which converts a pure brittle material, cement mortar styropor, and cellular concrete blocks into a ductile composite material. This occurs because of using ferrocement layers.

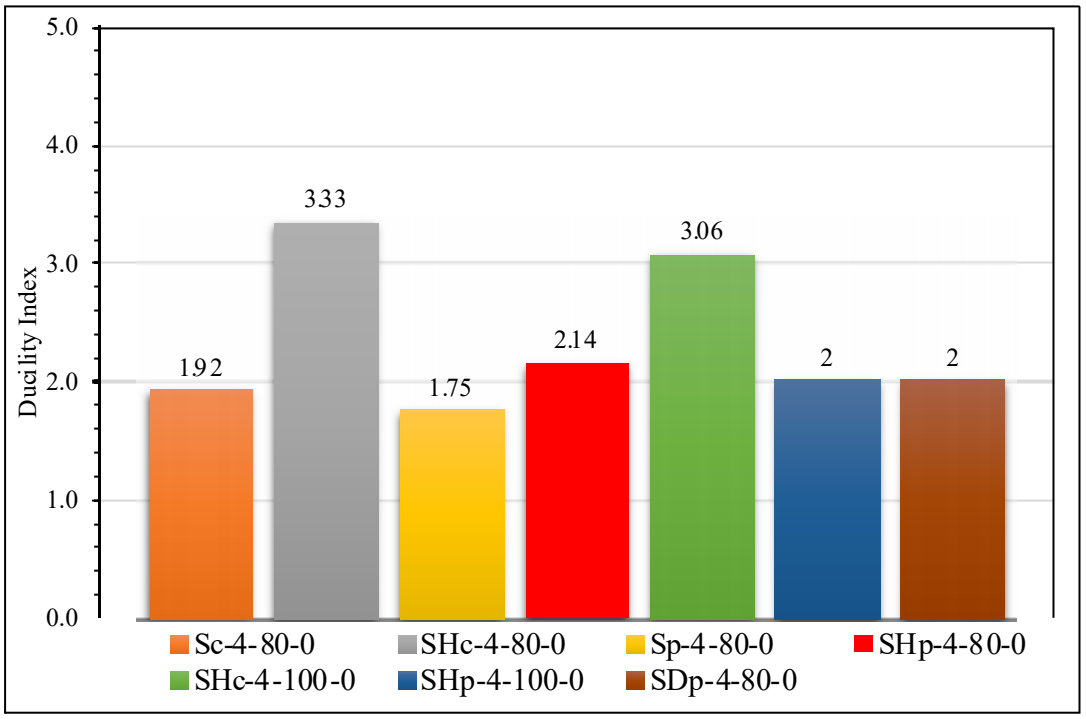

Figure 4-13: Ductility index results for ferrocement sandwiched slabs specimens G_3.

4.4 Failure Modes

The failure modes for all groups of specimens G_1, G_2, and G_3 conducted in the current study are discussed in this section.

Failure modes for all jack arch slabs specimens of group G_1 considered as a control are shown in Figure 4-14 (a-e). For those specimens, failure is characterized in all jack arch slabs made from perforated and solid clay brick specimens by the sudden collapse of brickwork slabs due to initiate cracks at the bond joints between clay brick units. This characterized failure in the control of traditional jack arch slab specimens because the bond joints between brick units are the element's weakest region. The failure mode is characterized by a brittle failure, this is due to the jack arch slab constituent materials being brittle and having low tensile strength. The observation during the test show that the compression faces of the specimens are not crush and that the clay bricks do not fracture or crush, see Figure 4-14 (a-d). For jack arch slab specimen made with cellular concrete block, the failure mode is similar to that of jack arch slabs made with perforated and solid clay brick specimens. The failure is characterized by brittleness and the sudden collapse of cellular concrete block. The fracture occurs in the cellular concrete block unit at mid-span instead in the bond joint between units. This failure mechanism because cellular concrete blocks have brittle and low tensile strength. During the test of this specimen, no crushing in the compression face occurred, see Figure 4-14 (e). From the above explanation, the flexural failure mode is dominated the jack arch slab specimens of group G_1 at mid-span for jack arch slab specimens made with cellular concrete block and nearer the bond joint at mid-span for jack arch slab specimens made with perforated and solid clay brick.

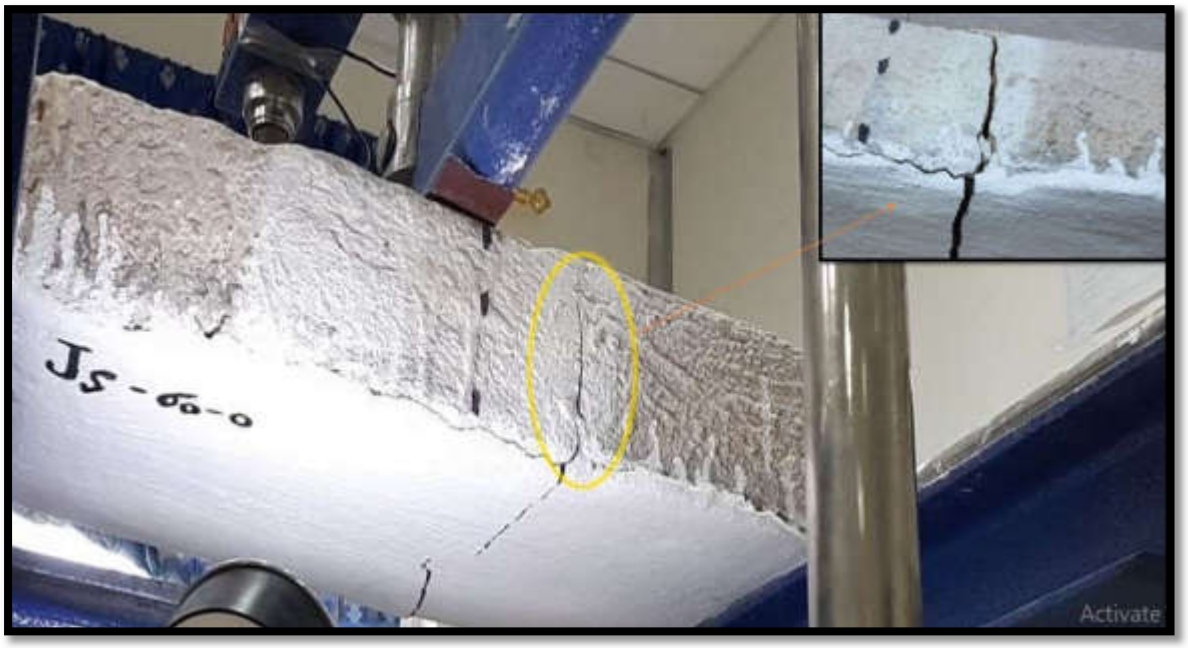

(a) Mode of failure for Js-60-0 specimen.

(b) Mode of failure for Js-80-0 specimen.

Figure 4-14: Modes of failure for jack arch slab specimens (G_1).

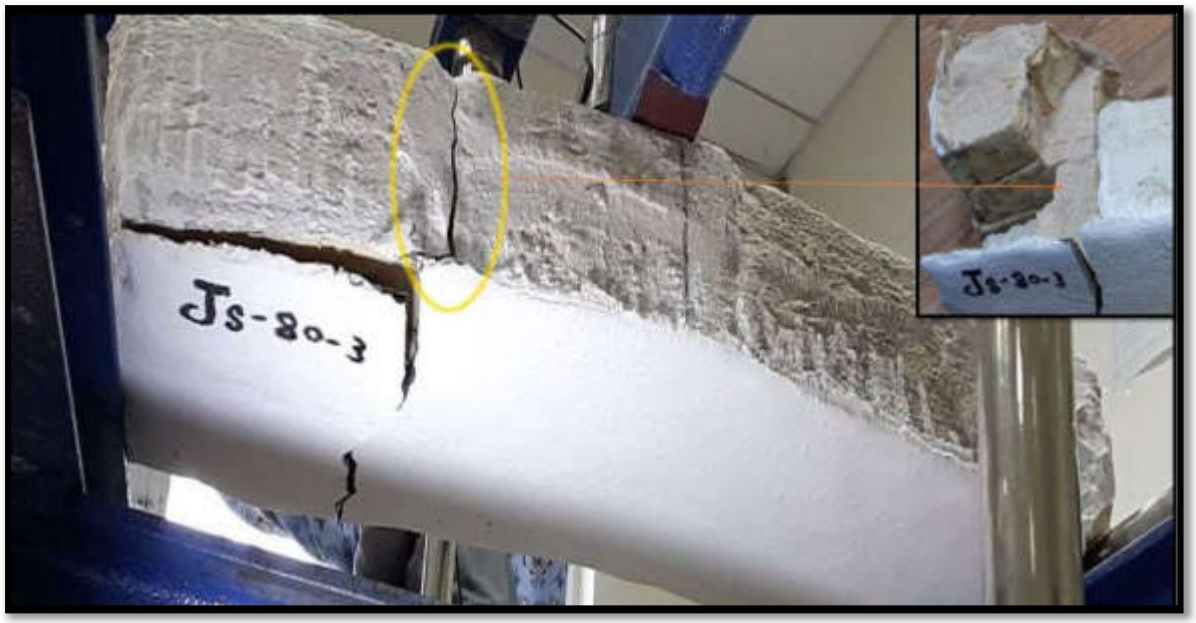

(c) Mode of failure for Js-80-3 specimen.

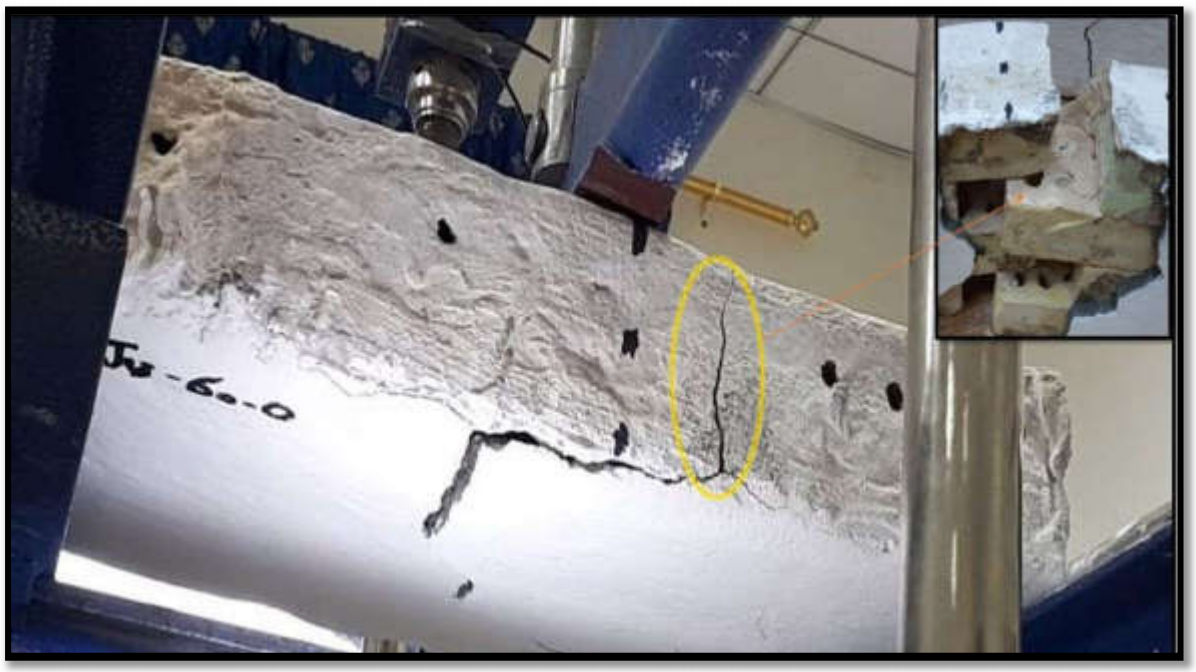

(d) Mode of failure for Jv-60-0 specimen.

Figure. 4-14: Continued.

(e) Mode of failure for Jc-60-0 specimen.

Figure. 4-14: Continued.

The testing failure mechanism and crack pattern for all five ferrocement precast panel specimens, P-2-60-0, P-4-60-0, P-4-80-0, P-4-80-3, and P-4-100-0, are shown in Figure.4-15(a-e). During the test, no crushing of cement mortar is observed on the compression top faces of the panels. All of the cracks start on the bottom face of the specimens. When the applied loads applied increases, multiple cracks often start and concentrate in the central mid-span area of the panels. As can observe from this figure, the spacing between cracks is smaller, the cracks are finer, and there are a greater number of cracks for specimens P-4-60-0, P-4-80-0, P-4-80-3, and P-4-100-0 that has a higher volume fraction than the specimen P-2-60-0. The failure mode indicates that the volume fraction of wire mesh has a significant impact on crack patterns of ferrocement precast panels.

(a) Mode of failure for P-2-60-0 specimen.

(b) Mode of failure for P-4-60-0 specimen.

Figure.4-15: Failure modes for all five ferrocement precast panels specimens.

(c) Mode of failure for P-4-80-0 specimen.

(d) Mode of failure for P-4-80-3 specimen.

Figure. 4-15: Continued.

(e) Mode of failure for P-4-100-0 specimen.

Figure. 4-15: Continued.

Failure modes of all eleven ferrocement composite-brick slab specimens are discussed in this paragraph. Figure. 4-16 (a-k) depicts the failure mechanism and crack pattern for all eleven tested ferrocement composite-brick slab of (G_2) specimens. For all specimens, testing observation show that the compression top faces of the cross-section that is made from gypsum mortar has no gypsum mortar crushing. At the increasing applied load to the ultimate load stage, the failure occurs at layer of clay brick units, cellular concrete block units, and gypsum mortar used for bonding the units. During testing, all-composite specimens show separation between the precast panels and the second layers of clay brick units or cellular concrete block prism and gypsum mortar at ultimate load. After reaching ultimate loads and increasing displacement under constant applied load, all of the cracks occurred on the bottom faces of the precast ferrocement panels of the specimens. From above, the modes of failure show that the ferrocement composite specimen elements have a ductile behavior. That is due to using a precast panel of ferrocement.

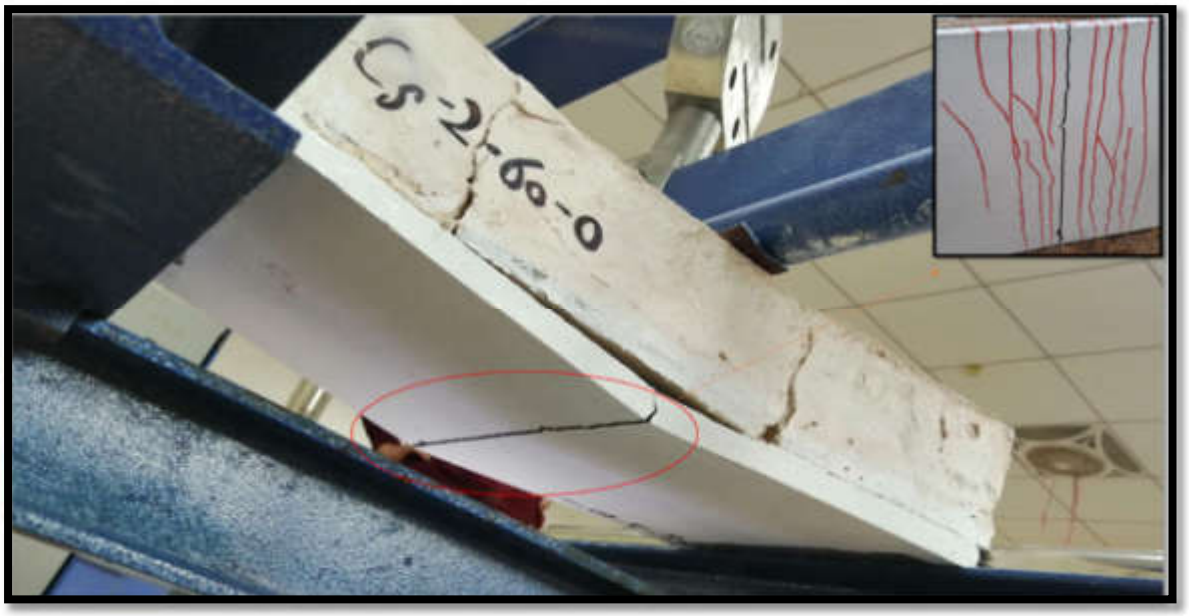

(a) Mode of failure for Cs-2-60-0 specimen.

(b) Mode of failure for Cs-4-60-0 specimen.

Figure. 4-16: Failure modes for all ferrocement composite- brick specimens.

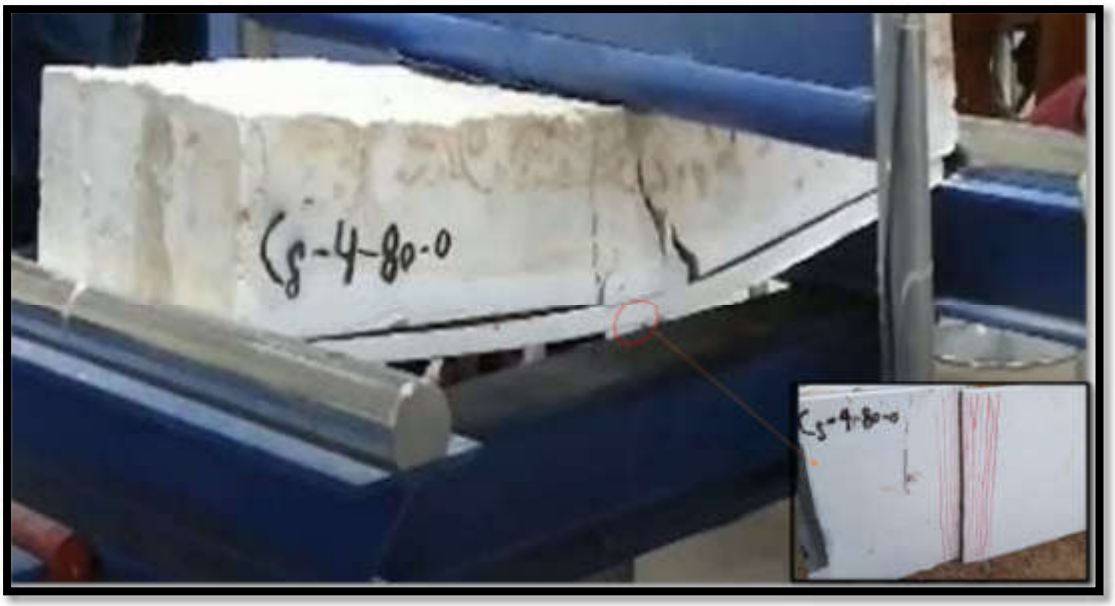

(c) Mode of failure for Cs-4-80-0 specimen.

(d)

Mode of failure for Cs-4-80-3 specimen.

Figure. 4-16: Continued.

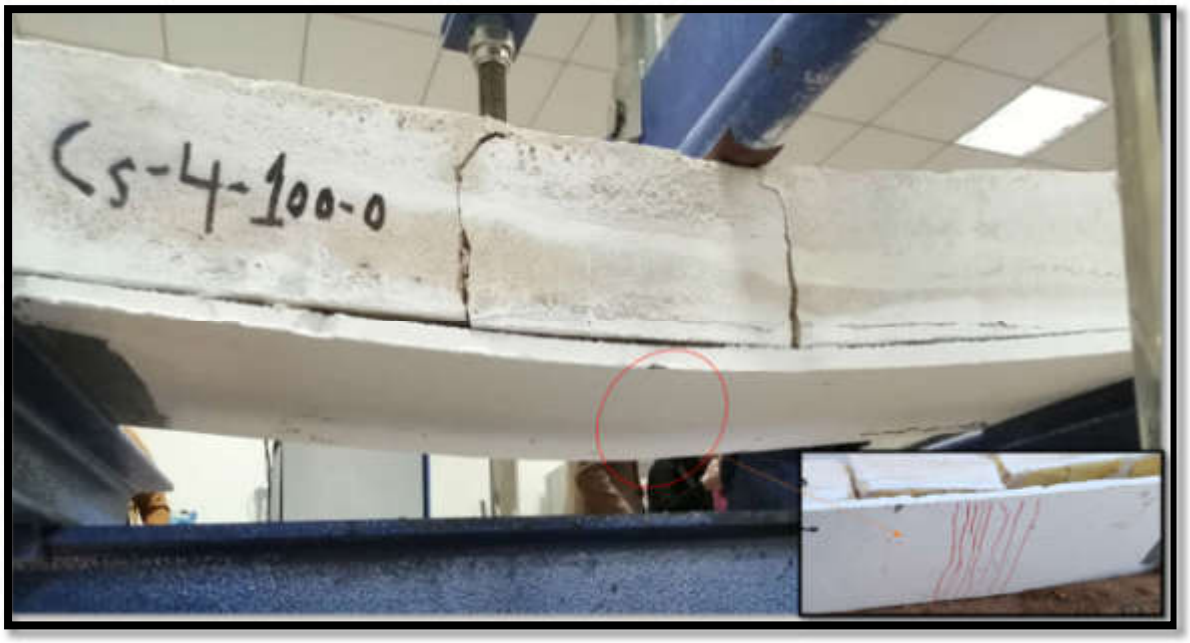

(e) Mode of failure for Cs-4-100-0 specimen.

(f) Mode of failure for Cs-6-100-0 specimen.

Figure. 4-16: Continued.

(g) Mode of failure for Cs-6-100-3 specimen.

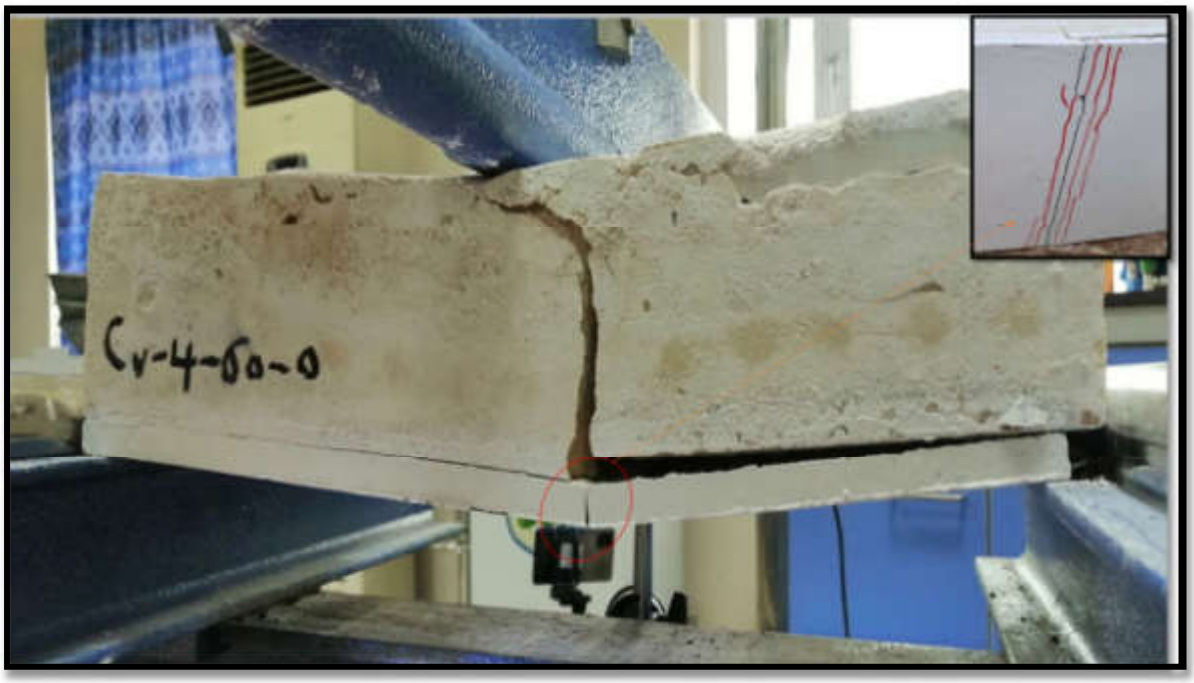

(h) Mode of failure for Cv-4-60-0 specimen.

Figure. 4-16: Continued.

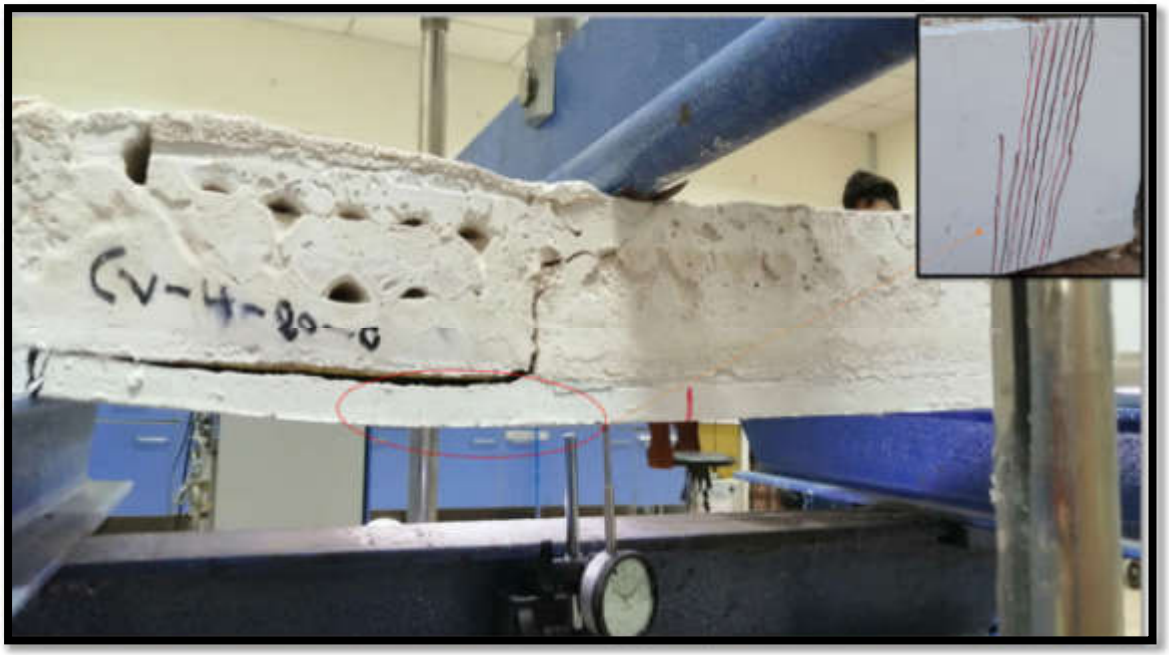

(i) Mode of failure for Cv-4-80-0 specimen.

(j) Mode of failure for Cc-4-60-0 specimen.

Figure. 4-16: Continued.

(k) Mode of failure for Cc-4-80-0 specimen.

Figure. 4-16: Continued.

Failure mechanisms and crack patterns for all ferrocement sandwiched slab specimens of group G_3 are demonstrated in Figure 4-17. The failure modes of specimens Sc-4-80-0, SHc-4-80-0, and SHc-4-100-0 that are made with cellular concrete prisms as core material, enclosed by two layers of ferrocement, are shown in Figure 4-17 (a, b, and e). It can note that the specimens fail due to the yielding of steel wire mesh reinforcements. During the test, flexural cracks occurs at a distance or around the mid-span of the bottom face of specimens. As the applied load increase, the cracks extend vertically, resulting in the generation of additional flexural cracks. The cracks start to form and propagate diagonally along with the cellular concrete prisms as the specimens reach their ultimate load. The diagonal pattern of cracks develops because of the poor shear resistance of the cellular concrete block prisms. Significant diagonal cracks occur at the end of the specimen during failure. Horizontal separation is seen between the top and bottom ferrocement layers and the cellular concrete block prisms in specimen Sc-4-80-0 that is without

shear connectors. For the specimens SHc-4-80-0 and SHc-4-100-0 that contain shear connectors, there is no horizontal separation that occurs between the top and bottom ferrocement layers and the cellular concrete block prisms. This mode of failure due to shear connectors that enhance interaction between ferrocement top and bottom layers and cellular concrete prisms. Also, the observations made through the tests of all specimens indicated no crushing of cement mortar at the compression face of the cross-section. These specimens failed due to reaching the ultimate stress of the reinforcing steel mesh, and the mesh bars rupture, indicating that the strain in the steel mesh has reached its ultimate strain. The failure modes and crack patterns of sandwich ferrocement specimens of Sp-4-80-0, SHp-4-80-0, SHp-4-100-0, and SDp-4-80-0 with styropor prisms as the core material are depicted in Figure 4-17 (c, d, f, and g). They are similar in behavior to specimens with cellular concrete prisms as core material, in which specimens fail due to reaching the ultimate loads of the reinforcing steel mesh, and the mesh bars rupture, indicating that the strain in the steel mesh has reached its ultimate strain. During testing, flexural cracks occur at a distance or nearer the mid-span of the bottom face ferrocement sandwiched slab specimens. As the applied load increased, the cracks extend vertically, resulting in the generation of additional flexural cracks. The cracks start to propagate diagonally along with the styropor as the specimens reached their ultimate load. The diagonal pattern of cracks develops because of the poor shear resistance of the styropor. Also, significant diagonal cracks occur at the end of the specimen during failure. Horizontal separation is seen between the top and bottom ferrocement layers and styropor in specimens without shear connectors. For the specimens SHp-4-80-0 and SHp-4-100-0 that contain shear connectors, there is no horizontal separation seen between the top and bottom ferrocement layers and the styropor. This failure mechanism due to shear connectors that enhance interaction between ferrocement

layers and styropor prisms. Also, for these specimens, no crushing of cement mortar is observed on the compression face of the cross-section.

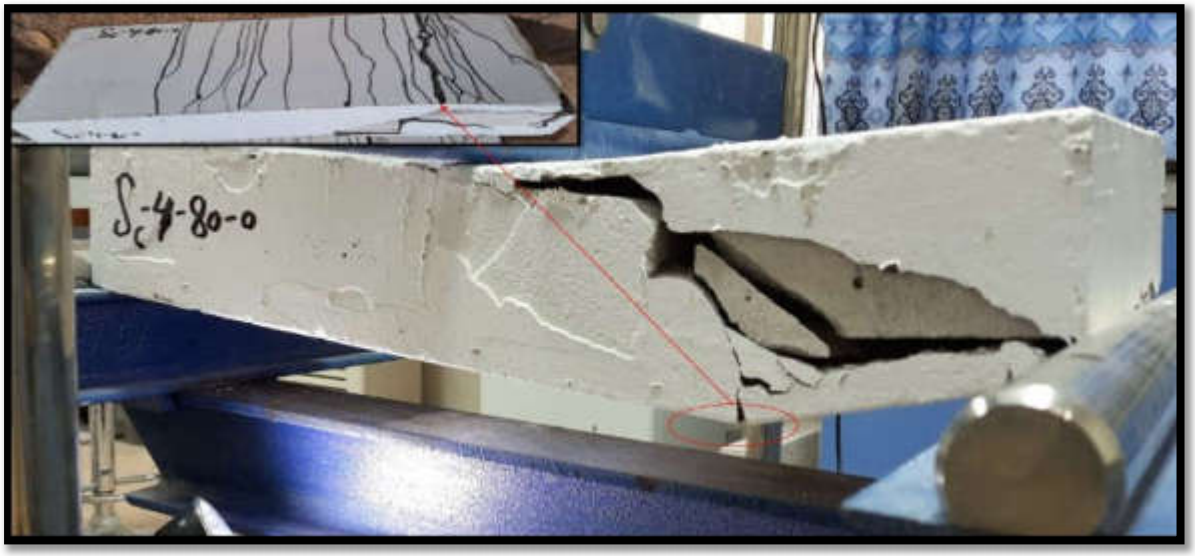

(a) Mode of failure for Sc-4-80-0 specimen.

(b) Mode of failure for SHc-4-80-0 specimen.

Figure 4-17: Failure modes for all ferrocement sandwiched slabs specimens.

(c) Mode of failure for Sp-4-80-0 specimen.

(d) Mode of failure for SHp-4-80-0 specimen.

Figure. 4-17: Continued.

(e) Mode of failure for SHc-4-100-0 specimen.

(f) Mode of failure for SHp-4-100-0 specimen.

Figure. 4-17: Continued.

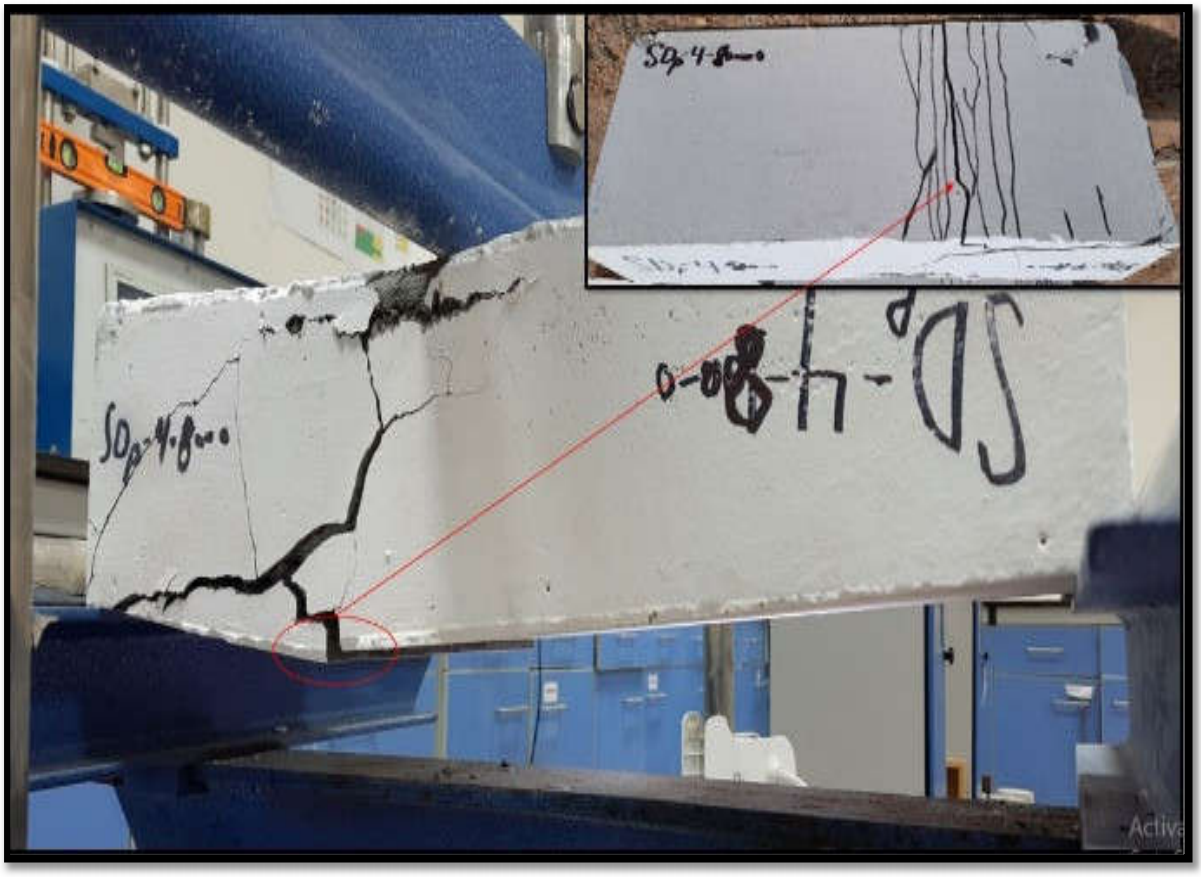

(g) Mode of failure for SDp-4-80-0 specimen.

Figure. 4-17: Continued.

CHAPTER FIVE: CONCLUSIONS AND RECMMONDATIONS

5.1 Conclusions

The following are the main conclusions of the current experimental study based on the experimental results that are obtained from the current study:

5.1.1 Conclusions for jack arch slab control specimens

1. In the construction of jack-arch slabs, the perforated bricks can use due to their lightweight, and acceptable structural performance.
2. Cellular concrete blocks can use to construct jack-arch slabs due to their lightweight and acceptable structural response. However, it is only utilizing for a span of 600 mm due to being available only as a precast unit with 600 mm in length dimension, which increases the demand for utilizing a greater number of steel I-section beams than other types of bricks.
3. Flexural bond failure dominates the jack arch slab specimens at mid-span for cellular concrete block specimens, and closer to the bond joint at mid-span for perforated, and solid brick specimens.
4. Increasing camber by 30 mm for solid clay brick specimens increase the ultimate load, and ductility index by 77.62 and 5.5% respectively.
5. From the result of the present work, the authors advise using jack arch slab in the construction of slabs for residential buildings due to fast work, less expensive, and appropriate for small areas when compare to reinforced concrete slabs with considering the proper engineering techniques for its construction.

5.1.2 Conclusions for ferrocement precast and composite brick specimens

1. All composite brick slab specimens performed better than control jack arch slab specimens regarding structural performance, and can resist normal design loads for residential structures and can use for jack arch slab applications.
2. Perforated clay bricks composite slab specimens showed higher structural performance than solid clay brick specimens. This is effective for reducing slab weight and having a positive effect on other structural elements of the structure due to their lightweight.
3. The ferrocement precast panel characteristics demonstrated that it can securely carry topping and construction loads without using a mid-support.
4. The mode of failure of the composite specimen elements indicates ductile and composite behavior, converting a brittle material (clay brick and cellular concrete blocks) into a composite ductile material. This occurs due to using a precast panel of ferrocement.
5. All-composite ferrocement slabs with solid and perforated bricks, as well as cellular concrete block specimens have a higher ultimate strength and ductility index than the reference jack arch slab specimens by range (19.53-264.33%) and (48.78-243.21%), respectively. This is due to the precast ferrocement panel, which improve the slab's flexural strength and ductility.
6. The specimens of composite slab made with perforated clay bricks have greater strength when compare to all ferrocement precast and composite brick specimens. This is due to perforated brick units and gypsum mortar having higher flexural bonding strengths. This is because they have perforations that enhance the bonding strength between units.
7. Precast ferrocement panel specimens have a greater ductility index than the reference jack arch slab specimens by ranges (22.73-105.7%), respectively, due to the steel wire mesh in them.

5.1.3 Conclusions for ferrocement sandwiched slabs specimens

1. The manufactured ferrocement sandwich composite specimens (G_3) have higher structural performance than control jack arch slab specimen (G_1) and (G_2), so can use as an alternative to the traditional brick-work slab.
2. The produced ferrocement sandwich composite jack arch slab specimens are lighter in weight than (G_1) specimens of the same span and depth section. The weight decrease of the ferrocement sandwich composite jack arch slab specimens ranges from 19.60 to 43.13 % depending on the core materials employed. This is effective in decreasing slab weight and having a positive impact on the other structural elements.
3. The mode of failure of the ferrocement sandwich composite jack arch slab specimens indicates ductile and composite behavior, converting a pure brittle material styropor and cellular concrete blocks into a ductile composite material.
4. All ferrocement sandwich composite slab specimens have a higher ultimate strength by ranges from 571.23-1216.89% and ductility index by ranges from 60.55-205.50% than the reference jack arch slab specimen, respectively.
5. Using shear connectors improve ultimate strength by 29.65, and 43.47%, and ductility index by 22.28, and 73.43%, respectively.
6. Increasing depth section of the ferrocement sandwich composite slab leads to an increase in the ultimate load and ductility ratio by 77.48 and 14.28%, respectively.

5.2 Recommendations for Future Works

The following are a list of problems on which further studies are recommended:

1. According to the flexural bonding strength test mentioned in the chapter three and failure mode for all specimens is due to poor flexural bonding strength

between clay bricks units and cellular concrete block prisms with gypsum mortar, experimental investigation to improve the flexural bond strength between brick units and mortar should be study.

2. Full-scale samples of jack arch slabs made from different types of clay bricks and cellular concrete blocks (thermostone) should be investigate.
3. For the traditional jack-arch slab, experimental investigation into strengthening the bottom face of the jack-arch slab by using jute fiber or other strengthening methods such as CFRP should be study.
4. Structural behavior of ferrocement composite and ferrocement sandwiched composite jack arch slabs with ferrocement layers reinforced by polypropylene or jute fiber should be investigate.
5. The finite element models, and empirical equations for the technique discussed in current study must be examine and evaluate.

APPENDICIES

APPENDIX A: PRODUCT DATA SHEET OF SIKA VISCOCRETE 5930L IQ

BUILDING TRUST

PRODUCT DATA SHEET

Sika® ViscoCrete®-5930 L IQ

HIGH RANGE WATER REDUCING ADMIXTURE

DESCRIPTION

Sika® ViscoCrete®-5930 L IQ is a High range water reducing and super plasticizing admixture for Concrete & Mortar utilizing Sika's 'ViscoCrete®' polycarboxylate polymer technology (3rd Generation) .

USES

Sika® ViscoCrete®-5930 L IQ is mainly used for the following applications:
1- Concrete Containing GGBS , Micro Silica , Fly ash , ... Etc.
2- Production of Ready Mixed Concrete, High performance Concrete .
3- Impermeable & dense Concrete with smooth surface , Water tight mix design proportion must be considered.
4- Production of Self-compacting Concrete (SCC) , SCC mix design proportion must be considered.
5- Production of complex & fine elements such as Slabs , Foundations , Walls , Beams & Columns even through congested reinforcement .

CHARACTERISTICS / ADVANTAGES

Sika® ViscoCrete®-5930 L IQ is a powerful superplasticizer which acts through several different mechanisms including surface adsorption and sterically effects separating the cementitious binder particles. The following advantages properties are achieved:
1- High water reduction, resulting in high density, high strength and reduced permeability
2- Superior plasticizing effect, resulting in improved flow, placing and compaction characteristics
3- Reduced shrinkage during curing and reduced creep when hardened .
4- Chloride Free thus; no corrosion effect on steel.
5- Reduced rate of carbonation of the Concrete .
6- NO need for vibration , thus NO noise pollution .
7- Suitable for Winter conditions .

APPROVALS / CERTIFICATES

Sika® ViscoCrete®-5930 L IQ meets the requirements of ASTM C-494 Types F.

PRODUCT INFORMATION

Composition	Aqueous solution of modified polycarboxylates
Packaging	Bulk Deliveries 1000 Kgs IBC 20 kg Pail
Appearance / Colour	Brownish liquid
Shelf life	12 months from date of production if stored properly in undamaged unopened, original sealed packaging.
Storage conditions	In dry conditions at temperatures between +5°C and +35°C. Protect from direct sunlight. It requires recirculation when held in storage for extended periods.
Specific gravity	1.085 ± (0.01) g/cm3
pH-Value	4 - 6
Total chloride ion content	Nil

TECHNICAL INFORMATION

Concreting guidance	The standard rules of good concreting practice, concerning production and placing, are to be followed. Laboratory trials shall be carried out before concreting on site, especially when using a new mix design or producing new concrete components. Fresh concrete must be cured properly and curing applied as early as possible.

APPLICATION INFORMATION

Recommended dosage	Recommended dosage for concrete: 1- For plastic Concrete (0.2 - 0.8 %) by weight of Binder (200 - 800 gm) for 100 kg cement . 2- For Flow & Self Compacting Concrete (0.8 - 1.8 %) by weight of Binder (800 - 1800 gm) for 100 kg cement . 3- Optimum dosage should be determined by site trials. When adjusting the consistency , high water reduction property of the admixture must be taken in consideration , excessive water addition must be prevented .
Compatibility	Sika® ViscoCrete®-5930 L IQ can be used in conjunction with : 1- SikaFiber® 2- Sika®PlastoCrete-N 3- Sika®Antifreeze 4- SikaRapid® 5- SikaRetarder® All admixtures must be added separately. Trials are always recommended before combining products . For additional information, please contact Sika technical personnel.
Dispensing	Sika® ViscoCrete®-5930 L IQ is added to the gauging water or added with it into the concrete mixer. To take advantage of the high water reduction, a wet mixing time, which is depending on the mixing conditions and mixer performance, of at least 2 mins. per cubic meter after the admixture addition is recommended. Sika® ViscoCrete®-5930 L IQ shall not be added to dry cement.
Restrictions	Over dosage effect An over dosage of Sika® ViscoCrete®-5930 L IQ with water excess will cause the following : 1- Increase of air entrainment . 2- Bleeding or Segregation .

BASIS OF PRODUCT DATA

All technical data stated in this Product Data Sheet are based on laboratory tests. Actual measured data may vary due to circumstances beyond our control.

IMPORTANT CONSIDERATIONS

When using Sika® ViscoCrete®-5930 L IQ the following points should be taken in consideration :
1- A suitable mix design has to be taken into account and local material sources shall be trialed.
2- Do not use with naphthalene based admixtures.

ECOLOGY, HEALTH AND SAFETY

For information and advice on the safe handling, storage and disposal of chemical products, users shall refer to the most recent Safety Data Sheet (SDS) containing physical, ecological, toxicological and other safety-related data.

APPLICATION INSTRUCTIONS

Application Method / Tools :
The standard rules of good concreting practice , concerning production as well as placing are to be followed , refer to relevant standards . Fresh Concrete must be cured properly .
Cleaning of tools :
Clean all tools & application equipment with water immediately after use .
Hardened / Cured material can only be mechanically removed .

LOCAL RESTRICTIONS

Please note that as a result of specific local regulations the declared data for this product may vary from country to country. Please consult the local Product Data Sheet for the exact product data.

LEGAL NOTES

The information, and, in particular, the recommendations relating to the application and end-use of Sika products, are given in good faith based on Sika's current knowledge and experience of the products when properly stored, handled and applied under normal conditions in accordance with Sika's recommendations. In practice, the differences in materials, substrates and actual site conditions are such that no warranty in respect of merchantability or of fitness for a particular purpose, nor any liability arising out of any legal relationship whatsoever, can be inferred either from this information, or from any written recommendations, or from any other advice offered. The user of the product must test the product's suitability for the intended application and purpose. Sika reserves the right to change the properties of its products. The proprietary rights of third parties must be observed. All orders are accepted subject to our current terms of sale and delivery. Users must always refer to the most recent issue of the local Product Data Sheet for the product concerned, copies of which will be supplied on request.

Sika Iraq (Sika Trading L.L.C.)
Erbil / Baghdad / Basra
Tel: +96 477 303 74451
info@iq.sika.com
iq.sika.com

REFERENCES

1. Hassoun, M. N., & Al-Manaseer, A. (2020). *Structural concrete: theory and design*. John Wiley & sons.

2. Sako, Z., & Levon, A. (2007). *Building construction.* University of Baghdad - College of Engineering - Department of Civil Engineering.

3. Resan, S. F., & Dawod, A. O. (2015). Behavior of Customary Jack-Arch Slabs in South of Iraq. *Journal of University of Babylon*, 23(2).

4. https://www.ina.iq/149475--.html, 2022.

5. Maheri, M. R., & Rahmani, H. (2003). Static and seismic design of one-way and two-way jack arch masonry slabs. *Engineering structures*, 25(13), 1639-1654.

6. Maheri, M. R., Pourfallah, S., & Azarm, R. (2012). Seismic retrofitting methods for the jack arch masonry slabs. *Engineering structures*, *36*, 49-60.

7. Zahrai, S.M., & Zahraei, S. A. (2006). Passive seismic control of masonry jack arch slabs. *World conference on structural control and monitoring*, 4, 1–8.

8. Zahraei, S. M., & Heidarzadeh, M. (2007). Destructive effects of the 2003 bam earthquake on structures. *Asian journal of civil engineering (building and housing)*, 8(3), 329-342.

9. *ACI Committee 549-R97: State-of-the-Art Report on Ferrocement.* ACI 549-R97, in Manual of Concrete Practice, American Concrete Institute, Farmington Hills, Michigan, 26 pages.

10. Naaman, A. E. (2000). *Ferrocement and laminated cementitious composites* (Vol. 3000, p. 26). Ann Arbor: Techno press.

11. Yardim, Y. (2018). Review of research on the application of ferrocement in composite precast slabs. *Periodica Polytechnica Civil Engineering*, *62*(4), 1030-1038.

12. Li, B., Lam, E. S. S., Wu, B., & Wang, Y. Y. (2013). Experimental investigation on reinforced concrete interior beam–column joints rehabilitated by ferrocement jackets. *Engineering Structures*, *56*, 897-909.

13. https://forum.susana.org/septic-tanks/20592-constructing-septic-tanks-on-site-using-ferrocement#, "Img_4724,".

14. de Andrade, S. A., Vellasco, P. C. D. S., da Silva, J. G. S., & Takey, T. H. (2004). Standardized composite slab systems for building constructions. *Journal of Constructional Steel Research*, *60*(3-5), 493-524.

15. *https://web.itu.edu.tr/~haluk/COMPOSITE%201.pdf,2005*.

16. Pourfallah, S., Maheri, M. R., & Najafgholipour, M. A. (2009). Experimental Investigation of the Jack Arch Slab Retrofitted by Concrete Layer. In *ICCD03: 3rd International Conference on Concrete & Development* (pp. 523-533).

17. Zahrai, S. M. (2015). Experimental study of typical and retrofitted jack arch slabs in a single story 3D steel building. *International Journal of Civil Engineering*, *13*(3), 278-288.

18. Alfeehan, A. A., & Alkerwei, R. H. (2014). Structural Behavior for Low Cost Roof System of Steel Frame and Thermo-Stone Blocks. *Engineering and Technology Journal*, *32*(12 Part (A) Engineering).

19. Dawood, A. O., & Resan, S. F. (2015). Seismic analysis of traditional jack-arch slab in south of Iraq. *Al-qadisiyah journal for engineering sciences*, *8*(3).

20. Shakib, H., Mirjalili, A., Dardaei, S., & Mazroei, A. (2015). Experimental investigation of the seismic performance of retrofitted masonry flat arch diaphragms. *Journal of Performance of Constructed Facilities*, *29*(4), 04014115.

21. Ozdemir, M. A., Kaya, E. S., Aksar, B., Seker, B., Cakir, F., Uckan, E., & Akbas, B. (2017). Seismic vulnerability of masonry Jack arch slabs. *Engineering failure analysis*, *77*, 146-159.

22. A. Majeed, S., & N. Mahmood, M. (2009). Flexural behavior of flat and folded ferrocement panels. *Al-rafidain engineering journal (AREJ)*, *17*(4), 1-11.

23. Gaidhankar, D. G., Kulkarni, M. S., & Inamdar, S. K. (2017). Behavior of ferrocement panels using welded square mesh. International journal for research & development in technology, 8(4), 138–150.

24. Nawar, M. T. (2018). Study on flexural behaviour and cracking of ferrocement slabs by neglecting very fine sand. *Iraqi journal of civil engineering*, *12*(2).

25. Mughal, U. A., Saleem, M. A., & Abbas, S. (2019). Comparative study of ferrocement panels reinforced with galvanized iron and polypropylene meshes. *Construction and Building Materials*, *210*, 40-47.

26. Memon, N. A., Sumadi, S. R., & Ramli, M. (2006). Strength and behaviour of lightweight ferrocementaerated concrete sandwich blocks. *Malaysian journal of civil engineering*, *18*(2).

27. Memon, N. A., Sumadi, S. R., & Ramli, M. (2007). Ferrocement encased lightweight aerated concrete: a novel approach to produce sandwich composite. *Materials Letters*, *61*(19-20), 4035-4038.

28. Yardim, Y., Jafaar, M. S., Noorzaei, J., Khan, S. R., & Kamal, N. M. (2008). Performance of precast ferrocement panel for composite masonry slab system. In *International Conference on Construction and Building Technology (ICCBT2008). ICCBT* (pp. 397-407).

29. Thanoon, W. A., Yardim, Y., Jaafar, M. S., & Noorzaei, J. (2010). Structural behaviour of ferrocement–brick composite floor slab panel. *Construction and Building materials*, *24*(11), 2224-2230.

30. Thanoon, W. A., Yardim, Y., Jaafar, M. S., & Noorzaei, J. (2011). Structural response of interlocking composite masonry slab. *Proceedings of the Institution of Civil Engineers-Structures and Buildings*, *164*(6), 409-420.

31. Fahmy, E. H., Shaheen, Y. B., Abou Zeid, M. N., & Gaafar, H. M. (2012). Ferrocement sandwich and hollow core panels for floor construction. *Canadian Journal of Civil Engineering*, *39*(12), 1297-1310.

32. Cheah, C. B., & Ramli, M. (2013). The structural behaviour of HCWA ferrocement–reinforced concrete composite slabs. *Composites Part B: Engineering*, *51*, 68-78.

33. Waryosh, W. A., Abtan, Y. G., & Dawood, M. H. A. (2013). Structural behavior of composite sandwich slab panels. *Journal of Engineering and Sustainable Development*, *17*(4), 220-232.

34. Abushawashi, N., & Vimonsatit, V. (2014). Use of Ferrocement Panel as Reinforced Concrete Slabs with Lightweight Blocks Infill. In *Second Australasia and Southeast Asian Conference, Bangkok, Thailand* (pp. 245-250).

35. Dharanidharan, S. (2016). Flexural behavior of ferrocement composite slab. *International journal of engineering sciences & research technology [IJESRT], ISSN*, 2277-9655.

36. Shaheen, Y. B., Eid, F. M., & Dayer, M. A. S. (2019). Developing of Light Weight Ferrocement Composite Plates. *AICSGE*, 10, 861–872.

37. Huang, W., Ma, X., Luo, B., Li, Z., & Sun, Y. (2019). Experimental study on flexural behaviour of lightweight multi-ribbed composite slabs. *Advances in Civil Engineering*, *2019*.

38. Iraqi specifications 25/1993: *Clay Buildings Bricks*. Central Organization for Standardization and Quality Control. Iraq (in Arabic).

39. Iraqi specifications 24/1989: *Method of Testing and Sampling Clay Buildings Bricks*. Central Organization for Standardization and Quality Control. Iraq (in Arabic).

40. Iraqi specifications 28/2010: *Physical Properties Testing of Gypsum for Building Purposes.* Central Organization for Standardization and Quality Control. Iraq (in Arabic).

41. Iraqi Refernce guide 810/2009: *Method of Testing Cellular Concrete Blocks*. Central Organization for Standardization and Quality Control. Iraq (in Arabic).

42. Iraqi specifications 1441/2013: *Requirements of Testing Cellular Concrete Blocks.* Central Organization for Standardization and Quality Control. Iraq (in Arabic).

43. Khalaf, F. M. (2005). New test for determination of masonry tensile bond strength. *Journal of materials in civil engineering*, *17*(6), 725-732.

44. Iraqi Refernce guide 198/1990: *Method of Testing Physical Properties for Cement*. Central Organization for Standardization and Quality Control. Iraq (in Arabic).

45. Iraqi Refernce guide 472/1993: *Method of Testing Chemical Properties for Cement*. Central Organization for Standardization and Quality Control. Iraq (in Arabic).

46. Iraqi specifications 5/2019: *Portland Cement.* Central Organization for Standardization and Quality Control Iraq (in Arabic).

47. Iraqi Refernce guide 30/1984: *Method of Testing for Fine Aggregates.* Central Organization for Standardization and Quality Control. Iraq (in Arabic).

48. Iraqi specifications 45/1980: *Aggregates from Natural Sources for Concrete and Building Construction*. Central Organization for Standardization and Quality Control. Iraq (in Arabic).

49. *Standard specification for concrete aggregates (ASTM C33/C33M-13)*. 2013.

50. Iraqi specifications 1703/2018: Water Used for Concrete. Central Organization for Standardization and Quality Control Iraq (in Arabic).

51. Batson, G. B., Castro, J. O., Guerra, A. J., Iorns, M. E., Johnston, C. D., Naaman, A. E., ... & Zubieta, R. C. (2018). Guide for the design, construction, and repair of ferrocement. *ACI Structural Journal*, *85*(3), 325-351.

52. *Standard test method for compressive strength of hydraulic cement mortars (using 2-in. or [50-mm] cube specimens) (ASTMC109/C109M − 13)*. 2013.

53. *Standard test method for flexural Strength of hydraulic-cement mortars (ASTMC348 − 14)*. 2014.

54. Azizinamini, A., Darwin, D., Eligehausen, R., Pavel, R., & Ghosh, S. K. (1999, November). Proposed modifications to ACI 318-95 tension development and lap splice for high-strength concrete. *American Concrete Institute*.

55. Abdulraheem, M. S. (2018). Experimental investigation of fire effects on ductility and stiffness of reinforced reactive powder concrete columns under axial compression. *Journal of Building Engineering*, *20*, 750-761.

الخلاصة

تقترح هذه الدراسة طريقتين جديدتين لبناء سقوف العقادة. الطريقة الأولى تتكون من طبقتين. الطبقة الأولى تكون عباره عن الواح مسبقة الصب من الفيروسمنت التي تعمل عمل القالب الدائم مركبة مع أنواع مختلفة من الطابوق الطيني (الطابوق الطيني المصمت والطابوق الطيني المثقب)، ووحدات من الخرسانة الخلوية (الثرمستون)، مع مونة الجص. الطريقة الثانية تتكون من طبقتين من الفيروسمنت مفصولة بواسطة الفلين أو الخرسانية خلوية (الثرمستون) بشكل ساندويش. يكون السمك الكلي للنموذج 130 مم (15 مم لكل طبقة من الفيروسمنت و100 مم لوحدات الفلين او الثرمستون). جميع طبقات الفيروسمنت تم صبها من مونة اسمنتية ذات قابلية تشغيل عالية ومقاومة انضغاط 68 ميجا باسكال. المحددات الرئيسية المدرجة في هذه الدراسة العملية هي طول الفضاء، وارتفاع المنحني، ونسبة التسليح، وأنواع الطابوق، ونوع المادة الفاصلة بين طبقتي الفيروسمنت (الفلين أو الثرمستون)، وطول الفضاء، وسمك السقف. تم تصنيع واختبار 28 عينة أحادية الاتجاه تحت حمل انحناء خطي. خمسة منها كانت عبارة عن عينات من العقادة مكونة من الطابوق الطيني أو الثرمستون ومونة الجص لتمثل العينات المرجعية. العينات الثلاثة والعشرون الاخرى ستة عشر منهم كانت عينات من الألواح المسبقة الصب من الفيروسمنت مركبة مع أنواع مختلفة من الطابوق الطيني، خمسة منها عبارة عن الواح فيروسمنت مسبقة الصب لتقييم قدرتها على تحمل الاحمال المسلطة اثناء العمل، وسبع عينات أخرى كانت عبارة عينات من سقف مكون من طبقتين من الفيروسمنت بشكل ساندويش. أظهرت النتائج المتعلقة بالتحمل الأقصى ومؤشر المطيلية أن جميع العينات من الفيروسمنت المركبة لديها (19.53-264.33%) و (48.78-243.21%) تحمل اقصى ومؤشر مطيلية اعلى من العينة المرجعية على التوالي. عينات الواح الفيروسمنت المسبقة الصب كانت قادرة على تحمل أحمال البناء بشكل آمن دون استخدام أي اسناد لها. تتمتع جميع عينات السقف المكون من الفيروسمنت بشكل ساندويش بمؤشر أعلى للتحمل الاقصى والمطيلية، يتراوح بين (571.23-1216.89%) و (60.55-205.50%) من العينة المرجعية، على التوالي. أدت زيادة سمك السقف المكون من طبقتين من الفيروسمنت بشكل الساندويتش إلى زيادة التحمل الاقصى ومؤشر المطيلية بنسبة 77.48 و14.28% على التوالي. عند المقارنة بالعينات المرجعية، تم تقليل وزن السقف المكون من الفيروسمنت بشكل ساندويش بنسبة 19.60 إلى 43.13٪. طبقا للنتائج المشجعة لهذه الدراسة، يمكن استخدام الطرق المقترحة كبديل لسقوف العقادة التقليدية.

جمهورية العراق
وزارة التعليم العالي والبحث العلمي
جامعة ميسان / كلية الهندسة
قسم الهندسة المدنية

التصرف الانشائي للسقف المركب من الفيروسمنت والطابوق

من قبل

احمد هاتف عبيد

بكالوريوس هندسة مدنية، 2016

رسالة

مقدمة الى كلية الهندسة في جامعة ميسان

كجزء من متطلبات الحصول على درجة الماجستير في علوم الهندسة المدنية / انشاءات

جامعة ميسان

2022 تموز

بإشراف

الأستاذ الدكتور: عبد الخالق عبد اليمة جعفر